Development of Cell-Scaffold Construct for Cartilage Tissue Regeneration

Parinita Agrawal

Department of Biotechnology & Medical Engineering

NATIONAL INSTITUTE OF TECHNOLOGY, ROURKELA

Development of Cell-Scaffold Construct for Cartilage Tissue Regeneration

Dissertation submitted to the

National Institute of Technology, Rourkela

In partial fulfilment of the requirements for the degree of

Doctor of Philosophy

in

Biotechnology and Medical Engineering

by

Parinita Agrawal

(**Roll No. 513BM1002**)

Based on the research carried out under the supervision of

Dr. Krishna Pramanik
Principal Supervisor

and

Dr. Ranjan Kumar Patra
Co-Supervisor

November 2018

Department of Biotechnology and Medical Engineering

National Institute of Technology, Rourkela

Department of Biotechnology and Medical Engineering
National Institute of Technology, Rourkela

Certificate of Examination

Roll Number: *513BM1002* 27th November, 2018

Name: *Parinita Agrawal*

Title of Dissertation: *Development of Cell-Scaffold Construct for Cartilage Tissue Regeneration*

We the below signed, after checking the dissertation mentioned above and the official record book(s) of the student, hereby state our approval of the dissertation submitted in partial fulfilment of the requirements of the degree of Doctor of Philosophy in Biotechnology and Medical Engineering at National Institute of Technology Rourkela. We are satisfied with the volume, quality, correctness, and originality of the work.

----------	----------
Krishna Pramanik	Ranjan K. Patra
Principal supervisor	Co-supervisor
----------	----------
A. Thirugnanum	Amit Biswas
Member (DSC)	Member (DSC)
----------	----------
Sujit Kumar Bhutia	Ram Shanker Verma
Member (DSC)	External Examiner
----------	----------
Mukesh K. Gupta	A. Thirugnanum
Chairman (DSC)	Head of the Department

Department of Biotechnology and Medical Engineering
National Institute of Technology, Rourkela

Dr. Krishna Pramanik
Professor

Dr. Ranjan K. Patra
Senior Consultant, Orthopaedic

27th November, 2018

Supervisor's certificate

This is to certify that the work presented in this dissertation entitled "Development of Cell-Scaffold Construct for Cartilage Tissue Regeneration" by Parinita Agrawal, Roll Number 513BM1002, is a record of original research carried out by her under my supervision and guidance in partial fulfilment of the requirements of the degree of Doctor of Philosophy in Biotechnology and Medical Engineering. Neither this dissertation nor any part of it has been submitted for any degree or diploma to any institute or university in India or abroad.

Ranjan K. Patra
Co-supervisor

Krishna Pramanik
Principal Supervisor

DECLARATION OF ORIGINALITY

I, *Parinita Agrawal*, Roll Number *513BM1002* hereby declare that this dissertation entitled "*Development of Cell-Scaffold Construct for Cartilage Tissue Regeneration*" represents my original work carried out as a doctoral student of NIT Rourkela and, to the best of my knowledge, it contains no material previously published or written by another person, nor any material presented for the award of any other degree or diploma of NIT Rourkela or any other institution. Any contribution made to this research by others, with whom I have worked at NIT Rourkela or elsewhere, is explicitly acknowledged in the dissertation. Works of other authors cited in this dissertation have been duly acknowledged under the section "References". I have also submitted my original research records to the scrutiny committee for evaluation of my dissertation.

I am fully aware that in case of any non-compliance detected in future, the Senate of NIT Rourkela may withdraw the degree awarded to me on the basis of the present dissertation.

27th November, 2018 **Parinita Agrawal**

NIT Rourkela

ACKNOWLEDGEMENT

At this moment of accomplishment, it is important to look back and pen down the recognition to many people who have helped me to achieve such a crucial stage of my life.

I take this opportunity to thank my supervisor Dr. Krishna Pramanik for the inspiration and guidance she has offered throughout my PhD. She has provided me with a logistic vision to understand the subject and concentrate on important matters. She extended her support in every possible way be it as a critic or praise, she has always been there to promote me for my improvement. She has been instrumental in directing my thoughts towards the betterment of my work at every step and provided me space to chase my ideas, complete the experiments and write this thesis in a best possible way. I extend my gratitude to my co-supervisor Dr. Ranjan Kumar Patra for providing timely knowledge that helped me to maintain the enthusiasm throughout this study.

My sincere gratitude to Professor Animesh Biswas, Director National Institute of Technology Rourkela for providing the opportunity to pursue my research at the institute. I also extend my thanks to Professor Sunil Kumar Sarangi, ex-Director NIT Rourkela, who had been a guiding spirit for me and many research scholars at the institute. I thank Ministry of Human Resource Development, Government of India for providing financial support throughout the research period.

My sincere thanks also go to doctoral scrutiny committee chairman Dr. Mukesh Kumar Gupta and members Dr. Amit Biswas (Department of Biotechnology and Medical Engineering), Dr. Arunachalam Thirugnanum (Department of Biotechnology and Medical Engineering) and Dr. Sujit Bhutia (Department of Life Science) for evaluating my work and ensuring that every essential requirement for the fulfilment of this degree is met. I am also highly thankful to all the faculty members and staff of my department and the institute for extending their facilities that supported the completion of this thesis.

My thanks go to everyone I had the opportunity to work with during this study including my seniors Akalabya Bissoyi, Nadeem Siddiqui, Varshini Vishwanath, Bhisham Narayan Singh, and current lab member Amit Singh. This acknowledgment would be incomplete if I do not

mention my friends form the department and institution Senthil Guru, Tejinder Kaur, Veena Vyas, Seetarashmi Sahu, Shambit Ray, Sahely Saha and Swarnima Kashyap for the informative discussions and sharing the bittersweet moments during my stay.

Special thanks to my family, particularly my parents and brother for constant encouragement that was the power booster in this journey to pursue my dreams. Their patience and never-ending trust helped me maintain peace of mind and led me put the best foot forward. I am highly obliged to my in-laws for the love and perseverance they have shown that helped me remain focused in my work. I also extend my deep regards to the critics and those who periodically raised concerns on my caliber, for it was not to prove them wrong, this thesis would not have seen this day of completion. I feel 'thanks' would not be enough to describe how indebted I am to my husband, Dr. Ritu Raj for the motivation he offered throughout my PhD, and being the strength that helped me chase my dream. Finally, I would like to thank the almighty for programming my life in such a wonderful way filled with lovely people and fantastic opportunities that enabled me to work harder and succeed in my attempts!

Parinita Agrawal

ABSTRACT

The treatment of cartilage tissue damage and /or diseases is a great challenge because of the limited self- repair ability of cartilage tissue and several limitations prevailed in current clinical methods. In this context, development of cartilage construct by tissue engineering technique using scaffold derived from suitable biopolymers and stem cell is the most promising approach. In this study, silk-fibroin/chitosan (SF/CS) and its composite scaffolds, as artificial extra cellular matrix (ECM), and umbilical cord blood (UCB) derived human mesenchymal stem cells (hMSCs) as potential cell source, were used for developing cartilage construct. Firstly, hMSCs were isolated from UCB as a potential stem cell source, cultured and characterised. Phase contrast microscopy showed fibroblast-like morphology thus confirmed the cultured cells are of mesenchymal in nature. Flow cytometry analysis revealed >95% expression of CD105, CD73, and CD90, with <2% for CD45, CD34, CD11b, CD79α and HLA-DR expression by hMSCs at 4^{th} passage. *In vitro* differentiation potential of UCB-hMSCs into osteocytes, chondrocytes, and adipocytes, the characteristic mesenchymal lineages, was confirmed by histological analysis. UCB-hMSCs seeded on SF/CS scaffolds was cultured and differentiated under static and dynamic culture (spinner flask) conditions to generate cartilage construct. Constructs cultured in spinner flask bioreactor consisted of 62% live cells, and showed 543% more cell density at the core than the constructs obtained in static system. The progression of chondrogenic differentiation during 21 days of culture in chondrogenic media was assessed by glycosaminoglycans (GAG) synthesis, alcian blue staining for proteoglycan matrix, and immunofluorescence staining for collagen-II (Col II) and aggrecan (Acan). This was further confirmed by quantitative PCR (qPCR) analysis, showing low Col I expression and upregulated Sox9, matrilin 3 (MATN3), Col II and Acan genes. The results demonstrated superiority of culture condition in promoting hMSCs proliferation and ECM formation.

Secondly, effort has been given to improve the differentiation of hMSCs, thereby cartilage type ECM formation by using SF/CS scaffolds loaded with glucosamine (Gl) and chondroitin sulfate (Ch) individually. The Gl loaded SF/CS scaffolds (SF/CS-Gl) showed improved hMSCs attachment and viability (82.45±2.6% live cells) together with an increase in cell metabolic activity and proliferation than SF/CS scaffolds. The presence of Gl in the scaffold has enhanced the synthesis of cartilage-specific GAG with maintained chondrocyte

phenotype and significant gene up-regulation. Similarly, the chondrogenic potential of SF/CS scaffolds was also enhanced by the incorporation of Ch into SF/CS scaffold (SF/CS-Ch). An improvement in chondrogenic differentiation of hMSCs was evident by higher GAG secretion (247±20 µg/mg) than SF/CS (83.2±7 µg/mg) and SF/CS-Gl (130±6 µg/mg) scaffolds. Though cell viability and proliferation were comparable to SF/CS-Gl scaffold, the expression of chondrogenic genes and matrix proteins were higher in SF/CS-Ch scaffolds implying the positive effect of Ch in supporting chondrogenic differentiation leading to the cartilage specific ECM formation.

Considering the beneficial effect of GI and Ch in combination, an effort was further given to investigate the chondrogenic differentiation of hMSCs over Gl and Ch loaded composite SF/CS scaffolds (SF/CS-Gl-Ch). Among the scaffolds with varied concentration of Ch (0.5-1.5 wt%), SF/CS-Gl loaded with 1.5% Ch showed superiority in promoting cell attachment, viability, and proliferation. The DNA content of hMSCs in SF/CS-Gl-Ch (342.2±4 ng/ml) was two times higher than SF/CS-Ch (163±5 ng/ml) and SF/CS-Gl (153±5.2 ng/ml) scaffolds. The proteoglycan matrix staining was more prominent in SF/CS-Gl-Ch scaffold with higher GAG synthesis of 383±7 µg/mg and fluorescence intensity of Col II and Acan. The cartilage specific ECM produced in this study is higher than the constructs developed in reported literature. The chondrocytes in SF/CS-Gl-Ch showed higher expression of Sox9, Col II and Acan genes representing its superior chondrogenic potential than other constructs developed in this study. Therefore, Gl and Ch loaded SF/CS scaffold is proven to be an excellent scaffold matrix possessing superior tailor properties that can offer enhanced chondrogenic differentiation of hMSCs, and thus cartilage-specific ECM formation in a dynamic bioreactor system. The generated cartilage construct may pave the way for cartilage tissue regeneration for future clinical application.

Keywords: Cartilage tissue engineering, chitosan, chondroitin sulfate, glucosamine, mesenchymal stem cell, silk fibroin, spinner flask

Table of Contents

List of Figures

List of Tables

List of Abbreviations

%	Percentage
µ	Micro
3D	Three dimensional
Acan	Aggrecan
ADSCs	Adipose-derived stem cells
APC	Allophycocyanin
B-cell	B lymphocytes
BM	Bone marrow
BMP	Bone morphogenic protein
˚C	Degree Celsius
CD	Cluster of differentiation
cDNA	Complimentary deoyribo-nucleic acid
Ch	Chondroitin sulfate
CLSM	Confocal laser scanning microscope
CO_2	Carbon dioxide
Col I	Collagen type I
Col II	Collagen type II
CPDA	Citrate-phosphate-dextrose-adenine
CS	Chitosan
DMEM	Dulbecco's Modified Eagle's Medium
DMMB	Dimethylmethylene blue
DNA	Deoxyribonucleic acid
dNTP	Deoxynucleotide triphosphate
dsDNA	Double stranded deoyribo-nucleic acid
ECM	Extra cellular matrix
EDTA	Ethylenediaminetetraacetic acid
Et al.	And others
etc	Et cetera
EthD-1	Ethidium homodimer
FBS	Fetal bovine serum
FESEM	Field emission scanning electron microscope
FGF	Fibroblast growth factor
FITC	Fluorescein isothiocyanate
FTIR	Fourier transform infrared
GAG	Glycosaminoglycan
Gl	Glucosamine
h	hour
H&E	Hematoxylin and eosin
HA	Hyaluronic acid
HARV	High Aspect Ratio Vessel
HLA-DR	Human Leukocyte Antigen – antigen D Related

ICAM	Intercellular Adhesion Molecule
IGF	Insulin-like growth factor
IGH	Ispat General Hospital
ISCT	International Society for Cellular Therapy
M	Molar
m	mili
mAb	monoclonal antibody
MATN3	Matrilin 3
MHC	Major histocompatibility complex
min	minute
ml	Millilitre
MNCs	Mononuclear cells
MPC	Mesenchymal progenitor cells
MSCs	Mesenchymal stem cells
MTT	3-(4,5-Dimethylthiazol-2-yl)-2,5-Diphenyltetrazolium Bromide
NK cell	Natural killer cell
nm	nanometre
NP	Nanoparticle
O_2	Oxygen
OA	Osteoarthritis
PBS	Phosphate buffer saline
PCR	Polymerase chain reaction
PE	Phycoerythrin
PEG	poly(ethylene-glycol)-based
pH	hydrogen ion concentration
PLA	Polylactic acid
PLGA	Poly lactide-co-glycolide
PVA	Polyvinyl alcohol
RGD	Arginine-glycine-aspartate
RNA	Ribo nucleic acid
rpm	Rotation per minute
RT	Reverse transcription
s	Second
SF	Silk fibroin
Sox9	SRY-related high-mobility group box 9
STLV	Slow turning lateral vessel
SYSADOA	Symptomatic slow-acting drug for the treatment of osteoarthritis
SZP	Superficial zonal proteins
T-cell	T lymphocyte
TGF-β	Transforming growth factor beta
UCB	Umbilical cord blood
WJ	Wharton’s Jelly

Chapter 1

Introduction

1.1 Background

Cartilage tissue damages and diseases are arising due to aging, accidental injury and developmental abnormalities cause severe pain and loss of mobility (Kock et al. 2012). The treatment of such defects is a major challenge because articular cartilage has a limited potential for intrinsic repair due to its low cellularity, avascular, alymphatic and aneural nature (Beddoes et al. 2016). Furthermore, the current clinical treatments such as microfracture, tissue grafting and autologous chondrocyte transplantation used for cartilage repair offer several limitations including poor tissue integration, donor site morbidity, and involvement of invasive procedure, limited mobility and longevity of implants. As a consequence, the patient can't restore normal cartilage function and thus pain continues. Therefore, in recent years research focus has been directed towards the development of cartilage construct with desired properties through tissue engineering (TE) approach by considering it as a promising technique to cure cartilage defects.

In TE, three dimensional (3D) biopolymeric scaffolds with extracellular matrix (ECM) mimicking properties and suitable cell source are prime factors for the success of this method and for the generation of cartilage tissue construct. In recent years, a number of biomaterials have been explored and used for *in vitro* cartilage tissue regeneration (Stoddart et al. 2009; Rawal et al. 2013). Among these, silk fibroin (SF) and chitosan (CS) were reported to be potential for scaffold development. SF, a protein obtained from silk worm, can be regenerated in various forms depending on the application. SF shows a minimal inflammatory reaction and its repetitive glycine-alanine-glycine-alanine-glycine-serine (GAGAGS) sequence forming β-sheet structure provides excellent mechanical strength making it suitable for cartilage TE application. However, SF lacks hydrophilicity that limits its TE application. On the other hand, CS has intrinsic antibacterial activity, excellent biocompatibility, hydrophilicity and cell supportive property, but CS has poor mechanical strength. So, the blend of silk fibroin and chitosan has been reported to be a potential matrix for TE application (Bhardwaj and Kundu 2011; Vishwanath et al. 2016). Though various studies have shown the potentiality of the SF/CS blend scaffolds for tissue engineering application, but not much work has been done so far for their use in generating cartilage construct by investigating the chondrogenic differentiation, in particular, of a suitable cell on this scaffold, which calls for further research work.

Another important aspect in TE is the culture environment that profoundly influences the properties of the generated construct. A two dimensional (2D) system comprising of culture dishes is most preferred method owing to its simplicity. However, uneven distribution of cells in the scaffold and time required for construct generation are issues that can be overcome by using advanced methods like dynamic culture. Spinner flask is the simplest dynamic system that provides continuous stirring environment leading to efficient mass transport and mechanical stimulation, which are beneficial for cartilage construct generation (Darling and Athanasiou 2003). Studies have shown the phenotype maintenance of chondrocytes when cultured in spinner flask (Lee et al. 2011; Xu et al. 2014). However, these studies were restricted to the intrinsic capability of autologous chondrocytes to form aggregate to generate a 3D structure or get encapsulated into the gel beads that suffered from size limitation and rupture on implantation (Gigout et al. 2009). Therefore, there is a need of systematic study for construct generation in spinner flask bioreactor using the combination of appropriate cells and scaffold, and validate their performance over the widely used static culture technique.

Cell source also plays an important role in the success of generating construct. Mesenchymal stem cells (MSCs) are attractive cell source for cartilage TE, because of their intrinsic differentiation ability to cells of mesenchymal lineage and can be harvested from a variety of sources including bone marrow (BM), placenta, umbilical cord blood (UCB), adipose tissue and other adult tissues (Kern et al. 2006). UCB derived hMSCs are less immunogenic and offer a comparatively lower rate of post-transplant infection and rejection (Hu et al. 2013). Thus, UCB-hMSCs are promising cell source for seeding on the SF/CS scaffolds to generate cartilage construct. Furthermore, in order to achieve biomimetic property of cartilage extracellular matrix, use of growth factors and bioactive molecules like transforming growth factor, collagen, glucosamine (Gl), chondroitin sulfate (Ch) and hyaluronic acid, are of prime interest (Awad et al. 2004; Derfoul et al. 2007; Yan et al. 2013). In addition to structural benefits provided by the use of SF/CS as biomaterials, the incorporation of these factors may accelerate differentiation of hMSCs and help in achieving desired phenotype. Thus, the present research focuses on the development of cartilage construct using SF/CS based scaffolds and UCB-hMSCs under the influence of dynamic culture environment provided by spinner flask bioreactor for cartilage TE application.

1.2 Importance of tissue engineering

As defined by Langer and Vacanti, TE is an interdisciplinary field that applies the principles of engineering and life sciences towards the development of biological substitutes that restore, maintain, or improve tissue function or a whole organ (Vacanti and Langer 1999). Thus, TE can provide a permanent cure for cartilage defects by repairing or replacing the diseased or damaged tissue with a biocompatible construct, which restores the functionality of the tissue. An overview of TE process is shown in the flow chart (Figure 1.1). The important aspects of a TE process are- cell derived from either biopsies or stem cells, a scaffold, which has the required tailor properties, seeding technique to place cells on the scaffold and appropriate culture condition that provides required growth factors and mocro-environment for cell proliferation and organization to a viable tissue-engineered construct, to be implanted into patient's body for filling the defect site.

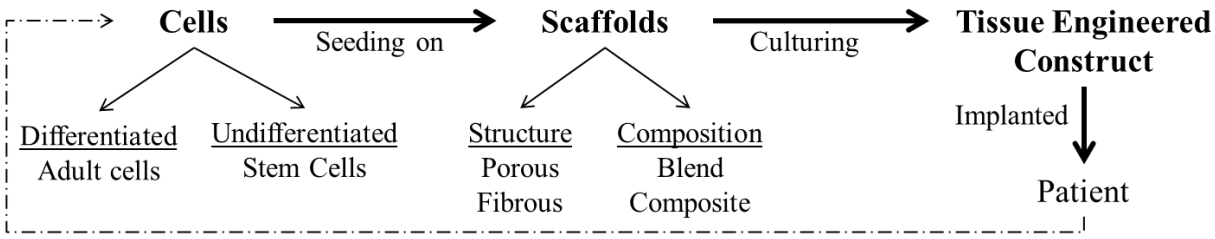

Figure 1.1 Overview of tissue engineering process

The ultimate aim of TE is to provide vital tissue substitutes with the abilities to function, grow, repair, and remodel. TE can be applied for the treatment of various tissue defects and diseases, including skin burn, bone and cartilage defects, muscular disorders, vascular defects, neural diseases, and so on.

1.3 Cartilage tissue

Cartilage is a smooth white connective tissue that covers the ends of the bones and provides a smooth surface to move without friction (Sherwood et al. 2002). Cartilage tissue is distinguished into three categories on the basis of functional differences, as described here- hyaline, fibro, and elastic cartilage. Hyaline cartilage is non-fibrous, white tissue that is found in knee joints. The hyaline cartilage covering the articular surface of bones is commonly termed as articular cartilage. The fibrocartilage is composed majorly of the collagenous extra cellular matrix (ECM) and supports the ends of tendons and ligaments. The elastic cartilage

has elastin in its ECM and is present in ear and nose (Temenoff and Mikos 2000).

1.3.1 Composition and defects

Cartilage tissue comprises of sparsely scattered cells and dense ECM whose composition and arrangement define the function of the tissue. The cells found in cartilage are called chondrocytes, which secrete and get embedded into the matrix comprising of collagenous and proteoglycan components. The cartilage tissue is anatomically distinguished into four zones (Figure 1.2). The superficial or the top most zone towards the articular surface is 10-20% of the thickness and functions to provide shear resistance and frictionless joint movement (Rawal et al. 2013). The collagen fibrils are densely packed tangentially oriented in this region and chondrocytes have flattened disc-like morphology, arranged parallel to the tissue surface (Izadifar et al. 2012). The cells secrete superficial zonal proteins (SZP) known as lubricin that provides surface lubrication and cushion effect (Chung and Burdick 2008). The ECM contains the highest amount of collagen compared to other zones along with fibronectin and water. The middle zone is 40-60% of articular cartilage thickness and contributes to providing high compressive modulus by entrapping water, building osmotic swelling effect (Izadifar et al. 2012). The collagen fibrils are thick, large, random and obliquely oriented and chondrocytes become spherical in this zone. The cells in the middle zone are rich in mitochondria, Golgi bodies and endoplasmic reticulum (Temenoff and Mikos 2000). The third deep zone comprises of 30-40% of the thickness of articular cartilage (Rawal et al. 2013). This region is richest in proteoglycan, and collagen fibrils have a larger diameter and are radially oriented. The chondrocytes in the deep zone have slightly elongated morphology, arranged in columns and present in lowest density as compared to other zones (Wirth and Rudert 1996). The fourth zone is the calcified region of hyaline cartilage where it meets the basal subchondral bone. In this, the ECM is highly mineralized and collagen type X is profoundly found instead of collagen type II (Col II) and chondrocytes are elongated, smaller and very less in number (Stoddart et al. 2009; Izadifar et al. 2012). Cells in this zone lack endoplasmic reticulum and show very less metabolic activity. The deep and calcified zones are distinguished by the tidemark, whose composition is still under investigation (Temenoff and Mikos 2000; Decker et al. 2014).

Worldwide, cartilage defects are estimated to be the fourth leading cause of disability, and in India, it has been reported to be growing at rapid rate, which is estimated to increase by 274%

by the end of 2040 (Akhter et al. 2011; Fransen et al. 2011). Cartilage diseases are more common in elder people but cartilage defects have been reported in all the age groups, including athletes. Age-related defect arises from the degeneration of joint cartilage that can sustain for years if it is not treated properly, and eventually lead to a permanent and incurable disease like osteoarthritis (OA). Another form of cartilage damage caused by accidental or sports injuries is the blunt trauma. These cartilage damages involve matrix disruption, which at primary level are repaired by the synthetic activity of the viable chondrocytes, but the critical ones involving the loss of chondrocytes along with the matrix needs clinical care (Temenoff and Mikos 2000). Other damages that affect the tissue anatomy are partial and full thickness defects, whose severity depends upon the depth of injury. The disruption confined to the surface of cartilage is termed as partial thickness defect. It has been observed by various researchers that the defects of superficial layers in cartilage tissues are usually not self-cured. While full thickness defects reaching subchondral bone are initially filled with granulation tissue, which subsequently forms fibrous cartilage (Wirth and Rudert 1996). The tissue replaced by fibrocartilage is inferior in mechanical property than the native cartilage and also shows increased permeability to body fluids that cause its degradation with time, leading to a reoccurrence of the defect or its symptoms (Sherwood et al. 2002).

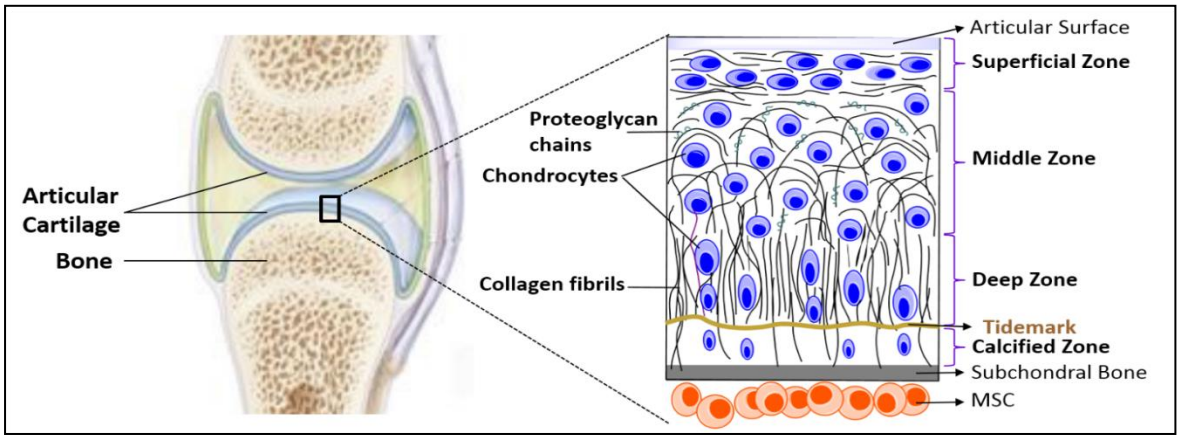

Figure 1.2 Cross section of knee joint and organization of articular cartilage representing arrangement of chondrocytes and matrix components in different zones.

1.3.2 Current clinical treatment methods for cartilage defects

Treatment of cartilage defects is a major challenge because articular cartilage has a limited potential of intrinsic repair due to its low cellularity, avascular, alymphatic and aneural nature that makes its repair process completely dependent upon diffusion of oxygen and nutrients

from the surrounding tissue (Yokoyama et al. 2005). The current clinical cartilage defects treatment methods are based upon grafting technique that involves three different approaches depending upon the source of graft, namely autograft, allograft or xenograft. Though widely used, each of these practiced methods has disadvantages that limit their application. Autograft involves implanting a tissue from one site of a patient's body to another. In this case, the chances of graft rejection are very less, but it has an inbuilt disadvantage as the patient is already suffering from disease, thus grafting in the same body will be painful and grafted tissues might fail to regenerate after harvest, which is commonly observed in the elderly people (Temenoff and Mikos 2000). Moreover, diversity in the composition of cartilage tissue present in different parts of the body is also a limitation in autograft process. As obtaining the sufficient amount of cartilage tissue from other (healthy) part of the body that possesses exact properties as required to restore the damaged tissue may not be possible (Zhao et al. 2016). Thus, the graft is obtained from sources other than the patient's body by allografting or xenografting approaches. Allograft is a method where the tissue to be grafted is from another person of same species, while a xenograft is taken from different species. Allograft and xenografts suffer from the additional problem of donor scarcity, disease transmission or contamination, compatibility and immune rejection (Cancedda et al. 2003).

Other common reasons for graft failure include infection at the site of graft, shear-force of the body fluids that may disrupt the growth of new blood supply and development of hematoma (a collection of blood) or seroma (a collection of fluid) when the graft is placed over an active bleed area (Hutmacher 2000). In these approaches, there is always a chance that grafted tissue may not work as expected in the patient, which may eventually lead to the incomplete repair of damaged cartilage tissue.

The basis of strategies practised clinically, for the restoration of joint surfaces is to enhance intrinsic healing capacity of subchondral bone through the release of MSCs. This involves procedures such as subchondral drilling, autologous chondrocyte transplant, microfracture, abrasion arthroplasty, electrical and laser stimulation (Chung and Burdick 2008; Kock et al. 2012). In a survey involving 1000 arthroscopies, it has been reported that surgical procedures ideally show success in case of younger patients of age group lesser than 45 years (Hjelle et al. 2002). Moreover, in many cases, the repaired cartilage tissue by these techniques often possesses inferior mechanical properties as compared to native cartilage tissue, and also lacks

structural organization. Thus, to restore the anatomy of native cartilage tissue along with fulfilling functional requirements, a construct generated by tissue engineering has emerged as a promising solution.

1.3.3 Tissue-engineered cartilage construct

A tissue-engineered construct can provide a promising cure to cartilage defects as it includes stem cells, which have self-renewal capability, overcoming the limitation of cell availability and a biomaterial that is mechanically stable to withstand the load and perform biological functions. Thus, tissue engineering enables to develop a cartilage construct that has composition and structure resembling the native cartilage and is capable of restoring joint functionality. The important aspects of cartilage tissue engineering include biomaterials for scaffold fabrication; cell source for chondrocyte regeneration, microenvironment and seeding technique employed for cartilage construct generation. The cartilage tissue comprises of ECM that consists mainly of Col II, proteoglycans and non-collagenous proteins (Stoddart et al. 2009). Thus, the combination of cell and scaffold for making cartilage tissue construct should also support synthesis and deposition of abundant cartilaginous ECM.

1.3.3.1 Cell sources

An important component of tissue renewal is the implantation of cells that have the regenerative capability and do not elicit any immune response. An ideal cell source is one that provides ease of isolation, *in vitro* expansion and capable of abundant ECM synthesis (Kock et al. 2012). For cartilage tissue engineering application, the most studied cell sources are chondrocytes and stem cells.

Chondrocytes

Chondrocytes are the cells found in cartilage tissue that comprises of only 5-10% of the total volume of the tissue. Being less in number, these cells have a high metabolism to maintain the matrix molecules of the tissue, which is essential for its functionality (Yamane et al. 2005). The metabolism of cartilage is mainly anaerobic, due to no vasculature, though the chondrocytes located near to bone are supported by blood supply from the subchondral bone (Wirth and Rudert 1996). The chondrocytes are formed by differentiation of MSCs found in

BM during embryogenesis. During the process of chondrogenic differentiation, the MSCs pass through different stages and finally form chondrocytes. Depending upon the location, these newly formed chondrocytes either produce protein and calcified matrix in the central zone and become hypertrophic to facilitate bone formation, or secrete collagen and other cartilaginous matrix components to produce hyaline cartilage at the periphery (Temenoff and Mikos 2000).

Although the use of autologous chondrocytes will be advantageous for tissue engineering applications but its availability and expansion are always a challenge. The chondrocytes have limited proliferation capacity and with age, their division capability also decreases. When grown in monolayer, these cells lose their phenotype and start dedifferentiating with passaging (Cancedda et al. 2003). The use of adult cells further suffers from regulatory and production issues concerning sterilization, scale up, safety and quality control (Awad et al. 2004). Owing to these limitations with the use of chondrocytes, the research focus has shifted towards the use of stem cells, which have multi lineage potential and can be derived from various sources (Chung and Burdick 2008).

Mesenchymal stem cells

MSCs are multi-potential cells that readily differentiate into cells of mesenchymal origin particularly, bone, cartilage, adipose, and muscle. These cells can also generate cells of other tissue types upon induction by appropriate biological cues in-vitro (Tuan et al. 2003). The most promising factor for use of MSCs in tissue engineering is their immunosuppression and immunoprivileged properties. MSCs are able to terminate the proliferation and functions of immunocytes like T-, B- and NK cells by secreting some soluble factors and thus show immune suppression property (Bartholomew et al. 2002). Due to low expression of major histocompatibility complex-I (MHC I) and MHC II by MSCs, they do not trigger the host allogenic immune cells. Thus, MSCs are considered as immunoprivileged, the property that protects them from the immunological reactions from host tissue upon implantation to the defect site. Although upon differentiation, this immunoprivilege characteristic may get altered, which may then cause immune rejection (Huang et al. 2010).

MSCs can be characterized by the expression of various cluster of differentiation (CD) markers like CD29, CD44, CD73, CD90, CD105, STRO-1, CD106, CD146 and CD166.

Additionally, MSCs are negative for CD11a, CD14, CD19, CD34, CD45 and HLA-DR (Dominici et al. 2006). The primary identification of MSCs relies on their plastic adherence ability and high proliferation potential. The MSCs can withstand freezing temperatures without the loss of proliferation capability on thawing. This eases their preservation process and makes them a promising cell source for tissue engineering applications (Amini et al. 2012).

The MSCs reside in diverse host tissues and can be isolated throughout the life time. While other stem cells can be harvested only during particular time point from their sources, like embryonic stem cells can be obtained only from the blastocyst stage during embryogenesis. Different sources of MSCs are BM, umbilical cord, placenta, adipose tissue, periosteum, synovial membrane, muscle, dental and bone tissue (Hass et al. 2011). BM aspirate is considered as the richest source of MSCs, but its invasive collection procedure results in high-risk of infection. BM-MSCs show high differentiation capability, but their population doubling time is slow. Conversely, MSCs derived in a non-invasive manner from the placenta, dental tissues, and adipose tissues, though possess limited differentiation potential, but they show higher proliferation ability than BM-MSCs (Gimble and Guilak 2003; Hass et al. 2011).

MSCs can also be isolated from different parts of umbilical cord tissue namely blood, matrix, and Wharton's jelly. The most common among these sources is umbilical cord blood (UCB), which is considered as biological waste, and therefore its use does not involve ethical issues (O'Brien et al. 2006). Furthermore, the collection procedure of UCB is non-invasive that makes its usage advantageous compared to BM. The MSCs derived from UCB have shown a lower incidence of post-transplant infections and graft rejection as compared to other sources (Knutsen and Wall 1999). Owing to their chondrogenic differentiation potential and ease of availability, the UCB-derived MSCs can be preferably considered for tissue engineering research for potential therapeutic applications.

1.3.3.2 Potential scaffold biomaterials

Scaffolds are substrates that provide 3D support for growth and proliferation of anchorage-dependent cells to develop an engineered tissue. Cells isolated from various sources can be

grown on the scaffold of a specific composition suitable to allow their differentiation into different cell types *in vitro*. A scaffold provides an analogous structural framework as well as mimics the micro-environment of the tissue that is to be regenerated. An ideal scaffold is expected to show a controlled degradation that is in coordination with the tissue regeneration, allow the nutrient diffusion and removal of metabolites. Additionally, a scaffold should integrate with the surrounding tissue without eliciting an immunogenic response and provide mechanical support to the growing tissue (Chung and Burdick 2008). Appropriate scaffold material selection for a specific tissue engineering application is an important aspect as it should possess surface properties to promote cell proliferation, differentiation, and ECM production, which are vital for cartilage tissue engineering. Numerous synthetic and natural materials have been investigated for use as cell support and delivery agent in cartilage regeneration (Hutmacher 2000; Rawal et al. 2013).

Different types of materials used for scaffold fabrication are polymers, metals, ceramics, and composites. The primary interest has been in the use of polymeric materials, which can be easily molded into different forms like porous, hydrogels and fibrous scaffolds (Izadifar et al. 2012). Many polymers of natural origin are investigated for the potential application as scaffold for cartilage tissue engineering like, collagen, SF, alginate, hyaluronic acid (HA), CS, cellulose, fibrin glue, Ch, gelatin, Gl, agarose, etc. (Chung and Burdick 2008; Rawal et al. 2013). These naturally derived polymers are able to interact with cell surface receptors and indulge themselves in some of the vital regulatory pathways occurring in cells and tissues, making their use advantageous in obtaining a cellular response. A single polymer often does not contain all the desirable properties to be considered for a particular tissue engineering application and thus blends are prepared to combine two or more polymers of natural or synthetic origin. Use of synthetic polymers provides an advantage of tailorable properties but often lacks the direct interaction with cells. Moreover, their degradation by-products are more likely to be toxic and elicit an inflammatory response (Chung and Burdick 2008).

CS is a natural polymer derived from the shell of crustaceans, and possess innate biocompatibility and anti-microbial properties, which make it potential for biomedical applications (Kim et al. 2003). CS is obtained by partial de-acetylation of chitin. It comprises of the linear polysaccharide of D-glucosamine residues linked by β(1→4) linkage, and randomly arranged N-acetyl-glucosamine (Francis Suh and Matthew 2000). The cationic

amino group present in CS interacts with anion groups present in the bacterial cell wall, thereby inhibit biosynthesis of metabolites and disrupt the mass transport across the cell wall that accelerate bacterial death (Hu et al. 2003). CS is non-toxic, biodegradable and can be easily blended with other polymers to suffice the need of a specific application (Martino et al. 2005).

SF is a biopolymer obtained by a degumming method from silkworm cocoon. The common variety of silks are mulberry silk produced by *Bombyx mori* silkworm and non-mulberry silk, which is produced by silkworms of family *Saturniidae*. Mulberry silk possesses unique biological properties like biocompatibility, biodegradability, excellent mechanical strength, permeability to oxygen and water vapour. SF is considered for biomedical applications as it contains a repetitive glycine-alanine-serine sequence, which forms anti-parallel β-sheet structure. This secondary structure is cross-linked through strong inter and intra-molecular hydrogen bonds, which provide elasticity and mechanical strength to SF, making it an adequate choice for cartilage tissue engineering applications (Kundu et al. 2013).

1.3.3.3 Cartilage ECM

The cartilage tissue comprises of a small number of chondrocyte that secrete extensive ECM, containing 60-85% water and rest collagenous and non-collagenous components.

Collagenous matrix

The collagen matrix provides a framework that imparts tensile strength to cartilage tissue and protects it from tear and shear. Different types of collagens present in articular cartilage are collagen types II, VI, IX, and XI (Temenoff and Mikos 2000; Stoddart et al. 2009). Type II accounts for 90-95% of the collagen matrix and contains a high amount of bound carbohydrates, which facilitate binding of water molecules.

Non-collagenous matrix

The non-collagenous component of cartilage matrix comprises of proteoglycans that are made of 95% polysaccharides and 5% protein. The protein at the core binds with glycosaminoglycan (GAG), which is a linear polysaccharide consisting of disaccharide units. These disaccharide units contain repeating hexuronic acid residues (D-glucuronic acid, D-

iduronic acid or D-galactose) or hexosamine (D-glucosamine or D-galactosamine), one of which necessarily contains negatively charged carboxylate or sulfate groups that create an osmotic potential to enable interaction with water (Izadifar et al. 2012). Water binding capacity of proteoglycans provides elasticity and pressure handling ability to cartilage tissue that enables its compression to almost 20% of original volume, making the tissue more capable of withstanding compressive stress. GAGs mainly present in articular cartilage are keratan sulfate, dermatan sulfate, heparan sulfate and Ch (Wirth and Rudert 1996). Proteoglycans present as large aggregates in articular cartilage are called aggregans. This aggregation distributes stress in the tissue and prevents diffusion of proteoglycans out of the matrix. There are small proteoglycans, namely decorin, biglycan and fibromodulin that assist in the organization of collagen matrix (Temenoff and Mikos 2000).

Cartilage tissue damage disrupts its collagen framework causing loss of GAG components (Stoddart et al. 2009). Various researchers have attempted to reform the damaged cartilage ECM using native GAG components in combination with scaffolds, among which the use of Gl and Ch are the most promising for cartilage tissue regeneration (Messier et al. 2007). Gl is an amino-monosaccharide and one of the basic components of the disaccharide units of GAG, that ultimately forms functional proteoglycans present in cartilage matrix (Dodge and Jimenez 2003; Derfoul et al. 2007). It is also a major component of drugs used for the treatment of OA. Oral administration of Gl provides symptomatic relief from OA pain and efficiently prevents joint space loss thus altering disease progression (Pavelka et al. 2002; Chan and Ng 2011). Ch is a GAG component of articular cartilage ECM, made up of disaccharide units of D-glucuronic acid and sulfated N-acetylgalactosamine (Uebelhart et al. 1998). Ch has anti-inflammatory activity and controls the metabolism of cartilage tissue by synthesizing proteoglycans and inhibits proteolytic enzymes (Deal and Moskowitz 1999; Muzzarelli et al. 2012). It is usually administered orally or by intramuscular injection and has recently been utilized as a key component in the matrices combining with collagen, hyaluronic acid, poly(l-lactide), and other polymers, for chondrocytes culture (Gong et al. 2007; Zhang et al. 2011). Ch is present in aggrecan (Acan) molecules that bind to hyaluronan and link proteins to form huge aggregates and provides compressive strength to the tissue (Poole et al. 2002). Depending upon the location of sulfate group usually, two types of Ch are found in articular cartilage. Chondroitin 6-sulfate is mostly found in high amount in adults in superficial layers and serves to maintain the integrity of the tissue, whereas chondroitin 4-

sulfate content is rich in infant cartilage and lies in deep layers where it performs an important role in calcification process (Yokoyama et al. 2005).

1.4 Cell seeding techniques

Cell seeding means suspending cells on the scaffold in such a way that they spread on its surface and proliferate to occupy the maximum possible area. The ultimate aim is to generate a 3D construct, for which it is necessary that the cells infiltrate uniformly into the scaffold so that the neo-tissue develops mimicking the shape of the scaffold (Zhao et al. 2016). The distribution of cells on the scaffolds is largely affected by the seeding technique applied. The seeding methods can be broadly categorized as static seeding and dynamic seeding.

1.4.1 Static seeding

In static seeding, also termed as passive seeding, cells are placed on the top surface of scaffold and allowed to infiltrate under the effect of gravity. Transport of nutrients from the culture media, metabolites, and other macromolecules occurs primarily by diffusion due to concentration gradient (Sikavitsas et al. 2002). It does not involve any mechanical forces, which may damage the cells. The simplicity of process is advantageous as cell viability is not compromised. However, this method results in poor cell infiltration into thick and complex scaffold structures, especially the central areas of scaffolds contain fewer cells. This results in uneven cell distribution affecting construct generation (Solchaga et al. 2006). It is also reported that cells reaching to the interior of scaffolds return towards the superficial layers by chemotactic movement, where the nutrient concentration is comparatively higher. Thus, the low cellular density and limited nutrients supply have shown adverse effects on cell proliferation, ECM production, and differentiation (Vunjak-Novakovic et al. 1998). This limitation can be surmounted by the aid of an external force to facilitate cell infiltration. Different modified methods for improving the efficiency of static seeding use additional forces other than gravitation are- centrifugation, low pressure, and magnetic forces.

1.4.1.1 Centrifugation assisted static seeding

In this method, cell suspension is first laid on the dried scaffold and then centrifugal force is applied to assist the penetration of cells (Dar et al. 2002). The advantages of using

centrifugation with static seeding are better cell insertion and more uniform distribution (Godbey et al. 2004). However, it has disadvantages like difficulty in controlling scaffold orientation during seeding, and the centrifugal forces might show an adverse effect on cell function (Dai et al. 2009).

1.4.1.2 Low pressure assisted static seeding

Dai et al. have demonstrated that the entrapped air in pores of scaffolds prevents cell penetration. Additionally, when this tortuous scaffold is wetted with culture medium, the surface tension developed at air and culture medium interface hinders cell infiltration into scaffold interior. Thus, use of low pressure to remove air from a scaffold during seeding is expected to generate the suction of cells from culture medium towards scaffold pores. In this method, cell loaded scaffolds are placed into sterile desiccators and vacuum is applied to lower the pressure in the chamber to remove air from a scaffold and enhance cell entry into the scaffold (Dai et al. 2009). The ease of use and application of multiple types of porous scaffolds are the advantages provided by this method. However, the possibility of alteration in cell function, differentiation pathway, and genetic mutation are the disadvantages that always exist on the application of pressure during cell culture.

1.4.1.3 Magnet-assisted static seeding

To enhance entry of cells into a porous scaffold, magnetic particles are attached to the desired cell population and magnetic force is applied across the scaffold to physically pull cells into scaffold pores. In this process, the desired cells are characterized by particular surface receptors, and thus separated from a heterogeneous mixture, which is then conjugated to magnetic particles such as supermagnetic iron micro or nano beads. Magnet is placed under the scaffold, and nanoparticle (NP)-conjugated cells are then seeded onto the scaffold. The NP-cells get attracted (pulled) towards the magnet and align themselves inside the scaffold accordingly (Shimizu et al. 2006). The method provides an advantage of increased efficiency of cell seeding on scaffold and selectivity of desired cell type if antibodies conjugated magnetic particles are used. This method can also be utilized to localize cells in a particular area generating the desired pattern for different tissues. The ability to manipulate cells without physical contact is the benefit provided by this method (Sasaki et al. 2008). However, there is a possibility of nonspecific binding of magnetic NP to undesired cells, which may be

disadvantageous. The method depends upon cell and magnetic particle interaction, thus it may completely fail if the cells do not uptake the particles. The force exerted by the magnetic particles may affect cell viability and change levels of gene expression in the target cells (Berry et al. 2004).

These modified static seeding techniques improve the cell loading, but are still not very efficient in terms of cell distribution within the scaffolds. Moreover, there are some disadvantages varying from method to method that make the seeding protocol complex and time-consuming. Thus dynamic seeding methods are used to achieve quantitative loading and a more homogeneous and efficient cell distribution in less time (Solchaga et al. 2006).

1.4.2 Dynamic seeding

Dynamic seeding applies external continuous force via circulating media throughout the culture period, to facilitate cell infiltration into porous scaffolds. This increases the rate of mass transfer and also stimulates biological and mechanical responses of the growing tissue. Different assemblies of culture vessels augment the growth of cells and increase nutrient transport (Pazzano et al. 2000; Mauck et al. 2007). Developing a construct under the dynamic environment *in vitro* provides an advantage of mimicking *in vivo* environment to some extent. This prepares the tissue-engineered construct developed in a dynamic culture condition for better performance and adequate response (Zhao et al. 2016). The culture vessels used for dynamic seeding are termed as bioreactors that provide a sterile controlled environment for cell seeding on the scaffold and construct generation.

1.4.2.1 Bioreactors for cell seeding and culture

Application of bioreactors increases the efficiency of cell seeding, in addition to promoting growth, distribution, and differentiation of cells on scaffolds. These automated systems also provide a large number of construct generation in less time as compared to a static method, with higher productivity and ease of scalability (Temenoff and Mikos 2000). The tissue-engineered construct is generated with the synergistic effect of various forces provided inside a bioreactor system namely, fluid flow, compressive, shear, rotational and magnetic force and hydrostatic pressure. The major advantage is the circulation of media and growth factors that play a key role in cell survival, spatial distribution and provide an appropriate environment

for ECM production thus enhancing differentiation (Mahmoudifar and Doran 2005; Tandon et al. 2013). In a bioreactor, many operational conditions can be controlled according to the requirement like pH, flow rate, temperature and gas pressure, additionally, it could be aided with mechanical forces for stimulating a particular response in engineered tissue (Zhao et al. 2016). Bioreactors are designed into many types according to the application, though an ideal bioreactor fulfils following criteria-

i) Ease of sterilizing and assembling of the parts
ii) Made up of non-toxic materials
iii) The design allows unobstructed flow of media and gases
iv) Designed to avoid contamination
v) Allow controlled changes of different operational parameters
vi) Efficiency in tissue formation in short time span

Many bioreactors have been designed for the culture of cells on scaffolds for tissue engineering purpose and for *in vivo* implantation. Different types of bioreactors used for dynamic seeding are spinner flask, rotating vessel, and perfusion bioreactor.

Spinner flask bioreactor

Spinner flask is a simplest dynamic culture system, in which media is stirred continuously that replenishes nutrients and dilutes metabolites providing a uniform environment throughout the construct (Woodside et al. 1998). This system is readily scalable, simple in design and operation. It consists of a glass vessel of appropriate volume with an impeller in the middle that has attached magnetic bar, which rotates due to magnetic stirrer placed at the bottom. The scaffolds are fixed to needle hanging from the top lid of spinner flask (Sikavitsas et al. 2002). The unidirectional rotation of magnet generates convective force providing a directional cue for cell present in the media to penetrate into the scaffolds. This bioreactor provides a good control of pH and temperature but nutrient and metabolite concentration may change greatly if it is not replenished timely, that lead to decrease cell growth (Woodside et al. 1998). A spinner flask also contains additional ports to allow gas and media exchange and to ensure timely nutrient replenishment (Temenoff and Mikos 2000).

Rotating vessel bioreactor

The rotating vessel bioreactor was designed and developed by Schwarz and colleagues in

1992 at the NASA Johnson Space Center to investigate cell culture under-stimulated microgravity (Schwarz et al. 1992; Freed and Vunjak-Novakovic 1997). This reactor comprises of two concentric cylinders, the inner cylinder is stationary while the outer rotates in a particular axis. The inner cylinder is made up of porous membrane for gas exchange while the outer is non-permeable. Cell-seeded scaffolds are placed in the space between two cylinders that are filled with perfused media. The scaffolds are generally not fixed to any support that makes them fall freely due to the effect of gravity, which is balanced by centrifugal force generated by the rotation of the outer cylinder, creating microgravity like condition (Temenoff and Mikos 2000). This microgravity provides dynamic environment inside the reactor enabling efficient mass transfer and low shear stress. Two design configurations have been proposed, slow turning lateral vessel (STLV) and high aspect ratio vessel (HARV). The prime requirement for this bioreactor is that the scaffolds should have a density equivalent to water and dimensions such that it remains suspended into the free falling state without collapsing to inner vessel. Another problem with the operation of a rotating vessel bioreactor is the high possibility of collision of scaffolds with each other and to the walls of bioreactor that may damage scaffold structure and disrupts seeded cells (Amini et al. 2012).

Perfusion bioreactor

A perfusion bioreactor is the most efficient in terms of cell seeding into scaffolds having complex porous structure. The bioreactor chamber holds cell-seeded scaffolds and is connected with media circulation system, which is driven by a peristaltic pump. The media is continuously perfused through the pores of the 3D scaffold, which facilitates cell infiltration. The flow of media can be adjusted as unidirectional or bidirectional, steady, continuous, oscillating or pulsed as per the requirement. This setup provides efficient mass transport of gases and nutrients throughout the scaffold. The constructs generated in perfusion bioreactors have shown significant improvement in seeding efficiency, cell distribution, viability and greater stimulation for ECM production (Amini et al. 2012). In order to achieve desired benefits, a scaffold is required to possess the shape and size that matches the bioreactor specifications, which is a limiting factor. If the pores of the scaffold are inadequate in size or interconnectivity, it may block media circulation. The equipment is complex and requires accessory connections (peristaltic pump and media reservoir) to complete the setup, which further adds up to its cost thus limiting their widespread use for TE (Dai et al. 2009).

1.5 Factors influencing cartilage construct generation

The property of cartilage construct generated by tissue engineering approach depends upon several factors that may be related to the property of its components or physiological parameters. Scaffold related properties include physical, chemical and biological properties of biomaterials (Rawal et al. 2013). The properties of cells that influence the construct generation are type, source, and age of cells used for seeding on the scaffolds (Stoddart et al. 2009). While the culture condition includes physiological parameters maintained during construct generation (Zhao et al. 2016). Besides these, there are several other factors that administer the success of developed construct, like the method used for scaffold fabrication that determines its architecture, cell seeding density and use of growth factors in the culture media, some of these are discussed below.

1.5.1 Scaffold and its fabrication technique

Scaffolds may be porous or fibrous in nature on the basis of the method used for their fabrication. The fabrication techniques that generate fibrous scaffolds are electrospinning and blowspinning. Electrospinning applies electrostatic forces to produce fibers of nanometer diameter from the polymer solution. This method requires a high voltage power supply, a spinneret (for needle-based electrospinning) or solution reservoir (for needleless or free liquid surface electrospinning) and a grounded collector (Homayoni et al. 2009). Recently, blowspinning or airspraying method is employed for nanofibers formation for tissue engineering application. In this method, the polymer solution is driven by a high pressure usually provided in the form of gas and nanofibers are collected or directly targeted on the required defect site (Tutak et al. 2013; Behrens et al. 2014). The nanofibrous scaffolds are advantageous in mimicking the collagenous matrix structure of cartilage matrix and also provide a larger surface area for cell attachment. The nanofibrous scaffolds provide better tensile strength than porous scaffolds but often lack in compressive strength due to inadequate thickness, which can be improved by using collector of appropriate design to develop 3D scaffold.

The porous scaffold can be prepared by solvent casting, particulate leaching, gas foaming and freeze drying techniques. Solvent casting involves drying of a polymer solution placed in a mould to fabricate a scaffold of the desired shape. Whereas, in particulate leaching, pores are

generated by mixing soluble porogen (salt or sugar) particles in polymer solution and evaporation to obtain scaffold. Porogen is then removed by leaching in a particular solvent, which generates porous scaffold (Hutmacher 2000). In gas foaming, the polymer solution is compressed by applying gas under high pressure, a porous scaffold is obtained when this pressure is released and gas escapes rapidly leaving behind pores (Nazrov et al. 2004). The freeze-drying process involves separation of different phases of polymer solution where solute-rich phase solidifies at freezing temperature and solvent rich phase escapes by lyophilization leaving behind a porous scaffold (Subia et al. 2010). In all these techniques, the pore distribution are mostly irregular that results in varying physical characteristics. The most advantageous method is freeze drying as it does not involve any external chemical agent (porogen or gas) that may alter the scaffold properties and thus does not require additional efforts for their removal.

1.5.2 Cell seeding density

The number of cells seeded initially on scaffolds is an important factor that determines cell distribution, interactions, and ECM secretion. An abruptly higher cell density may cause cell aggregation thereby blocking scaffold pores and inadequate nutrient distribution. Similarly, very low cell density may result in the delayed establishment of cell to cell interconnection that could interrupt differentiation and tissue generation (Chung and Burdick 2008). A sparsely seeded cells also results in an uneven distribution that leaves a space for fibrous tissue growth, which may affect the characteristics of the regenerated construct (Temenoff and Mikos 2000). Thus it is very important to carefully consider the combination of initial seeding density and appropriate seeding technique for the required tissue generation.

1.5.3 Growth factors

Growth factors are the stimulating agents that induce and accelerate cell growth *in vitro* to form cartilage tissue. Soluble factors like transforming growth factor beta (TGF-β), bone morphogenic proteins (BMP), fibroblast growth factor (FGF), insulin-like growth factor (IGF) and insulin were studied for their effects in cartilage tissue engineering. TGF-β1 and TGF-β2 have been proved to regulate cell to cell interactions and hypertrophic differentiation of MSCs, respectively (Kim et al. 2003). BMP-2 and BMP-7 regulate chondrocyte differentiation by upregulating the expression of SRY-related high-mobility group box 9

(Sox9), col II and Acan, thus increasing matrix production. FGF-2 is a mitogen that functions in maintaining proliferation and chondrogenic characteristics of the cells growing in monolayer. IGF-1 induces cartilage type matrix synthesis by increasing production of col II and proteoglycans (Gan and Kandel 2007). These growth factors may be incorporated into the scaffold during fabrication or added to the culture media. While the growth factors supplemented culture media is readily utilized by growing cells, their release from the scaffolds mainly depends on degradation and diffusion properties of scaffold and growth factors respectively (Chung and Burdick 2008).

1.6 Thesis Outline

The present thesis has been organised in six chapters, which are as follows:

Chapter 1 describes the general introduction to the principles and important aspects of tissue engineering. Detail information on the specific aspects like, suitable biomaterial, cell source, ECM components and culture conditions required for developing cartilage construct through tissue engineering approach has been described in this chapter.

Chapter 2 presents an exhaustive literature review on the advancements in cartilage tissue engineering with a focus on different biomaterials and use of hMSCs. Recent advancements in the utilization of SF and CS scaffolds with glucosamine and chondroitin sulfate as possible scaffold components have been discussed. The application of bioreactors for cartilage construct generation has also been described.

Chapter 3 discusses the scope and specific objective of the research work.

Chapter 4 describes the methodology followed to conduct the required experimental study. All the necessary instruments used and protocol followed has been discussed in detail.

Chapter 5: The results and discussion of the experimental work has been presented in the following parts: **Chapter 5A** describes the isolation of hMSCs from UCB and their characterization to determine the purity in cell population for subsequent use. **Chapter 5B** describes the generation of the cell-scaffold construct using hMSCs and SF/CS scaffold in

dynamic culture condition for cartilage tissue engineering. **Chapter 5C** reports the construct generation using glucosamine loaded SF/CS scaffold and hMSCs and its *in vitro* assessment. **Chapter 5D** describes the effect of chondroitin sulfate incorporated SF/CS scaffolds on hMSCs proliferation and differentiation for cartilage construct generation. **Chapter 5E** presents the development of cartilage construct by culturing and differentiating hMSCs over combination of glucosamine and chondroitin sulfate loaded SF/CS scaffolds and comparison of the characteristics of generated construct with pelleted cell aggregates to determine their suitability for cartilage tissue engineering application. The comparison of the properties of the generated construct with the reported cartilage constructs has also been discussed.

Chapter 6 is a summary and conclusion of the present work, describing the important findings of the thesis work. The scope for future work of this research has also been suggested.

Chapter 2

Literature Review

2.1 History of cartilage tissue repair, challenges and treatment measures

In 1743, Hunter observed that the damaged cartilage tissue lacks self-repair mechanism, which was confirmed by Paget in 1853. But it took more than a century to attract the attention of researchers to understand and find alternative means of repair (Wirth and Rudert 1996). Investigations were started with the notion that cartilage tissues in young patients are automatically healed, though a cure is required for the lacerations occurring in elder people. A study in rats, mice, kitten, dog, and rabbits as experimental animals, showed that the chondrocytes present in articular cartilage perform an amitotic activity in young animals, which were absent on their maturity, but did not produce any result on complete repair of cartilage tissue (Elliott 1936). In 1972, experiments were performed in an injured rabbit cartilage showed that even a superficial damage to cartilage tissues in young animals failed to produce enough chondrocytes and matrix for tissue repair (Fuller and Ghadially 1972). Meanwhile, the study on full thickness defects proved that the damage reaching subchondral bone is healed by precursor cells released from BM irrespective of the age of animal (Campbell 1969). These findings initially led to the development of repair techniques involving drilling of subchondral bone to expose pluripotent cells from BM to the defect site with an objective of their transformation to chondrocytes and filling the defect (Ficat et al. 1979; Salter et al. 1980). With time, technique evolved into advanced practices, like marrow stimulation was modified to various forms like osteochondral grafting, which was applied clinically. However, painful surgical intervention, incomplete defect filling and production of fibrous cartilage instead of required hyaline cartilage tissue led to poor results in achieving the native state of tissue (Salter et al. 1980; Wirth and Rudert 1996). Thus, research focus was shifted to TE that emerged as a promising field for the development of substitutes having desirable properties to fill the tissue defect.

Recently, research on TE of cartilage has gained interest among the scientific community. TE approach involves the application of cells on biomaterials to generate cartilage construct. The native cartilage tissue consists of chondrocytes in less than 30% of total volume, whereas remaining mass contains water, collagenous and non-collagenous matrix components (Darling and Athanasiou 2003). The normal cartilage tissue consists of ~9626 chondrocytes/mm^3, and on an average, a single chondrocyte has to maintain the challenging volume of ECM ranging from 104040-160707 μm^3 (Stoddart et al. 2009). During *in vitro* regeneration of tissue-engineered cartilage, although the requirement of a small number of

chondrocytes is comparatively easy to achieve, yet this increases ECM producing responsibility on each cell in order to mimic native tissue composition. Thus, scaffolds are used as a substrate that can be loaded with bioactive molecules to help in ECM generation by chondrocytes in addition to providing structural support (Chung and Burdick 2008). One of the important components required to develop a scaffold is a biocompatible material (biomaterial) that has adequate structural and biological properties to support cartilage tissue regeneration. The biomaterial is seeded with an appropriate cell, which shows potential to differentiate to chondrocytes in a given culture condition (Tuli et al. 2003).

2.2 Biomaterials for cartilage tissue engineering

Numerous biomaterials have been investigated for required properties for cartilage TE application. The first synthetic polymer to be tested as a substrate for cartilage was polyvinyl alcohol (PVA) by Corkhill et al in 1990. PVA was later used in the form of the hydrogel as synthetic articular cartilage by Gu et al in 1998 (Rawal et al. 2013). In 1992, agarose gel was applied as support material for the growth of chondrocytes derived from calf articular cartilage. In a 10 week study, the newly developed tissue was shown to have a similar mechanical property with native articular cartilage. However, the rate of matrix biosynthesis was decreased within a month in the *in vitro* developed tissue (Buschmann et al. 1992). Later, various sets of experiments were performed using different biomaterials as scaffold components for the culture of chondrocytes derived from bovine and human articular and costal cartilage. Polyglycolic acid and polylactic acid (PLA) were used to make fibrous and porous matrices, respectively to demonstrate 3D neocartilage generation (Freed et al. 1993). Though various forms of biomaterials were studied, a highly porous scaffolds structure was reported to be the most desirable scaffold structure for cartilage tissue regeneration, as it retains chondrocytes and helps to reduce donor site morbidity (Temenoff and Mikos 2000). The attention of researchers was attracted towards the use of collagen as a scaffold matrix because of its abundance in native cartilage ECM. The suitability of different types of collagen for the growth of bovine chondrocytes was studied *in vitro* and successful development of matrix collagen network was demonstrated. A remarkable structural similarity with the native cartilage ECM was obtained, though the constructs generated were inferior in biomechanical properties (Riesle et al. 1998). The research for finding a suitable biomaterial was continued with various advancements, from modifying their structure to blending with other polymers to bring the desired characteristics of each to a single platform.

Some of the natural and synthetic potential biomaterials combinations studied recently for cartilage tissue engineering are listed in table 2.1.

Table 2.1 Biomaterial combinations for cartilage tissue engineering application

Biomaterial	**Procedure**	**Summary**	**Reference**
Gelatin-methacrylamide	Hydrogel	Compressive moduli 5–180 kPa. Low viscosity of polymer solution at 37℃ makes it incompatible with many scaffold fabrication process.	(Schuurman et al. 2013)
Alginate and agarose hydrogels Gelatin scaffolds	ADSC seeded on hydrogels and porous scaffold	When hydrogels come in contact with water, they show uncontrolled swelling that may compromise with the structural integrity of the construct. Mechanical and biochemical study demonstrated the stability of porous scaffold structure over hydrogels.	(Awad et al. 2004)
Poly(ethylene glycol)-terephthalate/ poly(butylene terephthalate) PEGT/PBT	Porous scaffolds prepared by compression-moulding/particulate-leaching and 3D fiber deposition were seeded with bovine articular chondrocytes	No observable change reported in the formation of Col II on culturing the cells in scaffolds of different architecture. *In vitro* less cartilaginous ECM formation and no increase in GAG synthesis after 14 days.	(Malda et al. 2005)
Gelatin and PCL	Electrospun scaffolds seeded with swine auricular cartilage and stacked one over another to develop a 3D construct	To provide shape to the construct Ti alloy was used as a support and cultured along with cell-seeded nanofibrous scaffolds. For evaluation, the constructs were stripped off from support damaging the integrity of developed construct. Inferior mechanical property of nano-fibrous scaffolds as compared to natural cartilage. PCL is hydrophobic that is unfavourable for cell attachment and interaction with the hydrophilic environment inside the body. Presence of PCL in the complex structure of the scaffold resulted in slow degradation of the scaffold that hindered homogenous cartilage tissue formation.	(Zheng et al. 2014)

2.2.1 Silk fibroin

SF has been a choice of scaffold biomaterial because of its higher mechanical strength. Being natural in origin, it provides good biocompatibility and bioactivity for the biomedical application (Marolt et al. 2006). The search on potential application of silk for clinical purpose dates back to 1959 when Goldenberg reported its property for use as a suture in surgery (Goldenberg 1959). Since three decades, silk fibroin obtained from *B. mori* has been under extensive study for its properties and application. The compatibility of silk proteins with mammalian fibroblast cells was first reported by studying the suitability of extracted SF over sericin to be used as a matrix material. Besides the presence of arginine-glycine-aspartate (RGD) amino acid sequences, electrostatic interactions between cells and substrate were observed to be responsible for promoting cell attachment (Minoura et al. 1995). Following this discovery, the researchers started considering silk fibroin for its potential use as *in vitro* scaffolds for tissue engineering. Its use in biomedical field started as sutures that got absorbed in the patient's body within 60 days (Altman et al. 2003). Ease of processing into various forms had made it one of the most extensively used polymers for biomedical applications.

Silk was also blended with other proteins, polysaccharides, polymers and inorganic particles to form scaffolds with desired properties for different applications. Human colon adenocarcinoma, lung carcinoma and mouth epidermoid carcinoma cells were cultured on SF coated plates and showed that the growth rate and protein production of cells were comparable with collagen-coated plates (Inouye et al. 1998). In another study, SF films were functionalized with RGD and the cultured Saos-2 (osteoblast-like) cells demonstrated successful mineralization over the scaffolds (Sofia et al. 2001). Following these observations, studies were carried out to demonstrate the osteochondral induction potential of SF based scaffold. The development of load-bearing tissue using SF scaffolds was studied by differentiating BM-derived stem cells to ligaments fibroblasts (Altman et al. 2002). In 2004, Meinel et al. explored the use of RGD coupled freeze-dried silk scaffolds by culturing and differentiating MSCs to chondrocytes. The suitability of scaffolds for cartilage TE application was demonstrated by studying its physicochemical properties. Favourable results were attributed to the high porosity, slow biodegradation, and structural integrity of SF scaffolds (Meinel et al. 2004). In 2005, independent research groups fabricated 3D porous matrices by salt leaching method and studied their physicochemical and biological properties. One group

developed water stable scaffolds and defined superior biocompatibility and biodegradability, which are appropriate for general tissue engineering applications (Kim et al. 2005). Another group of researchers cultured BM-derived hMSCs on porous SF scaffolds and demonstrated successful chondrogenesis (Wang et al. 2005). In 2006, regenerated SF films were linked with dextran and other proteins and studied for potential in drug delivery application (Hofmann et al. 2006). In 2008, the use of 3D porous SF as a substrate for the growth and proliferation of dermal fibroblast cells for tissue engineering applications was demonstrated (Mandal and Kundu 2008). The potentiality of SF as a prospective biomaterial was thus recognized by extensive study over half a century.

2.2.2 Chitosan

Cartilage tissue engineering requires scaffold not only for providing structural support but also expects a biological activity from a biomaterial. CS being cationic in nature is one such biomaterial that facilitates strong ionic interactions with the anionic ECM components and helps in their retention. Since a large number of matrix components found in cartilage tissue are anionic, CS based scaffolds are believed to help in colonization of chondrocytes *in vitro* and also upon implantation (Madihally and Matthew 1999; Yamane et al. 2005). Moreover, a remarkable structural similarity of CS with the proteoglycan components (GAG and HA) of cartilage ECM makes it a preferred biomaterial for cartilage TE (Chandy and Sharma 1990).

The potential of CS as a structural component for tissue engineering was investigated by fabricating CS scaffolds with different morphology (porous and micro carrier gel beads). And the suitability of porous structure was shown in which pore morphology was demonstrated to be an easily controllable feature (Madihally and Matthew 1999). On the other hand, CS also provides good biodegradability and biocompatibility. In 2003, microspheres of CS loaded with TGF-β were prepared and porcine knee chondrocytes were encapsulated to demonstrate the regeneration capacity of damaged articular cartilage (Kim et al. 2003). CS was used as a scaffold in 2005 for cartilage tissue regeneration in the rabbit. CS-HA fibrous scaffolds provided support for the adhesion, proliferation and ECM production for rabbit articular chondrocytes. The observed effect was due to the strong ionic interaction established between the cationic CS and anionic HA and ECM component, which increased the mechanical strength of scaffold as well as facilitated cell adhesion and proliferation (Yamane et al. 2005). Later, in 2009, the physicochemical properties of CS-based hydrogels was studied and

successful encapsulation of bovine chondrocytes was demonstrated (Tan et al. 2009a). Meanwhile, scaffolds were prepared using gelatin-CS-HA and integrated with poly lactide-co-glycolide (PLGA) microspheres to demonstrate its potentiality for cartilage TE application by culturing chondrocytes derived from rabbit ears (Tan et al. 2009b). These studies showed immense potential of CS in cartilage tissue regeneration, which led to further research on searching an adequate combination of scaffolds containing CS. To this end, CS was combined with crosslinking agents like genipin, glutaraldehyde, formaldehyde, etc., to improve degradation rate and mechanical strength of CS scaffolds. The use of crosslinkers was reported to improve biomaterials interaction with cells (Yan et al. 2010). However, crosslinking agents carry chemical groups that often show cytotoxicity and limit their use as a primary component in a scaffold. Thus, blending with other biopolymer is a preferred choice to obtain a scaffold with tailored properties. Recently, CS has been mixed with natural polymers including collagen, agarose and gelatin to fabricate porous scaffold for cartilage TE applications (Yan et al. 2010; Bhat et al. 2011; Bi et al. 2011; Anisha et al. 2013).

2.2.3 SF/CS blend as a potential scaffold

There are limited studies on blending of SF and CS for various TE applications, and even lesser that concentrates on cartilage tissue. In 2005, Gobin et al. first described the possibility of blending SF and CS into a sheet-like structure by freeze drying and studied their structural and mechanical characteristics. Analysis of three different combinations of SF/CS (25:75, 50:50 and 75:25 v/v) was performed, which demonstrated that blend with higher SF content showed higher mechanical strength, while more amount of CS resulted into an increase in water holding capacity (Gobin et al. 2005). In 2008, SF/CS blends were prepared in a different weight ratio to develop porous scaffolds by freeze drying. Besides studying physical properties of the scaffolds, their potential as a tissue-engineered substrate was demonstrated by culturing HepG2 cell lines (She et al. 2008). Another research group studied the interactions of adipose-derived MSCs with SF-CS scaffold that showed short-term cell attachment followed by migration into the 3D matrix. The kinetics of cell migration into scaffold was proven beneficial for implantation of cell-scaffold construct at the tissue repair site that are favourable for reconstructive surgical applications (Altman et al. 2010). These studies strongly supported the probable application of SF/CS blend scaffolds in various TE applications. Based on these studies, the SF/CS scaffolds were applied for cartilage TE (Table 2.2).

Table 2.2 SF/CS-based biomaterials and cell combinations for cartilage tissue engineering

SF: CS	**Method**	**Cells**	**Observation**	**Reference**
1:1	Freeze drying	Human hepatoma cell	Scaffold with porosity >95%, 100-150 µm pore size, controllable mechanical strength, biocompatible. General tissue engineering application	(She et al. 2008)
75:25	Freeze drying	Human adipose MSCs	Cell attachment, migration, infiltration for reconstructive surgical application	(Altman et al. 2010)
	Electro-spinning	Pig iliac endothelial cells	Crosslinking with genipin, glutaraldehyde and ethanol to improve the mechanical property. Characterization by FTIR, SEM and porosity and compatibility study *in vitro* by MTT and *in vivo* in rats proved potential use of genipin crosslinked scaffolds for TE.	(Zhang et al. 2010a)
	Freeze drying	Rabbit chondrocyte	Scaffolds supported cell adhesion, proliferation and GAG accumulation. *In vivo* generated construct showed good mechanical strength with increased deposition of cartilage matrix.	(Zang et al. 2011)
1:1 and 2:1	Freeze drying	Bovine chondrocyte	Scaffolds supported cell attachment, growth, and chondrogenic phenotype indicated by Alcian Blue and Col II/I expression.	(Bhardwaj et al. 2011)
	Freeze drying	Rat BM-MSCs	*In vitro* chondrogenesis of MSC in 3-week culture. SF/CS scaffolds were proven superior to pure SF and CS scaffolds by cell attachment, proliferation, differentiation, histological and immunohistochemical evaluations.	(Bhardwaj and Kundu 2012)
	Gelation	Rabbit chondrocyte	Hydrogels support cell proliferation, viability, GAG and Coll II production maintaining chondrogenic phenotype.	(Mirahmadi et al. 2013)
	Freeze drying	Rat BM-MSCs	Porosity, water absorption, and compressive strength of the scaffold. Cell supportive property by MTT, H&E (hematoxylin and eosin) staining and SEM observation.	(Sun et al. 2014)
1:1, 1:2, 2:1	Freeze drying	Goat chondrocyte	Better retention of Col II and GAG enriched matrix on scaffolds as compared to pure SF. Visco-elastic properties mimicking native cartilage tissue.	(Chameettachal et al. 2015)

2.2.4 Glucosamine and chondroitin sulfate

Glucosamine sulfate is known to resist the progression of OA and hence, is found in the composition of every drug for the same. Its use in clinical therapeutics was first reported in 1980, when it was found that the oral administration of Gl sulfate reduced the symptoms of the disease by two times and helped in rebuilding the damaged cartilage (Drovanti et al. 1980). Importance of sulfate group in the Gl for its role in proteoglycans synthesis was demonstrated by showing a remarkable reduction in GAG synthesis due to depletion of inorganic sulfate (Kraan et al. 1988). A parallel research reported that besides symptomatic relief, Gl also provides structural modifications of the cartilage defect areas (Theodosakis J, Adderly B 1997). Based on this, Deal and Moskowitz defined Gl as a nutraceutical that is applied as a therapeutic agent for the treatment of osteoarthritis. They also described that at physiological pH, Gl remains in a non-ionized form whose 90% is absorbed by the body upon oral administration. The radiolabelling studies performed in rats demonstrated that orally administered Gl absorbed by the body takes 4 h to reach cartilage tissue, where only 8-12% is retained by cartilage tissue. Pharmacokinetics study in dogs showed that the concentration of drug reaching cartilage tissue is five times lower in oral administration than that administered by other means, like intramuscular or intravenous injection. They concluded reason behind this to be the first-pass effect by the liver that metabolizes majority of ingested Gl to water, CO_2 and urea (Deal and Moskowitz 1999).

Later in 2002, by studying joint structure and function changes in human knee OA patients for three years, researchers reported that long-term treatment with Gl sulfate retarded disease progression, and thus demonstrated the possibility of their role in disease modification (Pavelka et al. 2002). Based on the study by Kraan et al., it was further confirmed that Gl is capable of stimulating proteoglycan synthesis as well as modulating Acan levels, which resulted in decreased degradation of proteoglycans that makes Gl a potential candidate for cartilage damage treatments (Dodge and Jimenez 2003). Based on human trials the recommended dose for daily intake of Gl was determined as 1500 mg that was capable to maintain plasma concentration of drug at 10 µM to show its effects in OA treatment (Chan and Ng 2011; Hammad et al. 2015). Their findings were validated and supported in a recent study on efficacy and availability of topically and orally administered Gl. They reported that 10-20% of the orally administered drug reaches articular cartilage, however, when an emulsion was applied locally, the transdermal delivery was about 20% to the joints in human

patients (Hammad et al. 2015). From these observations, it is evident that the administration method plays an important role in determining the availability and action of the drug.

Till date, very little literature is available on the use of Gl in combination with other polymers in tissue-engineered scaffold. In 2006, Hwang et al. added Gl with poly ethylene glycol (PEG)-based hydrogels and used as a scaffold to determine the optimum concentration of Gl beneficial for directing embryonic stem cells towards cartilage formation (Hwang et al. 2006). After a decade, researchers incorporated Gl in gelatin/HA cryogel and demonstrated its effect on structural properties of the scaffold. An increase in porosity of the scaffold on Gl addition was observed, without any change in pore size. Modulation of compressive strength was observed by increasing Gl content in the cryogel. The study was extended by implantation of Gl containing cryogels to cartilage defects in rabbits and demonstrated neocartilage formation, suggesting its suitability for cartilage tissue engineering application (Chen et al. 2016a).

Cartilage tissue damage or disease causes progressive loss of Ch from the tissue matrix, particularly in OA. Different researchers proposed rapid metabolism of Ch in the digestive tract as metabolites were not detected in blood plasma, thus the effectiveness of Ch as an orally administered drug for OA was doubtful (Ghosh et al. 1990; Baici et al. 1992). Nevertheless, subsequent research demonstrated the presence of non-metabolized Ch in plasma and also studied its beneficial effects on treating cartilage defects. Oral administration of Ch as a symptomatic slow-acting drug for the treatment for OA (SYSADOA) was proposed in 1993, following which, research and clinical trials were carried out to determine its effect in disease modification (Howell and Altman 1993). There were also questions regarding the mode of action of oral Ch on diseased cartilage, as symptomatic effects after drug intake were slower than regular analgesics. Later, it was found out that due to high molecular weight, the orally administered Ch is poorly absorbed by blood from the gastrointestinal tract. A study in rabbits demonstrated that the intramuscular injection of Ch led to less proteoglycan loss than orally administrated Ch (Uebelhart et al. 1997). Meanwhile, in an *in vitro* study, an increase in proteoglycan concentration in the ECM of human chondrocytes was observed when Ch added-culture media was used (Bassleer and Malaise 1997). However, with evolution and application of radiological methods in medicine, follow-up of changes occurring in knee joints after drug intake became possible. In 1998, with the

aid of radiographs and computerized image analysis, the ability of orally administered Ch in arresting the progression of knee OA in an animal model, particularly in femorotibial joint space, was demonstrated (Uebelhart et al. 1998). Meanwhile, based on numerous experiments with doses and their beneficial effects, the standard effective amount of Ch administration was defined to be 1200 mg per day (Deal and Moskowitz 1999). The effect of different modes of administration of Ch on cartilage ECM secretion was extensively studied in last decade and the findings from clinical trials demonstrated its benefits, which attracted researchers to pave the way for its application as a scaffold for cartilage tissue engineering (Uebelhart et al. 1998; Simánek et al. 2005; Garnjanagoonchorn et al. 2007).

Ch was first used in combination with PLA where porous scaffold was devised by salt leaching and solvent casting methods. The physical characteristics; porosity, mechanical properties and hydrophilicity of the scaffolds for cartilage TE were investigated (Lee et al. 2006). In 2007, Gong et al. showed the cytocompatibility of Ch incorporated collagen-PLA scaffolds prepared by layer by layer deposition (Gong et al. 2007). The chondrogenic potential of MSCs derived from goat iliac crest was investigated on the hydrogel prepared from Ch and poly ethylene glycol. In a six week study, cell supportive property of the hydrogels was demonstrated showing MSCs aggregation and chondrogenic differentiation by studying GAG, Acan and collagen synthesis (Varghese et al. 2008). In independent research, collagen-Ch-HA hydrogels and freeze-dried scaffolds were prepared and crosslinked with genipin. Ch and HA containing scaffolds were evaluated for *in vitro* compatibility with human chondrocytes and showed their suitability for cartilage regeneration by proteoglycans accumulation. Acan, Col II and cartilage oligomeric matrix protein gene expression by the cells on Ch-HA scaffolds were also demonstrated (Ko et al. 2009). In another research, compressive strength, swelling and *in vitro* degradation properties of the collagen-Ch-HA hydrogels was reported to be enhanced by crosslinking (Zhang et al. 2011). By application of different methods of scaffold fabrication, these studies proved that easy processing ability of Ch marks its widespread application.

The addition of Ch with SF or CS was reported in recent research. The stability of hydrogel consisting of CS and Ch in different pH range was demonstrated and chondrocyte proliferation and ECM formation supporting ability were shown. The CS-Ch hydrogels also prevented collagen degradation, thereby indicated their prospective role in maintaining cell

phenotype (Muzzarelli et al. 2012). In 2013, nano-Ch incorporated CS/HA sponge was developed by lyophilization and showed suitability for wound dressings by various physicochemical and biological characterizations. The porosity, water uptake capacity, swelling ratio and degradation of the sponges were demonstrated to be increasing on nano-Ch addition (Anisha et al. 2013). Later, in 2014, SF-Ch and sodium alginate scaffolds were prepared by lyophilization and obtained highly porous structure was obtained. The improvement in compressive strength of the scaffolds was demonstrated by crosslinking with 1-ethyl-3-(3-dimethylaminopropyl)carbodiimide-ethanol. The cell supportive property studied using rabbit chondrocytes showed improvement in cell attachment and gene expression in the composite scaffold as compared to pure SF scaffold, thereby demonstrated the advantage of this scaffold in TE (Naeimi et al. 2014). In 2015, different researchers added Ch with alginate and SF/gelatin/HA to show the application in cartilage TE (Huang et al. 2015; Sawatjui et al. 2015). Sawatjui et al. evaluated the chondrogenic induction property of freeze-dried SF/gelatin/Ch/HA scaffolds by culturing human BM-MSCs. An enhanced chondrogenic differentiation in composite scaffold as compared to SF scaffold or pellet culture was reported by studying GAG production and up-regulation of chondrogenic genes (Sawatjui et al. 2015). Recently, Ch was added with carboxymethylated pullulan to prepare an injectable hydrogel for the growth of porcine auricular chondrocytes. These hydrogels were also injected subcutaneously into mice, thereby tissue compatibility was demonstrated (Chen et al. 2016b).

2.2.5 Combined effect of glucosamine and chondroitin sulfate

In the incidence of cartilage disease or accidental damage, the severity of defect is reported to be directly proportional to GAG loss (Mankin and Lippiello 1971). The articular cartilage loses elasticity with GAG loss, which increases the problem every time there is movement in joints that further causes wear and tear in the tissue. Early in 1997, Hanson et al. attracted the attention of researchers by defining the expected role of a chondroprotective agent. They stated that the compound should enhance synthesis of macromolecules found in cartilage ECM, like GAGs, nucleic acids, proteoglycans, different types of collagen and other proteins. Meanwhile, the chondroprotective agent should also be capable of inhibiting the enzymes responsible for degradation of cartilage ECM components. These agents are also expected to stimulate the synoviocytes for synthesis of HA, as well as check the deposition of components that may accumulate and block synovial space and blood vessels present in

joints. Studies found that a single drug was unable to perform all these functions, thus the combinatorial use of Gl and Ch was proposed for therapeutic benefits to accomplish the requirements of chondroprotection and chondroregeneration (Hanson et al. 1997). This hypothesis was validated by Lippiello et al. in 2000 when an increased GAG synthesis was shown by the synergistic effect of this combination *in vitro*. A decrease in OA progression in rabbits was demonstrated, which suggested a disease-modifying effect of the mixture of Gl and Ch than using either of these agents alone (Lippiello et al. 2000). The effect of oral administration of Gl, Ch and manganese ascorbate in combination, on the metabolism of articular cartilage in cranial cruciate ligament-deficient dogs was studied by examining the amount of Ch epitopes in synovial fluid. The outcome of Gl-Ch-manganese ascorbate was reflected in 3-5 month period by an elevated concentration of Ch epitopes and GAG in synovial fluid that resulted in structural improvements in articular cartilage (Johnson et al. 2001). In 2003, the response of chondrocytes to Gl-Ch-manganese ascorbate was studied *in vitro*. The bovine cells were cultured under heat, cytokine, compression and matrix depletion stress conditions and effect of drug incorporation was demonstrated to be beneficial in combating chronic stress in cells obtained from aged joints (Lippiello 2003). In 2007, in a randomized study performed on 35 dogs suffering from OA of hips and elbows, an overall improvement in pain, weight-bearing capacity and other clinical conditions was reported. Slow onset of action of Gl/Ch oral administration was reported, but this generated positive symptomatic effect after 70 days (McCarthy et al. 2007). Subsequent studies on human OA patients compared their use in different combination, and demonstrated mixed results on benefits in the treatment of joint space loss as well as providing relief from pain (Sawitzke et al. 2008; Vangsness et al. 2009).

All these reports show the beneficial effects of oral or intravenous administration of Gl and Ch in combination. However, despite *in vitro* preliminary assessment of Gl/Ch on bovine chondrocytes by Lippiello et al. in 2003, there is no report available on their combinatorial study on OA regulation in the form of a scaffold. Furthermore, from these observations, it is hypothesized that direct administration of these drugs to the defect site, as an integral component of the scaffold, would decrease the response time eventually increasing efficacy in OA joint repair.

2.3 Cell sources and application: Chondrocytes and MSCs

Cell source is a very important factor that governs the fate of a tissue-engineered construct. Particularly for cartilage TE application, chondrocytes and MSCs are the most studied and considered as promising sources.

2.3.1 Chondrocytes for cartilage tissue engineering

Chondrocytes are considered as a potential cell source for cartilage TE owing to their niche and functional advantages. Chondrocytes are responsible for maintaining the dynamic metabolism of cartilage matrix that involves ECM production as well as regulation of expression of various inhibitors. Although these cells are excellently skilled in their function but their presence in the native cartilage tissue is very less in number, which becomes a major challenge as sufficient amount is not obtained for clinical use (Chung and Burdick 2008). It was identified as a cell of interest for cartilage tissue engineering applications, and their potentiality was studied by various researchers. In 1999, chondrocytes isolated from bovine were shown to maintain their phenotype in the presence of FGF-2. The cells showed dedifferentiation to primitive cells when cultured in monolayer *in vitro*, but on providing a suitable environment their redifferentiation ability to chondrocytes was also shown (Martin et al. 1999). However, in 2004, a study showed that chondrocytes lose their phenotype and chondrogenic potential in 5-8 passages *in vitro* and move towards apoptosis, which raises concern over their long-term use (Schulze-Tanzil et al. 2004). To assess their application in tissue engineering, in 2006 Goessler et al. performed a series of studies concentrating on different aspects of phenotype maintenance potential of chondrocytes *in vitro*. The expression profile of Col II, III, IV, VIII, IX and XI as well as, TGF β1, β2, β3 and β4 were studied for a period of 21 days in monolayer human septal chondrocytes. Col III, IV, VIII, IX and XI were identified as markers for dedifferentiation of chondrocytes, while Col II was reported to be an important molecule for anabolism of cells. The study concluded that TGF-β3 may assist dedifferentiation of chondrocytes that may trigger other regulatory factors to prepare the cells for future redifferentiation (Goessler et al. 2006a, b).

It was established that dedifferentiation of *in vitro* cultured chondrocytes in the monolayer is unavoidable. However, using other cell sources in combination with providing chondrogenic inducing factors, the problem of limited chondrocyte availability can be addressed. Thus,

researchers started exploring stem cells that may be induced to show chondrocyte like characteristics meanwhile showing unlimited division capability. Considering the mesenchymal lineage of origin of chondrocytes, MSC was first possible candidate that attracted the attention of researchers for exploring their cartilage tissue regeneration capability (Stoddart et al. 2009).

2.3.2 MSCs for cartilage tissue engineering

MSCs were first isolated from BM by Friedenstein et al. in 1976 and termed as clonogenic fibroblast precursor cells. The osteogenic and chondrogenic property of these BM-MSCs was also explored (Friedenstein et al. 1976). Following this study, numerous research was carried out for in-depth analysis of the characteristics of MSCs and their probable application in biomedical field. Although BM-MSCs are considered as the main source of MSCs for research use, the invasive and painful isolation procedure involved as well as significant decrease in cell count and differentiation potential with age encouraged the search for alternative sources. UCB gained the attention as it is a rich source of hemopoietic stem cells, which has been applied for clinical use. Initially, the presence of MSCs in UCB was controversial, but extensive research cleared the doubts. Erices et al. examined the cells harvested from UCB for MSCs like characteristics and termed them mesenchymal progenitor cells (MPC) based on the similarity in phenotype. The study also showed expansion capacity of UCB-MPC that was considered as a beneficial attribute for their therapeutic application (Erices et al. 2000). In 2004, individual reports by different researchers optimized the conditions to improve the quality of MSCs isolation from UCB. A study suggested that a unit of UCB not less than 33 ml should be processed within 15 h of collection for maximum isolation of MSCs. Moreover, the mononuclear cell (MNC) count of 1×10^8 cells was specified to be a crucial parameter for MSCs isolation. The *in vitro* differentiation capability of these cells into mesenchymal lineages was successfully demonstrated by providing specified culture condition (Bieback et al. 2004). The multipotency, specifically chondrogenic potential, of UCB-hMSCs was confirmed by culturing in pellet micromass culture for 3 weeks, followed by histological and molecular examinations of the chondrocytes (Lee et al. 2004). Based on these *in vitro* studies, from their discovery to characterization, the UCB-MSCs was established to be a promising alternative source to the BM-MSCs for the experimental and clinical purpose.

In the subsequent years, the properties of MSCs derived from BM, UCB and adipose tissue were compared in different studies and the highest expansion capability was reported by UCB-MSCs than other two sources (Kern et al. 2006). Following this, a wider classification of MSCs obtained from different tissues namely, BM, adipose tissue, birth-associated tissue (UCB, placenta, umbilical cord and Wharton's jelly) was performed by Hass et al. The isolated MSCs were compared for immunogenicity, proliferation and differentiation capacity under stress condition and showed proliferation capability of MSCs derived from neonatal tissues even under hypoxic conditions. The cells from these sources provide added advantage of harvesting in large quantities as well as in required number representing a promising cell population for application in cartilage TE (Hass et al. 2011).

2.4 Combination of cell and scaffold for cartilage construct generation

The generation of cartilage construct for its application in regenerative medicine requires a well-defined combination of cells and scaffolds. The studies performed using either cells or scaffolds alone suffered from various disadvantages. For example, researchers once considered to apply the scaffolds alone (without cells) onto the cartilage defect site using carbon-based, Dacron and Teflon matrices either alone or supplemented with growth factors to initiate tissue repair. This approach filled the defect site with an exact replica and initiated spontaneous healing capacity of cartilage tissue. However, failures were reported when these matrices were unsuccessful in allowing vascular invasion or hematoma formation thereby altered the complete tissue repair (Hunziker 1999).

Furthermore, the system solely based on cells have reported dedifferentiation of cells in two-dimensional monolayer cultures, producing Col I secreting cell population rather than the required Col II for cartilage regeneration (Temenoff and Mikos 2000). Also, upon implantation into the defect site, the cells fail to remain localized and get carried away by body fluids (Tuli et al. 2003). Owing to these difficulties, scaffolds were employed to host the cells into defect site that helps in the maintenance of cell phenotype in a favourable culture environment.

2.5 Bioreactor for tissue construct generation

For cartilage construct generation and deposition of adequate neocartilage matrix, initial

seeding with higher cell density and achieving a spatially uniform distribution of cells within the scaffold are prerequisite (Freed et al. 1994; Vunjak-Novakovic et al. 1998). Various studies were conducted to find an optimum culture condition that may show a profound effect on the quality of cartilage tissue produced *in vitro*. The cell-scaffold constructs were failing to imitate the native articular cartilage in terms of biological and mechanical properties. Researchers showed that mixing of culture media during cell seeding on the scaffold and subsequent culture enhanced cartilage development as compared to static culture methods (Freed et al. 1994; Freyria et al. 2004). The need of dynamic culture condition in cell growth and distribution was recognized when researchers reported beneficial effects of microgravity for the generation of tissue-engineered construct (Freed and Vunjak-Novakovic 1997).

Bioreactors offer several advantages in comparison to simple static flasks and petridish culture, such as enhanced mass transfer by convective fluid flow, provide mechanical forces that influence tissue development, and control over culture conditions. With a motive to provide the dynamic environment, an orbital shaker was used that maintained stirred suspension culture, to facilitate mixing of media in culture flasks for chondrocytes culture (Freed et al. 1994). These stirred containers were modified to spinner flask bioreactor that was used for cartilage tissue engineering by culturing bovine chondrocytes on a polyglycolic acid scaffold by different researchers. The effect of mixing of culture media on the composition and morphology of tissue-engineered cartilage was studied. The construct developed in spinner flask was superior to static culture in terms of cell number, sGAG and total collagen secretion. The morphology and histological examination revealed elongated cells and predominance of col I in ECM that indicated fibrous cartilage production instead of articular cartilage (Vunjak-Novakovic et al. 1996). Later, using same components and setup, the effect of hydrodynamic environment on tissue-engineered cartilage at different turbulent mixing intensities (80-160 rpm), demonstrated a beneficial effect in terms of maintenance of gaseous (CO_2 and O_2) concentration during the culture that together resulted into higher collagen and GAG synthesis. The ECM deposition remained unaltered at different mixing intensities. However, developed constructs failed to retain the synthesised ECM that may be due to higher turbulence generated, which could be controlled by lowering the mixing intensity (Gooch et al. 2001). Another group used PEG-terephthalate/poly(butylene terephthalate) scaffolds and seeded bovine chondrocytes to generate tissue-engineered cartilage in a spinner flask. The construct showed an increase in GAG/DNA only till 14 days

in vitro, which indicated the need for further optimization of spinner flask operation parameters (Malda et al. 2005).

In 2009, Gigout et al. used spinner flask to generate scaffold-free cartilage construct by culturing chondrocytes aggregate for 7 days in presence of a shear protective agent, Pluronic F-68. The cells in aggregates produced low or no Col I, whereas Col II was highly expressed, thereby, demonstrated convincing results for their use in cartilage repair (Gigout et al. 2009). As stated earlier, chondrocytes de-differentiate *in vitro* that affects the quality of construct and limits long-term use for tissue engineering applications. To address this issue, dynamic culture environment was used as an advantage to redifferentiate the dedifferentiated rabbit chondrocytes. A large amount of redifferentiated cell spheroids was obtained by using spinner flask (Lee et al. 2011). Though aggregates produced in these studies matched chondrogenic phenotype, but it was difficult to obtain a required shape to fill the defect site with 'cells only' system. Also, these cell clusters were fragile and often failed to withstand fluid shear and compressive stress inside the body. Thus, the use of a scaffold was considered that would host cells as well as provide structural support to form the construct.

Researchers modified polyethylene oxide/chitin/CS scaffold with elastin and poly-l-lysine, thereby demonstrated improved adhesion of bovine chondrocytes when cultured in a spinner flask for 4 weeks. Their study showed ample cartilage ECM secretion by cells and suggested the use of elastin and poly-l-lysine as surface activator molecules for biomaterial intended for cartilage tissue engineering application (Kuo and Chung 2012). In continuation, to check the *in vitro* dedifferentiation of cells, rabbit chondrocytes were encapsulated in alginate beads and cultured in spinner flask for 35 days. This resulted into redifferentiation of chondrocytes even at 4^{th} passage stage, but phenotype of cells was inferior that indicated the need of additional growth factors to maintain cells at higher passage stages (Xu et al. 2014). All these studies involved chondrocytes that largely suffer from issues like dedifferentiation and limited division capability. Thus, stem cells that easily differentiate in to chondrocytes were then explored for their behaviour in the dynamic spinner flask environment.

Liu et al. fabricated tubular cartilage grafts using rabbit BM-MSC micro-aggregates and PLGA scaffolds in spinner flask bioreactor with an aim to provide as substitute for tracheal cartilage tissue. In a 4 week study, PLGA was shown to degrade completely leaving behind

the differentiated chondrocytes embedded in a proteoglycan-rich matrix (Liu et al. 2010). Another researcher used ADSCs in suspension culture for the spheroid formation and reported enhanced chondrogenesis *in vitro* and *in vivo* upon implanting subcutaneously in mice. The study proposed that chondrogenic differentiation was attributed by the enhanced cell to cell interaction in spheroids and dynamic environment of spinner flask that also enabled large-scale production (Yoon et al. 2012). In addition, recently Song et al. studied the effect of dynamic environment on chondrogenic differentiation of ADSCs seeded on CS/gelatin hydrogel. The cells adhered to scaffolds showed chondrocyte-like morphology, enhanced function and ECM secretion showing a positive effect of dynamic environment provided in spinner flask bioreactor for chondrogenesis of stem cells (Song et al. 2015).

In recent years, many multifaceted bioreactor systems have been designed with the aim to provide enhanced mass transfer to facilitate growth of cells. TE of human cartilage was investigated by using PGA scaffolds and human chondrocytes in a perfusion bioreactor system. The recirculation method adopted by researchers was shown to stimulate increase in GAG and collagen synthesis, however, Col II levels were significantly lower than the required level for their application in cartilage tissue replacement (Mahmoudifar and Doran 2005). In another study, perfusion bioreactor was used to enhance the accumulation and retention of ECM in a cartilage construct comprising of similar system as stated in earlier study (Shahin and Doran 2011). In another study demonstrating the use of perfusion system for cartilage TE, human chondrocytes were cultured in alginate scaffolds and continuous media circulation was shown beneficial in terms of Acan deposition in cell matrix. Their study showed an overall low GAG retention by the cells in perfusion system. They also indicated the need of optimization of dynamic culture conditions to achieve enhanced ECM accumulation (Grogan et al. 2012). In addition, for cartilage tissue construct generation, researchers designed wavy-walled airlift bioreactor, to enhance mixing at controlled shear stress for *in vitro* chondrocyte culture. In a cells-only system they demonstrated stimulatory effect of hydrodynamic forces on GAG and collagen synthesis by rabbit chondrocytes (Patil et al. 2013). Although, advanced bioreactors have shown their efficiency in one or another aspect for application in cartilage TE, but these are associated with concerns, like requirement of scaffold to be in specific geometry which is the major limiting factor. Spinner flask bioreactor is less expensive than other dynamic systems, and advantageous in terms of ease of operation and scale-up as it does not involve complex machinery.

Chapter 3

Scope and Objectives

Cartilage tissue is prone to damage due to age related degeneration, accidental injury, disease or trauma that may affect any age group. Treatment of cartilage defects is a major challenge because of the limited potential of cartilage tissue for intrinsic repair. Moreover, the existing clinical methods for treating cartilage defect have a number of shortcomings. In this context, cartilage tissue engineering has been evolved as a promising method to treat cartilage defect by developing cartage tissue construct from stem cell and scaffold that can be derived from biopolymers with desired composition mimicking ECM of the damaged cartilage. The success of tissue engineered cartilage construct relies on various factors such as an easily accessible cell source and a 3D scaffold that provides structural support for cell growth and controlled environment thereby facilitates stem cell differentiation to chondrogenic lineage. Though research and development work has been initiated in this field in recent years, a viable cartilage construct is not yet developed that may be used for clinical application. Silk fibroin and chitosan are natural biopolymers and their blend has shown to be potential for tissue engineering application. hMSCs isolated from UCB are considered as promising cell source because of their self-renewal property and inherent chondrogenic differentiation ability. In tissue engineering, *in vitro* culture environment greatly influences the properties of generated construct, which can be well regulated by using a dynamic culture system. Keeping this in mind, the present research has been undertaken to develop cartilage construct by culturing and differentiating hMSCs over SF/CS and their composite scaffolds under dynamic culture condition using spinner flask bioreactor.

Objectives

i. To isolate human mesenchymal stem cells from umbilical cord blood and their expansion

ii. To develop cartilage construct by the culture and differentiation of hMSCs over silk fibroin/chitosan scaffold

iii. To develop cartilage construct by the culture and differentiation of hMSCs over glucosamine improvised silk fibroin/chitosan scaffold

iv. To develop cartilage construct by the culture and differentiation of hMSCs over chondritin sulfate improvised silk fibroin/chitosan scaffold

v. To develop cartilage construct by the culture and differentiation of hMSCs over glucosamine-chondritin sulfate improvised silk fibroin/chitosan scaffold

Scope of the work

1. hMSCs isolation from UCB and *in vitro* expansion

Cells are important component of tissue engineering that grows on scaffold to generate tissue construct. An ideal cell source is thus expected to have regenerative capability and minimum immune response. Additionally, it should provide ease of isolation, *in vitro* expansion and capable of abundant ECM synthesis. MSCs have shown to possess these properties and additionally it shows innate differentiation ability to chondrogenic lineage. MSCs are present in many tissues of the body, however their isolation in adequate amount and obtaining a population with adequate number are the key challenges. Thus, in this part of the study, hMSCs were isolated from UCB, cultured *in vitro* and characterization was done to assess their morphology, immunophenotype and trilineage differentiation ability for further use in cartilage construct generation.

2. Generation of construct by *in vitro* culture of hMSCs over SF/CS scaffold

In TE, 3D biopolymeric scaffold with tailor properties plays important role in supporting cell attachment, proliferation and ECM formation. In this context, the scaffold derived from SF and CS blend is an attractive biomaterial having numerous properties that are desired for TE application. Therefore, this part of the present study shall investigate the suitability of blend of SF and CS as a platform for the recruitment and subsequent differentiation of hMSCs towards the formation of cartilage construct. The success of tissue construct generation greatly depends on the *in vitro* micro environment that facilitates homogenous cell distribution and cell-scaffold interaction, which could be achieved in a suitable bioreactor system. In this context, the dynamic culture condition provides better microenvironment for the cells than static one. Therefore, research work shall further investigate the effect of dynamic culture system using spinner flask as the simplest bioreactor system on culture and differentiation of hMSCs over SF/CS scaffold resulting into the generation of cartilage construct. The generated construct will be assessed by histology, sGAG secretion, immunofluorescence and quantitative polymerase chain reaction (qPCR) analysis.

3. Development of cartilage construct by chondrogenic differentiation of hMSCs over glucosamine loaded SF/CS scaffold

The integrity of cartilage ECM is primarily affected due to damage or disease of cartilage tissue. Therefore, for *in vitro* generation of tissue engineered cartilage construct, there is need of much chondrocyte like ECM formation, which is a great challenge. In this context, Gl is a promising bioactive component, which is a basic GAG unit in chondrocytes ECM. Owing to its stimulatory role in proteoglycan synthesis it has been used in medicines for the treatment of cartilage defects and diseases. However, its role as an integral component of tissue engineered scaffold in promoting chondrogenic differentiation of stem cells has not been studied systematically. Therefore, the present study investigates the effect of the addition of glucosamine in SF/CS scaffolds on the proliferation and differentiation of hMSCs for the development of cartilage construct. In order to examine the possible role of Gl in regulating initial stages of cell-scaffold interaction, the generation of construct shall be studied under both static and dynamic culture conditions. The developed cell-scaffold constructs will be assessed for cell attachment, viability, metabolic activity, proliferation and finally chondrogenic differentiation by histological, sGAG secretion, immunofluorescence and qPCR analysis.

4. Development of cartilage construct by culture and chondrogenic differentiation of hMSCs over Chondroitin sulfate loaded SF/CS scaffold

A tissue engineered cartilage construct is expected not only to promote chondrogenic progression but also to halt tissue degeneration. Ch, a GAG component is found in articular cartilage ECM that exhibits chondrogenesis as well as chondroprotection properties. Ch is thus an interesting bioactive component that has potentiality to be used in scaffold for cartilage construct generation. Using Ch in formulations with different biopolymers, preliminary studies have been performed that demonstrated its regulatory effect on cartilage type matrix production. Considering the beneficial effects of Ch, this part of research work focused on the study of the effect of Ch as a key component in SF/CS scaffolds on the behaviour of hMSCs under static and dynamic culture conditions and its role in accelerating chondrogenic differentiation. The developed construct shall be studied for attachment, viability, metabolic activity and proliferation of hMSCs on SF/CS-Ch scaffolds. Furthermore,

histological, sGAG secretion, immunofluorescence and qPCR analysis shall be performed to evaluate the extent of chondrogenic differentiation and to compare with the pure SF/CS as control scaffold.

5. Development of cartilage construct by chondrogenic differentiation of hMSCs over improvised glucosamine- Chondroitin sulfate loaded SF/CS scaffold

Native cartilage ECM contains Gl and Ch that help the chondrocytes in maintaining anabolism of the cartilage tissue. Due to their advantageous role in cartilage ECM synthesis, Gl and Ch are used in combination as a drug for oral administration in case of cartilage damage treatment. Studies have reported their beneficial effects on chondrocytes or stem cells derived from non-human origin, though very few have demonstrated *in vitro* compatibility with cells of human origin. Furthermore, there is absolutely no published literature that discussed on the cartilage construct generation using the differentiation capability of UCB-hMSCs on SF/CS-glucosamine and SF/CS-chondroitin sulfate, or the combination of all the four components as scaffolds under dynamic culture condition. Therefore, a systematic research work was undertaken to demonstrate the generation of cartilage construct using hMSCs seeded and cultured on SF/CS-Gl-Ch scaffolds. The biocompatibility, sGAG deposition and chondrogenic differentiation ability of the constructs were investigated *in vitro* and the quality of construct was evaluated by comparing the properties with the cell aggregates formed using conventional pellet culture method.

Chapter 4

Materials and Methods

4.1 Materials

4.1.1 Preparation and characterization of scaffold

Chitosan powder of deacetylation degree >90 % was purchased from HiMedia India. *Bombyx mori* silk cocoons were procured from Central Tasar Research and Training Institute, Jharkhand, India. Acetic acid (M 60.05 g/mol), lithium bromide (LiBr), Hexane and sodium carbonate (Na_2CO_3) were obtained from Merck, India. Glucosamine, chondroitin sulfate (extracted from bovine trachea) and lysozyme were purchased from Sigma–Aldrich Company Ltd, USA.

4.1.2 Cell culture study

Ficoll-hypaque, fetal bovine serum (FBS), antibiotic-antimycotic 100x solution (containing 10,000 U Penicillin, 10 mg Streptomycin and 25 µg Amphotericin B per ml in 0.9% normal saline), Triton X100 and RNase free water were purchased from HiMedia, USA. Phosphate buffer saline (PBS) solution, Dulbecco's Modified Eagle Medium (DMEM) and trypsin (0.25%) were obtained from Gibco, USA. Chondrogenic differentiation medium containing high-glucose DMEM supplemented with 1,000 ng/ml BMP-7, 10 ng/ml TGF-β3, 100 nM dexamethasone, 50 µg/ml ascorbate-2-phosphate, 40 µg/ml proline, 100 µg/ml pyruvate, and 1:100 diluted ITS+Premix (6.25 µg/ml insulin, 6.25 µg/ml transferrin, 6.25 ng/ml selenious acid), 1.25 mg/ml bovine serum albumin, and 5.35 mg/ml linoleic acid), osteogenic and adipogenic induction medium were purchased from Stempro, Life technologies, USA. Paraformaldehyde, chloroform, alizarin red, alcian Blue, oil red-O, bisBenzimide DNA quantification fluorescence assay kit and primers for gene sequences were procured from Sigma–Aldrich, USA. Fluorescence dye (phycoerythrin (PE), fluorescein isothiocyanate (FITC), peridinin-chlorophyll-protein complex: cy5.5 (PerCP/cy5.5) and allophycocyanin (APC)) conjugated mouse anti-human antibodies CD73-PE, CD90-APC, CD105-PE, CD34-PE, CD11b-PE, CD79α-APC, CD45-PerCP/cy5.5 and HLA-DR-PerCP/cy5.5 were purchased from Becton Dickenson pharminogen, USA. Calcein-acetoxymethyl ester (AM) dye, ethidium homodimer (EthD-1), Hoechst 33258, phalloidin-FITC and 3-(4,5-Dimethyl-2-thiazolyl)-2,5-diphenyltetrazolium bromide (MTT) reagent were obtained from Invitrogen, USA. Dimethylmethylene blue (DMMB) and papain extraction reagent (PER, containing papain in 0.2 M sodium phosphate buffer, sodium acetate and ethylenediamine tetra acetic acid (EDTA), pH 6.4) were procured from Blyscan, Biocolor Ltd., UK. Anti-Col II antibody,

anti-Acan antibody Alexa Fluor 594 conjugated Goat Anti-Mouse secondary antibody were procured from Abcam, UK. Dimethyl sulfoxide (DMSO), glutaraldehyde, ethanol, phenol, isopropanol were obtained from Merck India Ltd. TRIzol reagent, High capacity cDNA Reverse Transcription kit, and real-time SYBR Green reagent are from Thermo Fisher Scientific Inc.

4.2 Methods

4.2.1 Collection of UCB

50 ml UCB were collected from Ispat General Hospital (IGH), Rourkela, India with prior consent of delivery patient. Commercially available blood collection bag containing 10 ml citrate-phosphate-dextrose-adenine (CPDA) and a buffer consisting of an anticoagulant was used for aseptic transfer of UCB sample to the laboratory for processing. The procedure for UCB collection, hMSCs isolation and culturing followed in our laboratory was approved by the institutional ethical committee [NITRKL/IEC/FORM 2/30-1-2014/06].

4.2.2 Isolation and *in vitro* expansion of hMSCs

hMSCs were isolated from UCB by density gradient centrifugation (Bissoyi and Pramanik 2013). UCB was slowly overlaid on Ficoll-Hypaque in a conical tube in 2:1 v/v ratio and centrifuged at 500 ×g for 20 min. Buffy coat layer formed below the top layer was collected in a separate tube and mixed with an equal volume of PBS. The tubes were incubated for 10 min at room temperature and then centrifuged at 400 ×g for 10 min. The supernatant was discarded and the cell pellet was suspended in DMEM followed by centrifugation at 200 ×g for 10 min to remove the traces of solutions used in earlier steps and other impurities. The obtained cell pellet was resuspended in complete media containing DMEM supplemented with 10% v/v FBS and 1% v/v antibiotic-antimycotic solution. The cell suspension was then plated into culture flasks at the cell density of 1×10^4 cells/cm^3. The cells were cultured under a humidified condition at 37 ℃ and 5% CO_2 with media change in every three days. Non-adherent cells were discarded at the time of media changing and adherent cells were washed with PBS followed by supplementing with freshly prepared complete media. This procedure was followed until the cells attained confluence in culture flask.

The confluent cell population was subcultured by treating culture flasks with 0.25% trypsin-EDTA for 3 min with occasional tapping to disassociate adherent cells. The contents of the flask were collected in a tube and mixed with equal volume of DMEM containing 20% v/v FBS followed by centrifugation at 400 ×g at 37℃ for 5 min. The supernatant was discarded followed by suspending the cell pellet in complete media and plating into culture flasks for further expansion (passaging). The cell suspension of every passage was mixed with 10% v/v DMSO as cryoprotectant in cryo-vial and immediately plunged into liquid nitrogen for preservation.

4.2.3 Characterization of cultured hMSCs

4.2.3.1 Morphology assessment

Change in morphology of the isolated UCB-hMSCs during *in vitro* culture was studied by observing under phase contrast microscope. After washing out unattached cells at the time of media change, images of cells attached to culture flask were captured using a camera (Zeiss Axiovert 40 CFL, USA) inbuilt with the microscope.

4.2.3.2 Immunophenotype study

During culturing of UCB-hMSCs, the expression level of hMSCs specific surface proteins was determined by flow cytometry using FACS Aria III (Becton Dickenson, USA). 1 x 10^6 cells were suspended in 1 ml PBS and incubated with fluorescence dye conjugated with mouse anti-human antibodies CD73-PE, CD90-APC, CD105-PE, CD34-PE, CD11b-PE, CD79α-APC, CD45-PerCP/cy5.5 and HLA-DR-PerCP/cy5.5, in dark for 15 min (Bissoyi and Pramanik 2013). For each sample, 10,000 events were acquired in a flow cytometer and analysed using BD FACS Diva 6.0 software. The un-tagged cell suspension was used as a control for analysis. The characterization was performed at each subculture until the hMSCs population of purity ≥ 95% was achieved.

4.2.3.3 Tri-lineage differentiation assessment

UCB-hMSCs were cultured in osteogenic, chondrogenic and adipogenic induction medium to determine their tri-lineage differentiation capability. 1 x 10^4 cells of 4^{th} passage were seeded in culture dishes containing culture medium supplemented with three different differentiation

media separately. These were incubated under a humidified condition at 37℃ and 5% CO_2 with media change twice in a week. After 21 days, cells were washed with PBS and fixed using 4% paraformaldehyde. The differentiation capability of cells was evaluated by histological staining using alizarin red for osteocytes, alcian blue for chondrocytes and oil red-O for adipocytes, followed by observing under a light microscope equipped with Jenoptik Prog Res CF scan digital camera (Optronics, USA).

4.2.4 Fabrication of porous scaffold

4.2.4.1 Preparation of silk fibroin powder

Bombyx mori silkworm cocoons were cut into small pieces and cleaned well to remove the traces of silkworm and other debris. Degumming of the cocoons was done by boiling with 0.01 M sodium carbonate for 60 min. Sericin was removed by thoroughly washing under running distilled water. The resultant fibres were dried overnight at 45℃ and dissolved in 9.3 M LiBr at 50℃. The silk solution was then transferred to dialysis cassette (slide-A-Lyzer 10K, Thermo Scientific) to remove LiBr residue. Dialysis was performed against distilled water for three days with a water change every 8 h. The dialyzed solution was freeze-dried to obtain SF powder and stored in an airtight container until further use.

4.2.4.2 Preparation of pure SF/CS blends and their composites by adding glucosamine and chondroitin sulfate

SF powder was dissolved in distilled water to form 1 wt% aqueous solution. CS was dissolved in 5% acetic acid/water solution to form 1 wt% homogenous solution (Bhardwaj and Kundu 2011). SF and CS solutions were blended with a ratio of 80:20 v/v (SF/CS) with continuous stirring to make a homogenous solution following the published literature (Vishwanath et al. 2016). Three batches of SF/CS composite biomaterials were prepared by adding Gl and Ch separately and in combination. In the first batch, 1% Gl powder was added to the SF/CS blend (Vishwanath et al. 2017), and the prepared composite was designated as SF/CS-Gl. SF/CS-Ch composite was prepared by mixing 1 wt% Ch powder to the SF/CS blend. Ch loaded SF/CS-Gl polymer composites were prepared by adding Ch in different concentrations (0.5, 1.0 and 1.5 wt%) to SF/CS-Gl solution, which was designated as SF/CS-Gl-$Ch_{0.5}$, SF/CS-Gl-$Ch_{1.0}$ and SF/CS-Gl-$Ch_{1.5}$. The polymer blend and composite solutions

were kept overnight with continuous stirring to form homogeneous mixtures.

4.2.4.3 Preparation of freeze-dried SF/CS blend and composite scaffolds

SF/CS blend, SF/CS-Gl, SF/CS-Ch and SF/CS-Gl-Ch composite solutions poured in plastic petri-plates were lyophilized in a freeze drier (Operon, Bell Technology Ltd., New Zealand) and maintained at -110℃ for 24 h. Porous scaffolds thus formed were stored in 4℃ until further use.

4.2.4.4 Physicochemical and structural characterization of scaffolds

Morphology of freeze dried scaffolds was studied using a scanning electron microscope (SEM, Jeol-JSM6480LV, USA). To prevent charging during imaging, the samples were sputter-coated with gold. ImageJ (USA) software was used to measure pore size of the scaffolds.

The porosity of the scaffolds (1 cm × 1 cm × 1 cm) was measured using liquid displacement method (Bhardwaj and Kundu 2011). The scaffolds were soaked in a measured volume of hexane (V_1) for 5 min. The scaffolds were then pressed to force air out and allow the liquid to penetrate and fill the pores, this total volume was recorded as V_2. The residual volume of hexane after removal of the hexane-impregnated scaffold was recorded as V_3. The porosity (P) of the scaffold was estimated from the following equation as- $P\ (\%) = [(V_1-V_3)/ (V_2-V_3)] \times 100$.

To assess biodegradation, scaffolds were weighed (recorded as initial weight (Wa)) and immersed in phosphate buffer saline (PBS, 0.01 M, pH 7.4) containing 500 U/mL lysozyme enzyme. The solution was changed regularly and weight loss of the scaffolds was determined every week for 28 days, using the following relation- Weight remain (%)= [Wa – Wb/Wa] × 100. Where, Wb is the weight of scaffold at different time interval (Anisha et al. 2013).

The intermolecular interaction between the scaffold components was determined by Fourier Transform Infrared (FTIR) spectroscopy using Spectroscope (IR-Prestige 21, Shimadzu,

Japan). Samples were pelletized with KBr powder using a Hydraulic press. The instrument was operated in transmittance mode in the scanning range 500 to 4000 cm^{-1} and a resolution of 8 cm^{-1}.

4.2.5 Development of tissue-engineered cartilage constructs

4.2.5.1 Cell seeding on scaffolds

Scaffolds were cut into 10 mm × 10 mm × 5 mm pieces and dipped in 70% ethanol overnight for sterilization and washed with PBS for neutralization. The scaffolds were then placed in 12-well plate and conditioned by overnight incubation in complete media. hMSCs suspension with density ~4×10^5 cells/ml were seeded into the scaffold by static method and incubated for 3 h to allow cell attachment. Then complete media was added to cell-seeded scaffolds and incubated at 37℃ under humid condition containing 5% CO_2.

4.2.5.2 Dynamic culture

Cell-seeded scaffolds were fixed in a sterilized needle and hanged inside the spinner flask filled with 300 ml freshly prepared complete media. The spinner flask was then put on the magnetic stirrer with continuous stirring between 20-120 rpm. These were placed inside the incubator set at 37℃ under humid condition and 5% CO_2.

4.2.5.3 Differentiation of UCB-hMSCs to chondrocytes on scaffold

UCB-hMSCs seeded scaffolds (cultured for 7 days) were further cultured in chondrogenic differentiation media for 21 days. The growth media was pipetted out from static and dynamic cultures; cell-seeded scaffolds were washed with PBS and culture vessels were replenished with freshly prepared serum-free chondrogenic medium. Both the culture systems were incubated at 37℃ under humid condition and 5% CO_2 with media change every 3^{rd} and 7^{th} day for static and spinner flask culture respectively. The cell-seeded scaffolds were also cultured under growth media without differentiation media, represented as non-induced cultures, in parallel with the induced cultures under different culture conditions.

4.2.6 Cell aggregation by pellet (Scaffold-free) culture

UCB-hMSCs were cultured in scaffold-free condition by a conventional pellet culture method, to determine the efficiency of the generated cell-scaffold construct by comparing various properties. The cell pellet was formed by centrifugation of ~1 × 10^5 cells/ml at 250 ×g for 5 min in 15 mL centrifuge tubes. The supernatant was discarded, tubes were filled with freshly prepared complete culture media and incubated at 37℃ in a humidified environment and 5% CO_2 with loosened caps to allow gaseous exchange. The cell pellets were cultured for four weeks with media change twice a week without disturbing the pellet. To study chondrogenic differentiation potential, cell pellets after 7 days of culture in growth medium were transferred into the 12-well plates and maintained in chondrogenic medium for next 21 days. The medium was replenished with freshly prepared differentiation media twice in a week. Individual pellets were fixed with 4% paraformaldehyde and sectioned into 0.5 mm slices for characterization.

4.3 *In vitro* characterization of cell-seeded scaffolds and cell aggregates

4.3.1 Cell attachment and morphology

Cell attachment and morphology were monitored during 7 to 14 days of culture using field emission scanning electron microscope (FESEM, Nova NanoSEM 450, FEI). Cell-seeded scaffolds and cell pellets were washed with PBS and fixed using 2.5% glutaraldehyde and incubated at 20℃ overnight. The samples were washed with PBS followed by dehydrating in 35%, 50%, 70%, 90% and 100% ethanol serially keeping for 5 min at each step. Samples were sputter coated with gold and observed under FESEM.

4.3.2 Cell viability and distribution study

The assessment of viable cell population seeded on scaffold as well as in aggregate formed by pellet culture was done for non-fixed samples by fluorescent microscopy. The samples were washed with PBS followed by staining with 1 µM calcein-AM and incubated in dark for 20 min. The calcein stained samples were re-stained with 1 µM EthD-1 and incubated in dark for 5 min. The samples were observed under confocal scanning laser microscope (CSLM, Leica Microsystems, SP8, Germany) to examine live and dead cells.

To quantify viable cell population, the stained samples were treated with 0.05% trypsin-

EDTA solution for 5 min. The supernatant was collected in tubes and fluorescence intensity was recorded at 494 nm excitation and 530 nm emission. Live cells percent was calculated using the equation; [100% × (measured signal - minimum signal)/ (maximum signal – minimum signal)] (Haugland et al. 1994).

Cell distribution onto the interior of the scaffold was studied by counting a number of live cells on a different plane of the confocal images taken at every 625 µm depth. Counting of live cells was performed with ImageJ software. Minimum five different frames were analysed for each plane and represented as a change in cell density on moving from surface to centre of the scaffold.

4.3.3 Metabolic activity

hMSCs seeded scaffolds and cell aggregate were quantified for cellular metabolic activity using MTT assay on 1st, 7th and 14th day of culture. Culture media was removed from the wells and samples were washed with PBS. 5 µl of MTT solution (0.5 mg/ml) was added to the samples and incubated at 37℃ under humid environment and 5% CO_2 for 4 h. Purple formazan crystals were solubilized by adding 200 µl DMSO. The absorbance was recorded at 570 nm in a plate reader (VictorX3, Perkin Elmer, USA) using DMSO as blank (Gini et al. 2016; Rahman et al. 2017).

4.3.4 Cell Proliferation Assay

Cell proliferation was estimated on the 1st, 7th and 14th day of culture by measuring DNA content of the cells using bisBenzimide DNA quantification fluorescence assay kit. The samples were treated with TRIzol reagent to lyse cells. Chloroform was added to the supernatant followed by centrifugation at 12000 ×g for 15 min at 4℃. DNA was isolated from the interphase of phenol-chloroform layer and washed with 70% ethanol followed by centrifugation at 10000 ×g to obtain DNA pellet. The DNA pellet was resuspended in distilled water and equal volume of bisBenzimide H33258 dye solution (0.1 µg/ml) was added followed by incubation in dark for 10 min. Fluorescence was recorded at 360 nm excitation and 460 nm emission in microplate reader (Biotek Synergy H1, India). DNA concentration of the samples was calculated from the standard curve prepared using 1 mg/ml calf thymus DNA (Cai et al. 2015).

4.4 Characterization of tissue-engineered cartilage constructs

4.4.1 Sulfated GAG (sGAG) estimation

sGAG secreted by the chondrocytes in construct was estimated by DMMB assay on 7^{th}, 14^{th} and 21^{st} days of culture. The constructs were treated with 1 ml PER and incubated at 65℃ in a water bath for 3 h followed by 37℃ overnight. sGAG was extracted by centrifugation at 10000 ×g for 10 min. The supernatant was collected in tubes and 1 ml DMMB dye was added followed by incubation for 30 min at room temperature. The tubes were centrifuged at 12000 ×g for 10 min. sGAG was precipitated along with DMMD dye at the bottom of tubes. 0.5 ml dissociation reagent was added to each pellet followed by vortexing that released the bound dye forming a clear light blue solution. Optical density was recorded at 656 nm using UV-Visible spectrophotometer (Double beam 2203, Systronics, India). A standard curve was prepared using chondroitin-4-sulfate. Since the presence of Ch in scaffolds may interfere with the results, sGAG content of constructs generated with Ch containing scaffolds was normalized by subtracting optical density of scaffolds without cells.

4.4.2 Histology study

The cell-scaffold constructs and cell aggregates prepared by pellet culture were assessed by histological analysis using alcian blue. The cells were fixed using 4% paraformaldehyde and 1% (w/v) alcian blue stain prepared in 3% acetic acid was added followed by incubation for 30 min at room temperature (Xu et al. 2014). The samples were washed with distilled water to remove the unbound stain and observed under light microscope. Total GAG content was quantified by estimating the extent of proteoglycan staining. The alcian blue stain was aspirated from samples and manoxol IB was added followed by incubation for 30 min. Finally, the optical density was recorded at 480 nm using plate reader.

4.4.3 Immunofluorescence study

The hMSCs seeded scaffolds and cell aggregate formed by pellet culture were analysed by immunofluorescence staining to detect antibody expression after 21 days of culture in chondrogenic differentiation medium. Samples were fixed with 4% paraformaldehyde for 20 min, washed in PBS and incubated in 0.1% Triton X100 at room temperature for 3 min. After washing with PBS, each sample was incubated with anti-Col II and anti-Acan antibodies for

12 h at 4 ℃. The samples were washed thoroughly with PBS to remove unbound primary antibody. Alexa fluor 594 conjugated goat anti-mouse secondary antibody was added to the samples and incubated in dark for 45 min at room temperature. The primary and secondary antibodies were used in 1:200 dilution prepared using PBS. After washing unbound secondary antibody, the samples were counter stained with FITC conjugated phalloidin, followed by incubation in dark for 30 min and Hoechst 33258 for 5 min. The samples were then visualized under CSLM.

4.4.4 Quantitative PCR (qPCR) analysis

qPCR analysis was performed to study the expression profile of hMSCs and chondrocyte-specific genes during the 21 days of chondrogenic differentiation of hMSCs seeded scaffolds and cell aggregate by pellet culture. The process of qPCR for estimation of gene expression involved 3 major steps, namely- total RNA isolation, reverse transcription (RT) of isolated RNA to complementary DNA (cDNA) and gene amplification.

4.4.4.1 Total RNA isolation

The cell-scaffold constructs and aggregate formed by pellet culture were acquired from their respective culture systems and placed in 24 well plates. Growth media was carefully removed from every well and 1 ml TRIzol reagent was added followed by incubation for 10 min to allow cell lysis. Supernatant from each sample was collected in separate tubes and 0.2 ml chloroform was added to separate nucleotide contents of the sample in different phases. The tubes were vigorously shaken for 15 s and incubated at room temperature for 2 min followed by centrifugation at 12000 ×g for 15 min at 4 ℃. The content of the tubes were separated into different layers, with RNA remaining exclusively in upper clear aqueous phase. The upper layer was collected into a separate tube and 0.5 ml isopropanol was added followed by incubation at room temperature for 10 min. RNA precipitate was obtained by centrifuging at 12000 ×g for 10 min at 4 ℃. RNA precipitate was washed with 75% ethanol and air dried. The isolated RNA was resuspended in RNase free water and placed in PCR 96-well plate.

4.4.4.2 Reverse transcription of isolated RNA to cDNA

The isolated total RNA was reverse transcribed with high capacity cDNA RT kit. RT master

mix was prepared by mixing RT buffer, dNTP, random primers, reverse transcriptase enzyme and nuclease-free water. RT master mix was added in equal volume to each well containing RNA and plate was sealed. The plate was placed in a thermal cycler and RT was performed with following program setting- Step 1: 25℃/10 min, step 2: 37℃/120 min, step 3: 85℃/5 min. The reverse transcribed cDNA products were stored at 4℃ until further use.

4.4.4.3 Gene amplification

Reverse transcribed cDNA products were amplified for genes Col I, Sox9, matrilin 3 (MATN3), Col II, and Acan using 7500 Fast Real-Time PCR system (Applied Biosystems, Thermo Fisher Scientific). SYBR Green reagent was used for the detection of PCR products during amplification. All the primers used in this study were purchased from Sigma Aldrich (sequence mentioned in Table 4.1). qPCR reaction mixture was prepared by adding nuclease-free water, SYBR green reagent, primers and cDNA for each gene in a separate well of PCR 96-well plate followed by placing the plate in thermal-cycler. The PCR protocol comprised of the following steps- an initial denaturation step set at 95℃ for 10 min followed by amplification for 45 cycles (94℃ for 30 s, 62℃ for 30 s, and 72℃ for 30 s). β-actin was used as an internal control for all the genes. Fold change of each target gene relative to their expression in hMSCs was calculated by $2^{-\Delta\Delta Ct}$ method (Xu et al. 2014; Lal et al. 2017).

Table 4.1 Gene sequences of the primers used for q-PCR analysis

Gene	**Forward sequence 5'- 3'**	**Reverse sequence 5'- 3'**
β-actin	TTCCAGCCCTCCTTCCTG	GCCCGACTCGTCATACTCC
Col I	GACCTCTCTCCTCTGAAACC	AACTGCTTTGTGCTTTGGG
SOX 9	GACTTCCGCGACGTGGAC	GTTGGGCGGCAGGTACTG
MATN3	CATGTTCAGCCACTGAGGAA	CAGAATGAATTAAAAATGGCAATG
Col II	CCGCCTTTGCTGGCTTAGGCCCG	ACCATTGATGGTTTCTCCAAACC
Acan	TGCAGGTGACCATGGCC	CGGTAATGGAACACAACCCCT

4.5 Statistical analysis

The statistical significance between data sets was calculated using two way ANOVA analysis. Data were taken to be significant when a *p*-value of 0.05 or less was obtained (showing a 95% confidence limit).

Chapter 5

Results and Discussion

Chapter 5A

Isolation, culture and characterization of hMSCs

Mesenchymal stem cells (MSCs) are considered as a promising cell source for tissue engineering including cartilage tissue regeneration due to its inherent potentiality to transform into different cells of connective tissue lineage (Dominici et al. 2006). MSCs can be isolated from various tissues like bone marrow (BM) and adipose, but their use is associated with invasive collection procedure and risk of infections to the donor (Majumdar et al. 2000; Hass et al. 2011). Therefore, umbilical cord blood (UCB) is a potential source because it is easily available as biological waste and involves non-invasive collection procedure. Although, there are contradictory reports relating to the frequency of MSCs in UCB, many successful studies have confirmed their substantial presence in UCB (Jin et al. 2013). Moreover, UCB is reported to host a more primitive cell population than other sources, thus MSCs isolated from UCB are expected to show higher proliferation and differentiation ability (Lee et al. 2004; Chang et al. 2016). The results of various studies have shown that UCB MSCs have higher population doubling and show less senescence than other sources. The reported mean population doubling of hMSCs for UCB, Wharton's Jelly (WJ), BM and adipose derived stem cells are 30 h, 24 h, 40 h, and 45.2 h respectively (Peng et al. 2008; Jin et al. 2013). Therefore, MSCs isolated from UCB was used in the present study.

UCB contains heterogeneous cell population including prevalent hematopoietic stem cells, so it is necessary to characterize the isolated cells for MSCs like properties before their use for cartilage tissue engineering. The mesenchymal and tissue stem cell committee of the International Society for Cellular Therapy (ISCT) defines MSCs as the cells that are plastic-adherent in standard culture conditions, express CD105, CD73 and CD90, and lacks the expression of CD45, CD34, CD14 or CD11b, CD79α or CD19, and HLA-DR. In addition, MSCs must essentially show differentiation potential to osteoblasts, adipocytes, and chondrocytes *in vitro* (Dominici et al. 2006; Rojewski et al. 2008). During isolation process, mononuclear cells (MNCs) present in UCB appear in the interphase of ficoll-hypaque mediated density gradient centrifugation. These MNCs comprises of mixed cell population, and can be expanded *in vitro* to achieve a purified population of MSCs (Xu and Lu 2016). The procedure of UCB-hMSCs isolation and maintenance was already established in our laboratory (Bissoyi and Pramanik 2013). However, the phenotype, proliferation and differentiation potential of cells may vary with different passage. Thus, for this thesis work, the isolation of hMSCs was repeated taking the fresh batch of UCB and entire procedure was followed that comprised of culture, characterization, expansion and differentiation.

Therefore, in this part of research, hMSCs was isolated from UCB and their morphology was assessed by microscopy and purity was studied by immunophenotype expression. The *in vitro* differentiation ability of the isolated cell was also assessed. The experimental result and discussion are described here-

5.1.1 Isolation and culture of MNCs

Density gradient centrifugation using ficoll-hypaque was performed to isolate MNCs from UCB. The MNCs were obtained from the buffy layer (density 1.077 g/cm^3) formed between plasma and ficoll-hypaque layer, whereas, granulocytes including erythrocytes were deposited at the bottom of centrifuge tube. The isolated MNCs include MSCs and hematopoietic stem cells along with other blood cells (Chang et al. 2016). MSCs were obtained based upon their distinguishing plastic-adherence property by culturing the MNCs in fibronectin-coated tissue culture flasks (Tarson) (Dominici et al. 2006). Non-adherent cells were removed by washing with PBS after 24 h of culture, and adherent cell population was expanded by replenishing the culture medium regularly. Cells adhered to the flasks were further characterized for MSCs like morphology and phenotype (Bissoyi and Pramanik 2013).

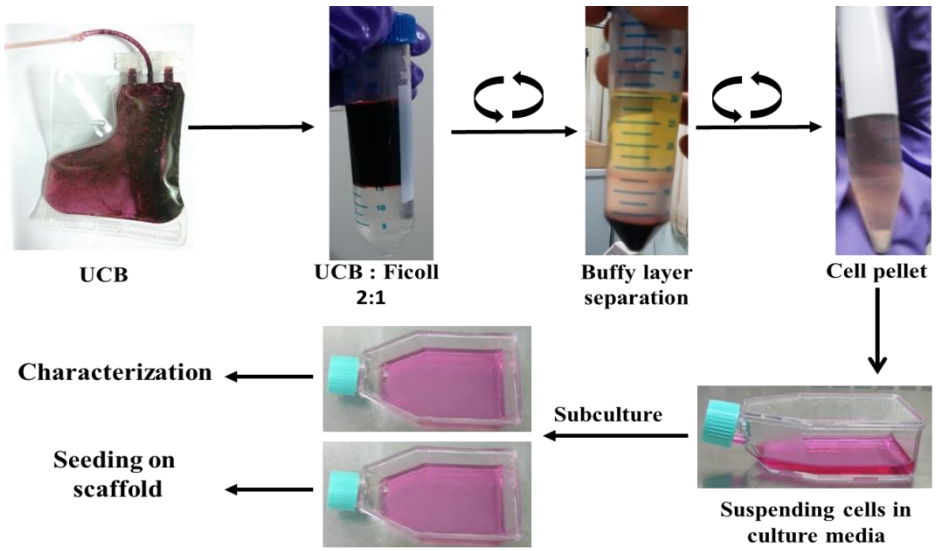

Figure 5.1.1 Schematic representation of hMSCs isolation from UCB by Ficoll-hypaque mediated density gradient centrifugation. The MNCs were collected from buffy layer by centrifugation in the form of cell pellet and cultured to obtain MSCs.

5.1.2 Cell morphology study

The isolated MNCs were regularly observed for their attachment to the culture flask and

change in morphology during the culture period to determine the attainment of MSCs population in the culture (Campbell and Pei 2012). On the first day, all the cells were round and appeared floating in the culture media (Figure 5.1.2A). After 24 hours some of the cells were observed to be attached to the culture flask. On 6th day, maximum population of round cells became elongated (Figure 5.1.2B). Cells were dividing rapidly occupying the available flask surface, as evident from increase in cell population on 12th day of culture (Figure 5.1.2C). The cells showed continuous division, and confluence was achieved on 18th day (Figure 5.1.2D) of culture.

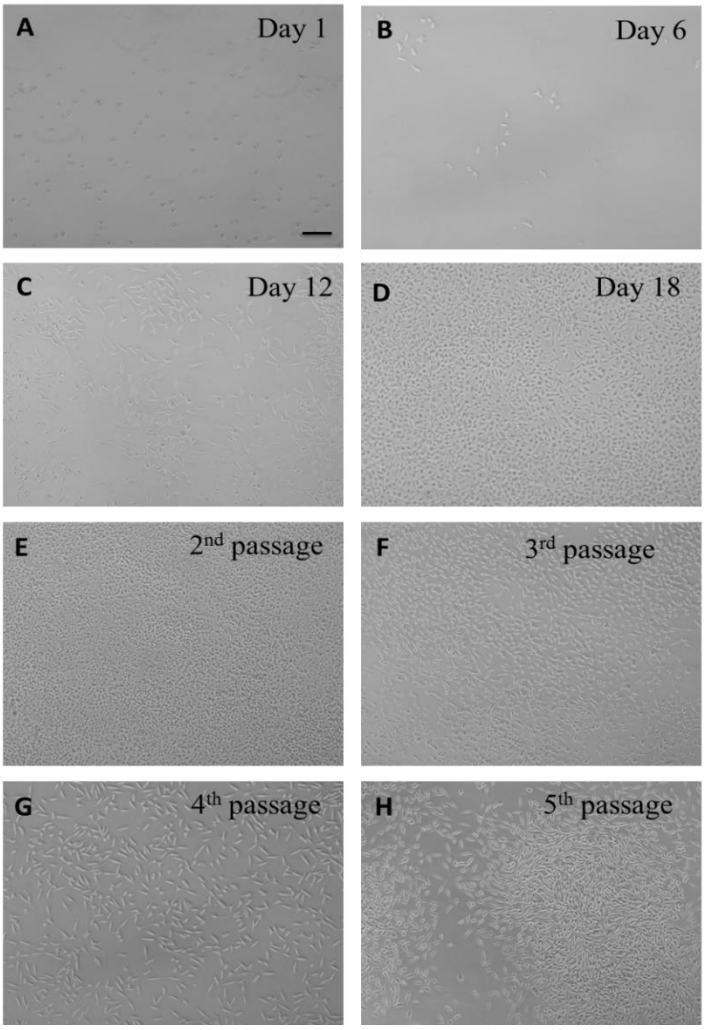

Figure 5.1.2 Phase contrast micrographs of MNCs derived from UCB on (A) 1st day showing round morphology. Fibroblast like morphology shown by cells on (B) 6th day, (C) 12th day and confluence achieved on (D) 18th day. Change in cell morphology with (E) 2nd, (F) 3rd, (G) 4th and (H) 5th passage stage showing colony formation. Scale bar = 100 µm

Change in cell morphology was also evident during subculture. Cells of 1st to 3rd passage stages were less elongated and spread over more area in available surface of culture flask

than cells of the subsequent passages. The cells attained bipolar fibroblast-like morphology, which is the characteristic of MSCs, at 4th passage stage (Figure 5.1.1E-G). The colony formation was observed in culture flasks with cell of 5th passage (Figure 5.1.1H). The cell colonies appeared denser in middle region and cells at periphery of colonies showed elongated morphology.

5.1.3 Immunophenotype characterization of cultured cells

The UCB derived hMSCs were characterized by flow cytometry to assess the cell surface marker expression thereby determining the change in cell phenotype during each passage. It was observed that 78% of cells were expressing CD73, while 81% and 74% expressions for CD90 and CD105 as showed by 2nd passage cells (Table 5.1). The expression of CD73, CD90 and CD105 increased during the progress of culture, with 84%, 89% and 82% expression, respectively at 3rd passage that reached to ≥ 95% at 4th passage. Thus, representing the attainment of MSCs phenotype by majority of cell population (Dominici et al. 2006; Alvarez-Viejo et al. 2013). Whereas, the expression of CD34 (hematopoietic marker), CD45 (pan-leucocyte marker), CD11b (marker for macrophage lineage), and CD79α (lymphoid cells marker) (Lai et al. 2000; Takahashi et al. 2003; Cajander et al. 2016) was decreasing with the progress of the passage attaining 22%, 25%, 7% and 11% expression, respectively at 2nd passage, and their expression decreased remarkably to 16%, 8%, 5% and 3.9% at 3rd passage, respectively. A further decrease in expression was observed at 4th passage that was 1.1% for CD34, 1.2% for CD45, 3% for CD11b and 2.6% for CD79α (Figure 5.1.3). Whereas, HLA-DR (monocyte marker) expression was comparatively less than that observed in the initial stage, with ≤ 1% cells expressing during the culture. The expression of HLA-DR corroborates with the published report stating that the biomarker remains supressed in MSCs unless stimulated by some immunological factors (Dominici et al. 2006). During initial passage, a larger population of cells expressed (> 20%) CD34 and CD45 due to the presence of hematopoietic stem cells (Alvarez-Viejo et al. 2013). UCB is well known to host hematopoietic stem cells that express many markers including CD45, CD34 and CD11b (Abreu et al. 2013; Chang et al. 2016). The decrease in cell population expressing CD34, CD45, CD11b, CD79α and HLA-DR with subsequent passage along with an increase in cell population showing higher expression of CD73, CD90 and CD105 was observed. At 4th passage stage, the majority (> 95%) of cells showed the expression of CD73, CD90 and CD105. The cells of 5th passage stage did not show further increase in the expression of these

markers. A decrease in proliferation ability of MSCs with increase in passage stage was also reported elsewhere (Lo Surdo and Bauer 2012; Chen et al. 2014; Ullah et al. 2015). Thus, the cells obtained at 4th passage stage were considered for further *in vitro* studies.

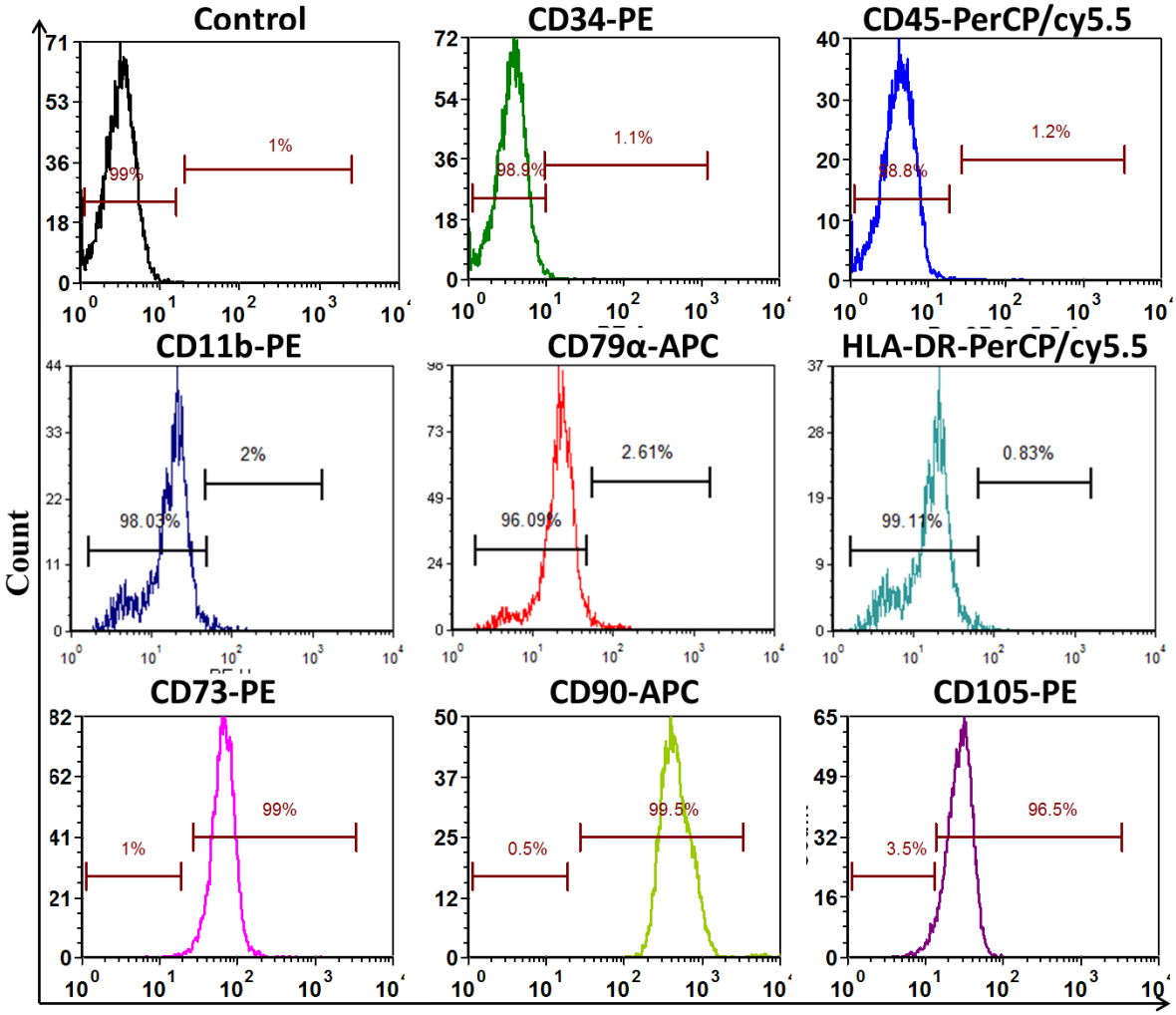

Figure 5.1.3 Surface marker expression profile of hMSCs by Flow cytometry, obtained at 4th passage. As indicated 99% cell population expressing CD73, 99.5% CD90 and 96.5% CD105, with only 1.1% population expressing CD34, 1.2% CD45, 2% CD11b, 2.6% CD79α and 0.83% HLA-DR.

Table 5.1 Expression of cell surface marker by flow cytometry analysis

Passage Stage		**2nd**	**3rd**	**4th**	**5th**
POSITIVE MARKERS	CD73	78%	84%	99%	99%
	CD90	81%	89%	99.5%	99%
	CD105	74%	82%	96.5%	96%
NEGATIVE MARKERS	CD34	22%	16%	1.1%	1%
	CD45	25%	8%	1.2%	1.2%
	CD11b	7%	5%	2%	2%

	CD79α	11%	3.95%	2.61%	2.6%
	HLA-DR	0.9%	0.7%	0.83%	0.81%

5.1.4 Tri-lineage differentiation potential

The ability of differentiation into specified lineage also helps in identifying MSCs. MSCs have self-renewal property and ability to differentiate into the cells of connective tissue of the mesoderm, namely, bone, cartilage, and fat (Lee et al. 2004). To assess this tri-lineage differentiation potential of the isolated UCB-hMSCs, histological analysis was performed. Figure 5.1.4D, E and F show culture dishes where staining was performed after culturing cells in osteogenic, chondrogenic and adipogenic media respectively, for 21 days.

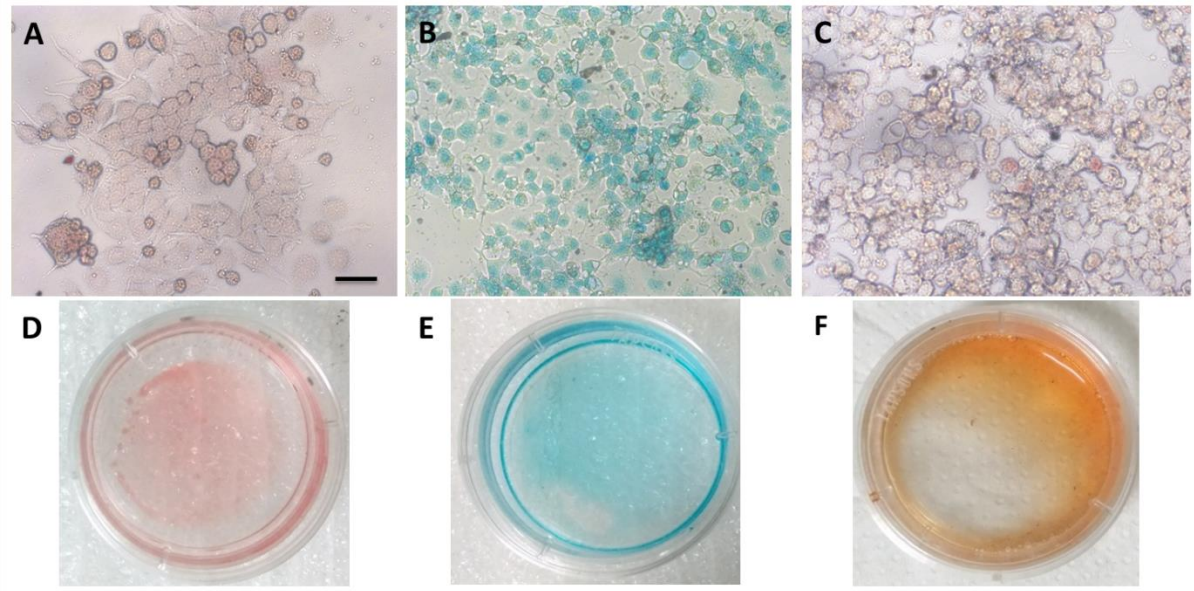

Figure 5.1.4 Light microscopy images showing trilineage differentiation potential of hMSCs assessed by (A and D) alizarin red staining for osteocytes, (B and E) alcian blue staining for chondrocytes and (C and F) oil red O staining for adipocytes. hMSCs derived from UCB has shown differentiation ability to osteocytes, chondrocytes and adipocytes. Scale bar= 50 µm

Osteoblasts are the cells that produce a mineralized matrix, mainly comprising of calcium ions, indicating the initial stages of osteogenesis that intensifies with time leading to bone tissue formation. Alizarin red forms a complex with calcium deposits and produces red coloration in cell matrix. Figure 5.1.4A shows the cell matrix stained with alizarin red, depicting osteogenic differentiation. Alcian blue is a dye that binds to the proteoglycan chains of the chondrocyte matrix. Figure 5.1.4B shows deep blue staining of cells with alcian blue dye depicting the chondrocyte cell population. Oil red-O is a fat-soluble pigment that is

widely used to detect the presence of fat and lipids in the tissue sections (Kern et al. 2006). Figure 5.1.4C shows larger cells with fat droplets stained with oil red O, representing the presence of adipocytes. Thus, this study has demonstrated that hMSCs isolated from UCB possesses differentiation ability to osteocytes, chondrocytes and adipocytes.

Conclusion

In this part of the study, MNCs were successfully isolated from UCB by Ficoll-Hypaque mediated density gradient centrifugation, and cultured to obtain MSCs. The elongated morphology and immunophenotype assessment for the expression of CD73, CD90, CD105, CD34, CD45, CD11b, CD79α and HLA-DR, determined the pure population of hMSCs obtained at 4^{th} passage and similar observation was made with 5^{th} passage cells. The derived MSCs showed successful *in vitro* differentiation into osteocytes, chondrocytes and adipocytes, the characteristic mesenchymal lineage, thereby further confirming the isolated cells are MSCs. Earlier studies have reported the reliability of using a single cell source (UCB) for chondrogenesis, as variations were not observed in the characteristics of MSCs harvested from UCB in different batches and volumes that offers the use of isolated cells for long period (Erices et al. 2000; Bieback et al. 2004). However, further investigation is needed for studying the differentiation potential of these cells on the scaffold to determine their efficiency towards cartilage tissue engineering, which is the main focus of the present research. Thus, the isolated UCB-hMSCs of 4^{th} passage were used to study their chondrogenic differentiation on SF/CS based porous scaffolds for cartilage construct generation.

Chapter 5B

Development of cell-scaffold construct by culturing and differentiating hMSCs over SF/CS scaffold

In the past decade, various combinations of SF and CS blend have been studied as a potential scaffold biomaterial for different tissue engineering applications, including cartilage tissue engineering. SF/CS scaffolds have been shown to support the proliferation of cells isolated from varied sources like BM, ADSCs, hepatoma and endothelial cells. However, their chondrogenic potential was not assessed (She et al. 2008; Altman et al. 2010; Zhang et al. 2010a; Bhardwaj and Kundu 2012; Deng et al. 2013; Li et al. 2017). In previous study in our laboratory, SF/CS porous scaffold with a ratio of 80:20 (v/v) was developed and proven to provide a suitable platform for cartilage tissue engineering applications (Vishwanath et al. 2016). So, in this part of work, attempt has been made to culture and differentiate UCB-hMSCs on SF/CS scaffolds for developing cartilage construct.

The success of generation of cartilage construct greatly depends on *in vitro* culture environment. The static culture using petri-plate or tissue flask essentially involving 2D culture is widely used. However, this method might result in poor infiltration of cell into thick and complex scaffold structures, causing an uneven cell distribution that affects construct generation (Solchaga et al. 2006). In this context, dynamic culture using bioreactors are advantageous offering uniform environment throughout the construct and efficient mass transfer (Tandon et al. 2013). The spinner flask bioreactor is less expensive than other dynamic culture systems like perfusion bioreactor and advantageous in terms of ease of operation and scale-up without involving complex machinery. Previous studies have reported the suitability of spinner flask bioreactor in maintaining differentiated state of chodrocytes (Gigout et al. 2009) and study on the chondrogenic differentiation potential of ADSCs and rabbit BM-MSCs (Liu et al. 2010; Yoon et al. 2012; Song et al. 2015).

In the present study, culture and differentiation of UCB-hMSCs over the SF/CS (80:20) scaffolds has been studied under dynamic culture condition using spinner flask bioreactor and the result was compared with static culture (Figure 5.2.1). The cell supportive property of scaffold under different culture condition was determined by FESEM, cell viability, MTT and DNA quantification study. The differentiation potential of hMSCs on SF/CS scaffolds was assessed by histological staining, total sGAG synthesis, fluorescence staining and qPCR study. The result and discussion of these experimental studies is presented in this chapter.

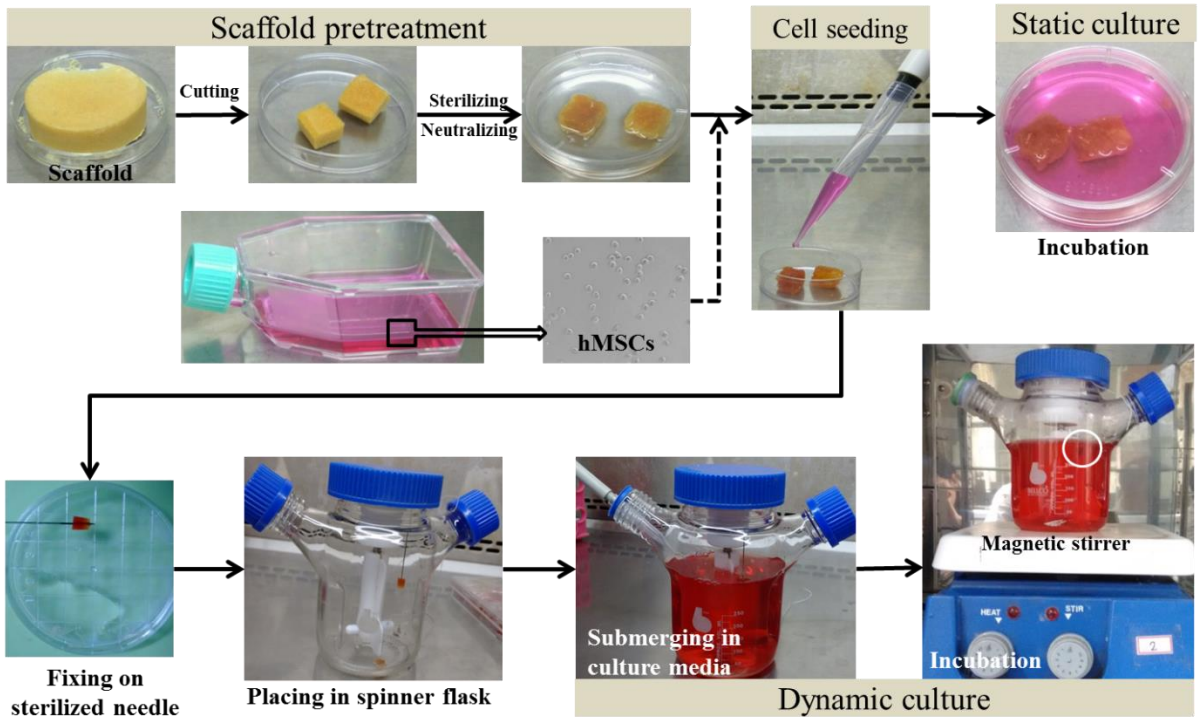

Figure 5.2.1 Schematic representation of construct development. The pretreated scaffolds were seeded with UCB derived hMSCs to culture under static condition and fixed in the needle then placed in spinner flask bioreactor and maintained under dynamic condition.

5.2.1 Preparation and physicochemical characterization of SF/CS scaffold

The freeze-dried SF/CS (80:20 v/v) porous scaffold possesses physicochemical properties desired for TE applications. The scaffold possess open pore microstructure with pore size in the range of 64-190 µm (transverse section) with elongated pores as evident by longitudinal section (Figure 5.2.2A and B), 84.28% porosity, hydrophilicity (49.9˚ contact angle) and controlled degradation rate with 13.36% weight loss when studied for 28 days.

The intermolecular interaction between SF and CS in the scaffold was determined by FTIR analysis. The characteristic peak for amide I bond was observed at 1634.56 cm^{-1} in both SF and SF/CS scaffold (Figure 5.2.2C). The intensity of peak for β-sheet structure at 1620.27 cm^{-1} present in SF was stronger in SF/CS scaffold indicating an increase in β-sheet chains in the scaffold resulting from enhanced intermolecular interaction. The band for glycine-alanine-glycine linkage was present in SF at 997.87 cm^{-1} and appeared as weak shoulder in the scaffold (Lu et al. 2007). The amide II band of amino group was observed at 1657 cm^{-1} in CS and scaffold. The characteristic –CH deformation peak was present at 1425 cm^{-1} in CS with a slight shift to 1434.57 cm^{-1} in SF/CS scaffold. Whereas, $–CH_3$ deformation was found

at 1381 cm^{-1} in the scaffold as well as in CS. The small peak at 898.92 cm^{-1} represented saccharine structure which was absent in SF/CS scaffold (Zhang and Cui 2012).

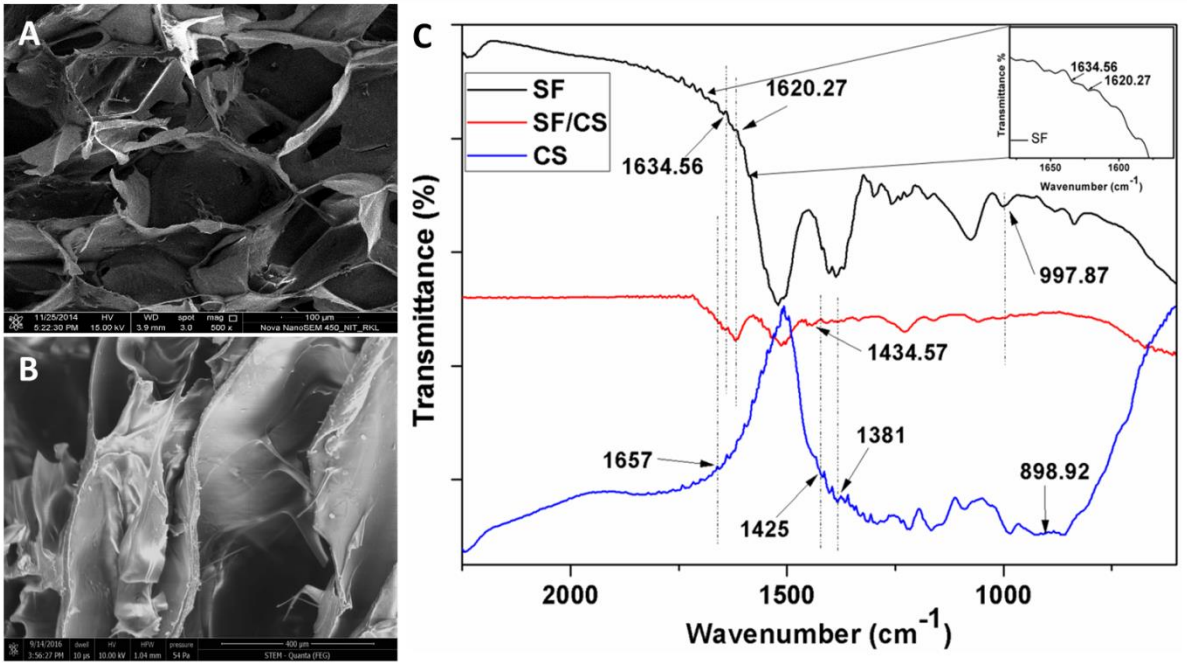

Figure 5.2.2 Physicochemical characterization of SF/CS scaffold. FESEM micrographs representing (A) transverse and (B) longitudinal sections of the scaffold. (C) FTIR spectra of SF, CS powder and SF/CS blend scaffold representing intermolecular interaction.

5.2.2 Assessment of cell-scaffold constructs

5.2.2.1 Cell attachment, morphology and spreading

hMSCs seeded SF/CS scaffolds cultured in static and dynamic culture (spinner flask) systems were observed under FESEM for studying the change in cell morphology, attachment and spreading on the scaffold surface. The rotational speed has a great influence in maintaining homogeneous culture and cell-scaffold interaction (Gooch et al. 2001; Darling and Athanasiou 2003; Wang et al. 2003; Gigout et al. 2009; Liu et al. 2010; Lee et al. 2011; Yoon et al. 2012; Song et al. 2015). Therefore, culture experiment for 7 day was conducted at varying rotational speed from 20 to 120 rpm to maximize cell attachment to the available scaffold surface with uniform spatial distribution.

FESEM (Figure 5.2.3) analysis revealed the variation in extent of cell attachment and spreading over scaffolds with stirrer speed. With increase in stirrer speed from 20 to 60 rpm,

an improvement in cell attachment to the scaffold was observed, which was later decreased at higher 80-120 rpm. As indicated in figure 5.2.3C, very few cells were attached to the pore walls of scaffold at lower mixing intensity of 20 rpm that was comparable with the static culture, where cells were observed to be attached to the edges of pore walls (Figure 5.2.3B). The less mixing intensity (lower rpm) may not be adequate enough to generate sufficient fluid shear for cell-scaffold interaction, thereby resulted in lower attachment and inferior distribution of cells. Similar observation was reported in a study where the attachment of fibroblasts were limited to the scaffold surface at 20 rpm, whereas cell attachment and spreading were improved at higher rpm (Wang et al. 2003). A higher attachment and spreading of cells on the scaffold surface were achieved in this study, with higher intensity at 40 and 60 rpm (Figure 5.2.3D and E). In comparison, more number of cells was observed to be infiltrated into the pores and spread over the entire scaffold surface with well-connected network formation at 60 rpm than at 40 rpm. There was no improvement in cell attachment and its distribution with further increase in rotational speed.

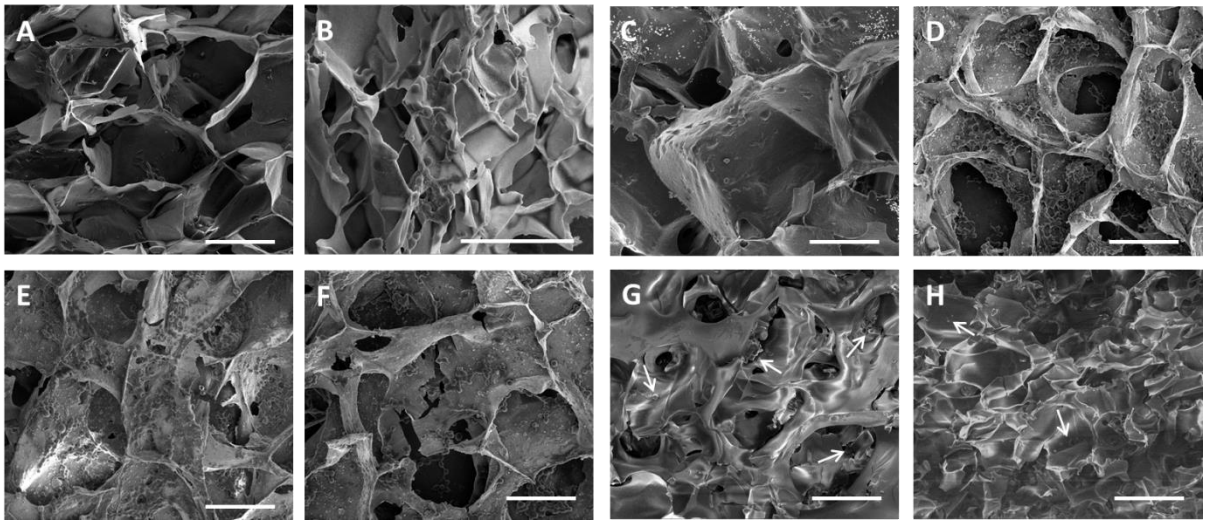

Figure 5.2.3 FESEM micrographs representing (A) porous structure of SF/CS scaffold, (B) hMSCs seeded scaffold maintained in static condition and (C-H) dynamic condition with different stirrer speed operating at (C) 20 rpm, (D) 40 rpm, (E) 60 rpm, (F) 80 rpm, (G) 100 rpm and (H) 120 rpm. Scale bar= 100µm. White arrows in G and H indicate cells attached to scaffolds. Maximum cells were retained on the scaffold at 60 rpm with no observable damage to the scaffold structure.

The rotational speed also had a great impact on the structural integrity of the scaffold. The scaffold structure was intact at 20-60 rpm, which was deteriorated with further increase in rpm. As indicated in figure 5.2.3F, at 80 rpm, the disruption of the scaffold pore wall started to occur, which further ruptured on increasing rpm to 100 (Figure 5.2.3G). The scaffold pore

walls were collapsed that resulted in complete closure of the pores at 120 rpm (Figure 5.2.3H)

Based on these observations, the culturing of cell-seeded SF/CS scaffolds was further extended upto 14 days under dynamic culture condition at 60 rpm. In both static (Figure 5.2.4B) and dynamic conditions (Figure 5.2.4C), the cell population was observed to increase on 14th day along with spreading and occupying available surface on the scaffold. However, the population of cells attached to the scaffold surface was higher in spinner flask than static culture system. This observation can be attributed to the effect of continuous flow of media in spinner flask bioreactor that resulted in cell spreading and distribution of nutrients essential for various cellular activities, ultimately leading to better results than the static culture (Gooch et al. 2001). Figure 5.2.4A represents the change in cell morphology from spindle shape in culture dish to round on attachment to the scaffold.

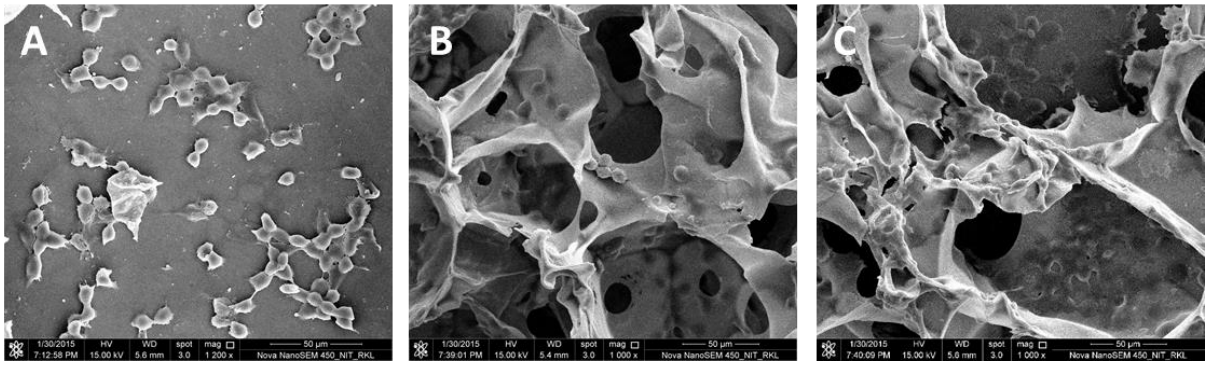

Figure 5.2.4 FESEM micrograph of hMSCs attachment on (A) culture dish and SF/CS scaffolds cultured under (B) static and (C) dynamic condition on 14th day, showing higher cell attachment and spreading on the scaffold in dynamic culture.

5.2.2.2 Cell viability and distribution assessment

Maintaining viable cell population and proper spatial distribution are important phenomenon particularly for chondrogenesis of hMSCs as upon differentiation they start losing division capability, which affects 3D construct generation (Solchaga et al. 2006). The cell viability on SF/CS porous scaffolds was assessed by staining with calcein-AM/EthD-1 and quantified by fluorescence intensity analysis. FESEM analysis of cell-seeded scaffolds cultured for 7 days under different mixing intensities (20-120 rpm) showed that 60 rpm is the most favourable so far as cell spreading and attachment are concerned. This observation was further validated to

assess their impact on cell viability by culturing hMSCs seeded scaffolds under 20-120 rpm for 7 days (Figure 5.2.5). The spreading of the green fluorescent live cell observed at static culture and 20 rpm were similar (Figure 5.2.5A and B, respectively). At 40 and 60 rpm, the number of live cells was more than other mixing intensities, with slight difference among the two (Figure 5.2.5C and D). At 40 rpm, the cells occurred individually whereas at 60 rpm small cell colonies were observed in some regions, which is in accordance with earlier observations, where 60 rpm showed higher live cell percentage and colonization (Wang et al. 2003; Malda et al. 2005; Gigout et al. 2009). There was a decline in live cell population on further increase in rotation speed to 80-120 rpm (Figure 5.2.5E-G), which may be due to the higher fluid shear that resulted into collapsed pores thereby obstruction in cell entry and spreading. A similar result was also revealed by fluorescence intensity analysis showing an increase in live cell population with increase in rotation speed to 60 rpm, and thereafter a decline in trend was observed (Figure 5.2.5H).

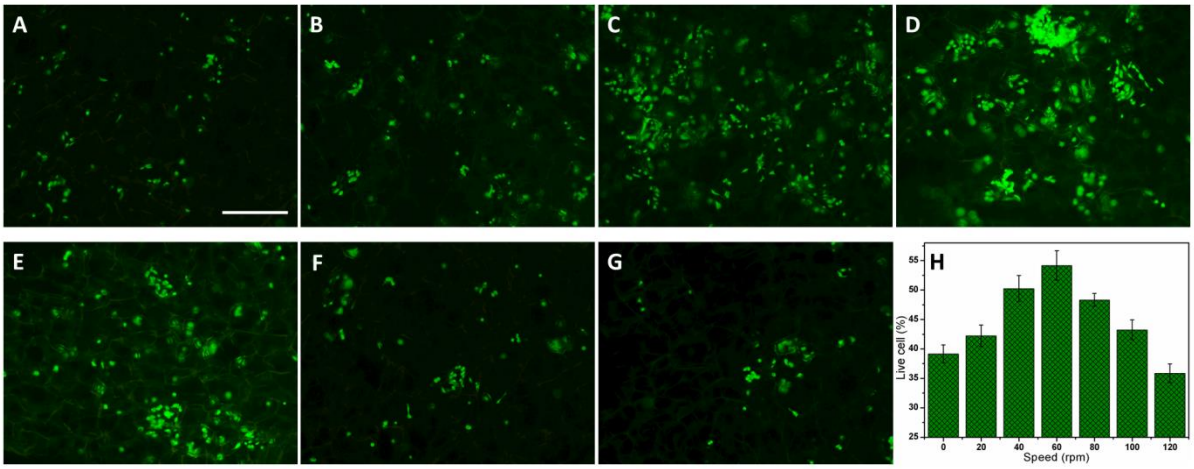

Figure 5.2.5 Calcein staining of hMSCs showing green fluorescence on SF/CS scaffold cultured for 7 days in (A) static condition and dynamic condition with different stirrer speed at (B) 20 rpm, (C) 40 rpm, (D) 60 rpm, (E) 80 rpm, (F) 100 rpm and (G) 120 rpm. Scale bar= 100µm. (H) Live cell % calculated by intensity analysis showing maximum viable cell population at 60 rpm.

The result of fluorescence analysis of live cells was in good agreement with the FESEM observation, where maximum cells were attached to the scaffold surface at 60 rpm. Thus, based on FESEM and fluorescence analysis, 60 rpm was found to be the most favorable in providing adequate dynamic environment for hMSCs attachment, spreading and viability maintenance on the scaffold, and hence used for further experiment.

On 14th day of culture, the SF/CS scaffolds were largely covered with green fluorescent hMSCs. In dynamic culture (Figure 5.2.6B), cell colonies were observed to be denser as compared to static culture (Figure 5.2.6A). The side view of the cell-seeded scaffold further showed more number of green fluorescent cell infiltrated into the depth of scaffold when cultured in spinner flask bioreactor (Figure 5.2.6D) as compared to static one (Figure 5.2.6C).

The cell viability was further quantified by fluorescence intensity analysis, which proved the efficiency of spinner flask bioreactor in supporting hMSCs proliferation (Figure 5.2.6E) over static culture. On 7th day, the percentage of live cells growing on scaffolds in spinner flask bioreactor was 54.16±2.4, while a significantly lower ($p < 0.05$) value of 39.16±1.4% was obtained in static culture. A significant difference ($p < 0.05$) in live cell population was observed on 14th day between two culture systems, with higher cell viability achieved using spinner flask (62±3.3%) than static culture (48 ± 2.2%).

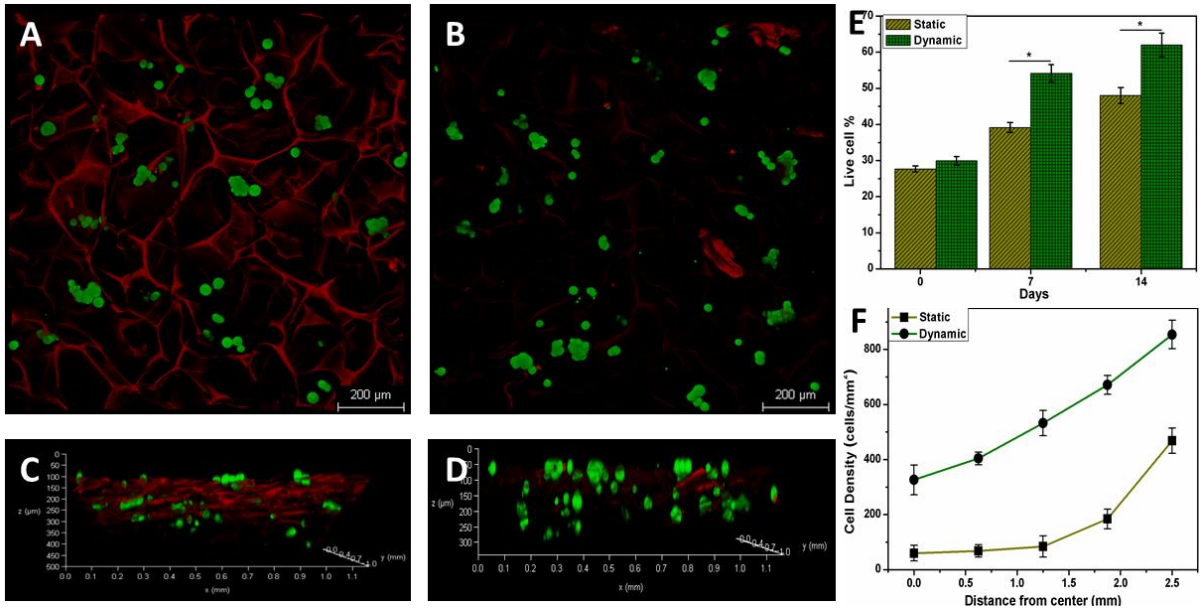

Figure 5.2.6 Fluorescence images of hMSCs seeded SF/CS scaffolds showing live cells stained green and dead cells stained red on 14th day cultured in (A and C) static and (B and D) dynamic condition (scale bar= 200 µm). (C and D) Side view of images A and B showing cell infiltration. (E) Bar graph showing live cell percentage by intensity analysis (n=3, *$p < 0.05$). (F) Cell distribution as a function of distance from centre of construct. hMSCs-seeded SF/CS scaffold cultured under dynamic condition showed homogenous cell distribution and higher viability than in static condition.

The calculation of vertical cell distribution by measuring area-normalized cell number as a function of depth of the scaffold, showed greater overall cell density in dynamic culture

(Figure 5.2.6F). In spinner flask system, a gradual decrease in cell density was observed, however, it dropped rapidly in static system with increase in distance from the surface. In static culture, a substantial difference ($p < 0.05$) in cell infiltration was observed within 0.625 mm depth, where only 184±36 cells/mm^2 were observed as compared to 468±46 cells/mm^2 on the scaffold surface. However, in spinner flask culture, there were 671±34 cells/mm^2 at 0.625 mm depth from the surface, where cell density was measured as 854±52 cells/mm^2. The drop in cell density on moving from scaffold surface to the core was insignificant in dynamic culture system. A significant difference ($p < 0.05$) was observed at the centre where dynamic culture showed 543% more cells per mm^2 (326±54 v/s 60±28 cells/mm^2) than the static culture. As evident from this analysis, majority of the cells were confined to upper area, in static culture. On contrary, in dynamic culture cell distribution was observed to be more uniform and penetrated till the core of construct, depicting the efficiency of spinner flask bioreactor in providing directional cue for cell infiltration into complex porous structure of the scaffold and homogenous dispersion.

5.2.2.3 Metabolic activity

The constructs prepared for clinical application should be able to maintain the natural processes occurring in cells (Bhardwaj and Kundu 2011). The maintenance of cellular metabolic activity during culture is one of the important natural processes. So, hMSCs seeded SF/CS scaffolds, cultured under static and dynamic conditions were analysed for cell metabolic activity by MTT assay. MTT is a colorimetric analysis, which indicates the presence of metabolically active cells, based on the ability of mitochondrial dehydrogenase enzyme to metabolise yellow tetrazolium salt to purple formazan crystals. The amount of formazan product indicates the number of metabolically active viable cells (Riss et al. 2016). The metabolic activity of hMSCs was found to increase with incubation time, and higher activity was shown by cell-seeded scaffold cultured under spinner flask bioreactor at every point of observation during the culture period under study (Figure 5.2.7A). A significant difference ($p < 0.05$) in absorbance was observed on 7th and 14th day between the static and dynamic systems, further showing the superiority of spinner flask bioreactor in supporting and maintaining cell metabolic activity. This higher efficiency may due to the 3D dynamic culture environment provided in spinner flask bioreactor that promoted comparatively quicker adaptation of cells to the culture environment as compared to the static culture (Xu et al. 2014).

5.2.2.4 DNA quantification

Cell viability was further assessed by DNA quantification of hMSCs by bisBenzimide assay using Hoechst 33258 dye. The dye binds to AT sequence in minor groove of double stranded DNA (dsDNA) and emits fluorescence at 460 nm, which is the direct indicator of the amount of DNA present in the test sample. The result shown in figure 5.2.7B reveals that the total amount of DNA was increased with the progress of the entire 21 days culture period both in static and dynamic culture system but with a varied degree of DNA content. In static system, the DNA content showed a linear increase till 14 days after which, it became stable. However, a higher DNA content was observed with dynamic culture system on 7th day (113±4 ng/ml) than static culture (27.86±2.75 ng/ml) with significant difference ($p < 0.01$). The maximum DNA content of the cells growing in spinner flask was measured as 137±6 ng/ml, whereas only 82±8 ng/ml was obtained with static culture on 21st day. The results indicate that although the cell proliferation slowed down after initial increment shown till 7th day, but it was continuous and significantly higher ($p < 0.05$) under the spinner-flask bioreactor as observed on 21st day. This result can be correlated with the cell distribution study, where more number of cells were obtained in the construct formed in dynamic culture that resulted in overall higher DNA content.

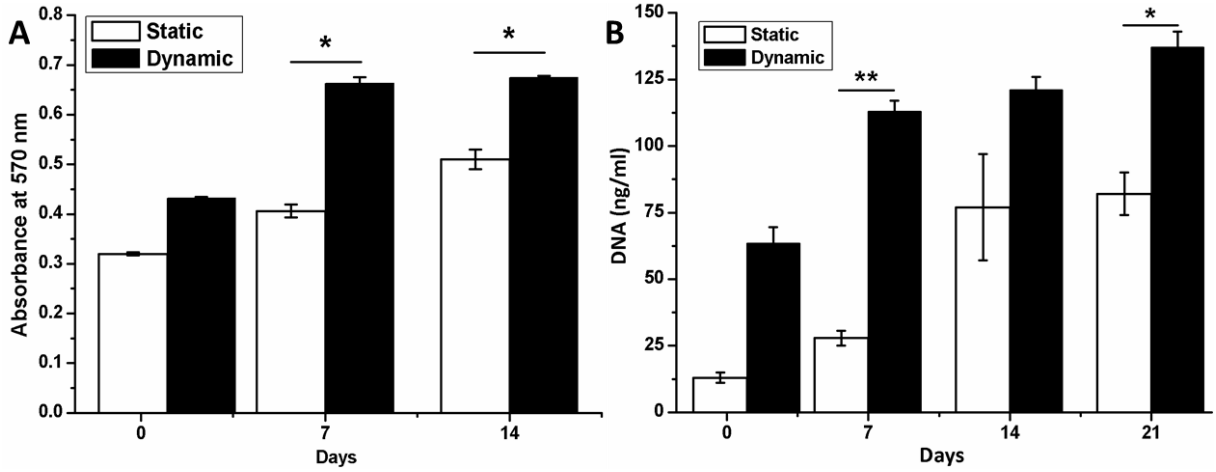

Figure 5.2.7 (A) Cell metabolic activity assessment by MTT assay on SF/CS scaffolds cultured under static and dynamic condition. (B) DNA quantification of hMSCs growing on the scaffolds for 21 days (n=3, *p< 0.05, **p < 0.01). The results represent superiority of the cell-seeded scaffolds cultured in spinner flask bioreactor in suporting cell metabolic activity and proliferation.

5.2.3 Assessment of chondrogenic differentiation

The *in vitro* studies for assessing cell supportive efficiency of SF/CS porous scaffolds under static and dynamic culture conditions revealed the superiority of the later culture condition. The effect of culture condition on chondrogenic differentiation of hMSCs seeded onto the scaffolds was further carried out by maintaining the cultures in chondrogenic induction medium for 21 days. The cultures were also maintained under growth media (not supplemented with chondrogenic differentiation media), represented as non-induced culture, to be used as negative control. The experimental results are discussed below-

5.2.3.1 Total sGAG estimation

The chondrogenic differentiation of hMSCs over SF/CS scaffold was further estimated by quantification of sGAG secretion, a characteristic predominant component of chondrocytes ECM (Sherwood et al. 2002). As observed in figure 5.2.8A, during 21 days of culture, sGAG concentration increased with progression of the culture, but no statistically significant difference was observed for first 14 days between the different culture conditions. However, on 21st day, a significant increase in sGAG content ($p < 0.05$) in spinner flask bioreactor was observed denoting faster chondrogenic progression of hMSCs as compared to static culture. The sGAG content (83.2±7 µg/mg) of the constructs developed in spinner flask bioreactor was more than double of static culture (35±4 µg/mg), implying the dependence of hMSCs response to chondrogenic culture conditions. This might be due to the effect of factors like nutrient diffusion and metabolic wastes removal (Bhardwaj et al. 2011).

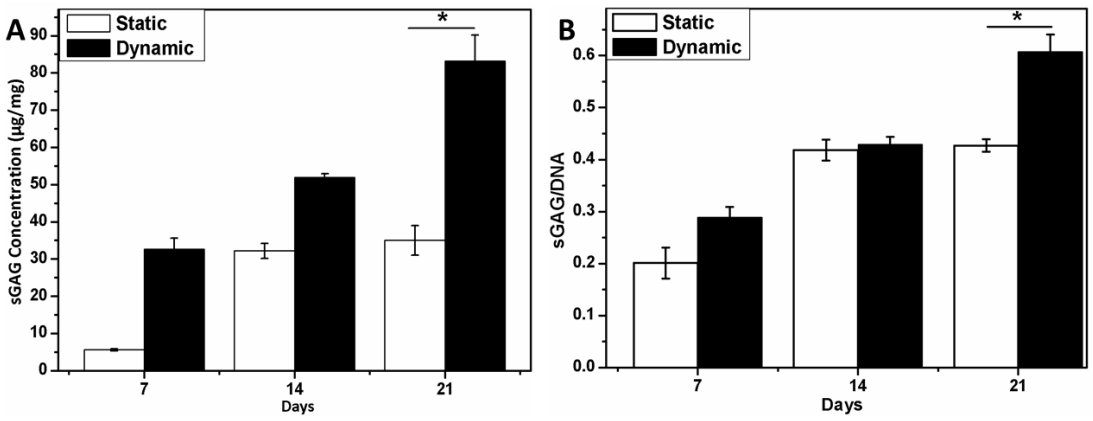

Figure 5.2.8 (A) Total sGAG secretion assessment by chondrocytes on SF/CS scaffolds cultured in static and dynamic conditions. (B) Normalised sGAG content with respect to DNA quantification of hMSCs growing on the scaffolds for 21 days (n=3, *$p < 0.05$). The results suggest chondrocytes like matrix synthesis along with cell proliferation in the constructs cultured in spinner flask bioreactor.

On comparing sGAG secretion result with DNA quantification, it was observed that the phenomenon of cell differentiation and proliferation were occurring in parallel for 14 days in both the culture conditions, but in static system, the differentiation was observed to decline after 2nd week (Figure 5.2.8B). In the constructs cultured in spinner flask, differentiation was continuous with linear increase in sGAG concentration throughout 3 weeks study, however, rate of proliferation started to decrease after 2nd week. The normalized values of total sGAG content with DNA concentration showed a similar trend, suggesting successful chondrogenic differentiation in dynamic culture as compared to static. This observation also suggests that upon differentiation for 21 days, the chondrocytes are metabolically active in sGAG synthesis even after achieving confluence in spinner flask bioreactor.

5.2.3.2 Histological evaluation

The extracellular matrix (ECM) of cartilage tissue comprises of proteoglycans that provides compressive strength to the tissue (Bhardwaj and Kundu 2012). Thus, production of proteoglycans through the differentiation of hMSCs may help as an indicator in determining the progress of chondrogenesis in *in vitro* culture. Alcian blue is a tetracationic dye that conjugates with proteoglycans and GAG under low pH thereby quantifies chondrogenic differentiation of hMSCs (Terry et al. 2000). On 21st day of culture in differentiation medium histological analysis by alcian blue staining showed a variation in the extent of staining between cell culture in static and dynamic conditions. The static culture showed individual cells surrounded by matrix stained in blue color (Figure 5.2.9A). Whereas cell-seeded scaffolds cultured in dynamic condition showed dense blue colored cells (Figure 5.2.9B). Cell aggregation, a characteristic chondrogenic phenomenon was also observed in the dynamic culture system along with proteoglycan synthesis. A significantly higher ($p < 0.05$) optical density for alcian blue staining was seen in samples cultured in dynamic culture compared to static culture (Figure 5.2.9C). Histological staining of proteoglycan matrix revealed that dynamic system supported cartilage type ECM deposition to a greater extent than static system that might facilitate the development of chondrocyte like phenotype of the differentiated hMSCs. In earlier reports it was demonstrated that ECM production has direct relation with many factors like, number of cells attached to the scaffold, fluid flow environment that improves nutrients availability and presence of therapeutic agents that enhance the synthesis process (Terry et al. 2000; Bhardwaj et al. 2011).

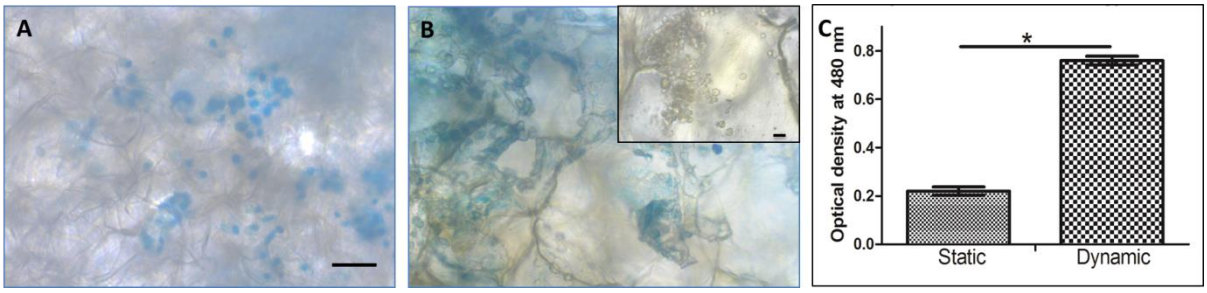

Figure 5.2.9 Histology staining for (A) static and (B) dynamic culture conditions showing proteoglycan matrix stained blue by alcian blue after 21 days of chondrogenic differentiation. Inset show absence of matrix coloration in non-induced culture (Scale bar= 50 µm). (C) Bar graph showing difference in optical density for alcian blue staining between the static and dynamic conditions (n=3, *p < 0.05). The dynamic environment provided in spinner flask served as better platform for proteoglycan matrix production by the hMSCs than the static condition.

5.2.3.3 Immunofluorescence study

Immunofluorescence staining of the cell in culture enables the study of different cellular components. Utilizing this approach, the predominant chondrocyte ECM components (Col II and Acan) were tagged using specific antibodies, and their expression was analysed by immunofluorescence staining after 21 days (Figure 5.2.10). Col II is a characteristic late chondrogenic marker secreted abundantly in ECM (Poole et al. 2002; Herlofsen et al. 2011). The hMSCs differentiating in static system showed weak expression of Col II (Figure 5.2.10A), while high expression was observed by cells cultured under dynamic system (Figure 5.2.10C and D). Furthermore, Acan is the most common proteoglycan matrix component that provides compressive stiffness to cartilage tissue (Poole et al. 2002). Immnofluorescence of Acan was detected in cytoplasm and extracellular space in both the culture conditions with higher expression shown in dynamic culture (Figure 5.2.10B, C and E). The strong immunostaining of Col II and Acan by cells present in construct cultured in spinner flask bioreactor was also reflected by integrated density analysis, signifying the cartilaginous matrix production that comprises of both collagenous and non-collagenous (proteoglycan) components.

Besides immunofluorescence, confocal microscopy was also studied to analyse the change in cell morphology on chondrogenic differentiation in comparison to undifferentiated hMSCs as depicted in Figure 5.2.10F. The undifferentiated hMSCs did not show immunofluorescence for Col II or Acan, and a remarkable difference in cell cytoskeleton arrangement was also evident from the differentiated cells. hMSCs exhibited parallel organization of β–actin (a

cytoskeleton component, stained green using Phalloidin), making the cells appear elongated and star-shaped, in contrast to the differentiated cells where cytoskeleton appeared constricted with circular morphology, thus attaining the characteristics of chondrocyte phenotype (Li et al. 2003). Remarkably, the circular packed arrangement of chondrocytes also indicated an increase in cell-to-cell interconnection that enhanced cell aggregation.

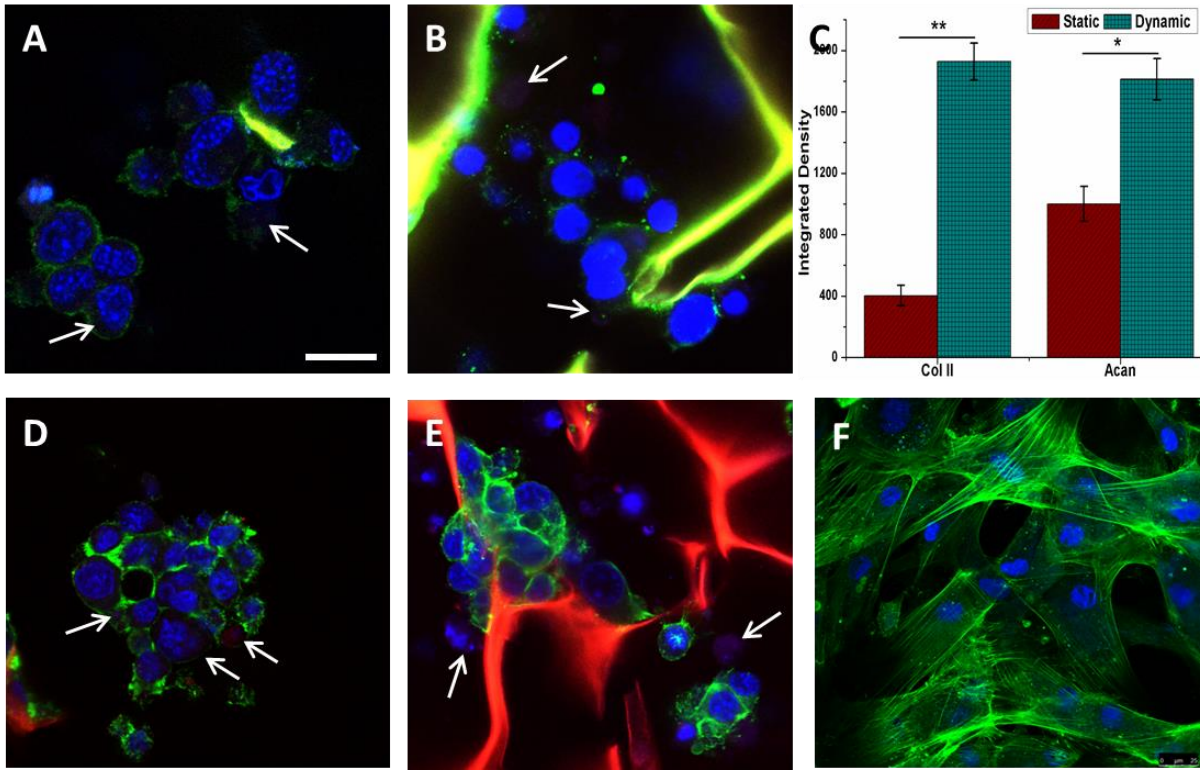

Figure 5.2.10 Immunofluorescence staining of Col II (A and D) and Acan (B and E) secretion in chondrocytes ECM (in red, indicated by white arrow) cultured under (A and B) static and (D and E) dynamic conditions. (C) Representing integrated density analysis of ECM staining (n=3, *$p < 0.05$, **$p < 0.01$). (F) Undifferentiated hMSCs showing elongated cells with no staining for Col II or Acan. Cell nucleus is stained blue and cytoskeleton in green. Scale bar= 50 µm. Constricted cytoskeleton and higher immunofluorescence of Col II and Acan reflected by the cells in spinner flask bioreactor represented chondrocyte phenotype development.

5.2.3.4 qPCR analysis

A quantitative analysis of gene expression during chondrogenic differentiation was performed by qPCR technique for a real time and precise detection. The expression profiles of Col I, Sox9, MATN3, Col II and Acan genes, representing their fold change with respect to undifferentiated hMSCs, is shown in figure 5.2.11. Col I, normally expressed by hMSCs, is not present in chondrocytes and it is responsible for the flattened appearance of hMSCs

(Yokoyama et al. 2005). Its presence in differentiating cells marks their dedifferentiation (Temenoff and Mikos 2000). The expression of Col I gene was more, initially on 7th day, which continuously decreased on 14th and 21st day as shown in both the culture systems (Figure 5.2.11A). A significant down-regulation ($p < 0.01$) of Col I expression was observed in dynamic system from 7th to 21st day. Sox9, an early chondrogenic marker, is expressed in hMSCs undergoing condensation during different phases of chondrogenesis (Bhardwaj and Kundu 2012). It is a transcription factor that binds to Col II specific gene sequences and regulates its expression (Lefebvre et al. 1997). The expression profile of Sox9 was observed to be similar in both the culture conditions with increasing trend from 7th to 14th day, which further up-regulated on 21st day (Figure 5.2.11B). Although, the early expression of Sox9 is important for triggering hMSCs condensation for differentiation, its expression at the mid stage is reported to further upregulate during the proliferation of chondroprogenitor cells, and at later stage for their transition to chondrocytes. Sox9 also stimulates the synthesis and expression of cartilage specific ECM components and participates in different phases of chondrogenesis (Lefebvre et al. 1997; Bhardwaj and Kundu 2012). Sox9 has been reported to be suppressed during hypertrophic stage, thus the duration of its expression indirectly corresponds to the maintenance of chondrocytes phenotype (Grassel and Ahmed 2007). MATN3, a gene that codes for non-collagen cartilage ECM component, is expressed during the mid-stage of chondrogenesis and regulates interaction between different matrix constituents thereby controls chondrocyte maturation (Pei et al. 2008). The expression of MATN3 was increased till 14th day with significantly higher ($p < 0.05$) expression in spinner flask culture (2.1±0.01 fold) than static culture (1.33±0.02 fold) (Figure 5.2.10C). The difference in expression of MATN3 was also significant between 7th and 14th day of observation in spinner flask culture, with a slight decrease on 21st day. Though, the expression profile of MATN3 was similar in static culture, but the difference between consecutive days of observation was statistically not significant. The expression of late chondrogenic genes namely Col II and Acan showed steady increase during the culture period. On 14th and 21st day, the expression of Col II was significantly higher ($p < 0.05$) when the cells were cultured in dynamic system than static one (Figure 5.2.11D). Similarly, a higher expression level of Acan was obtained in dynamic culture and significant up-regulation ($p < 0.01$) was evident from 7th to 21st day (Figure 5.2.11E).

The gene expression analysis of Col II and Acan was in accordance with the

immunofluorescence study that showed higher expression in dynamic system. Furthermore, the expression profiles of other chondrogenic genes represent progressive chondrogenic differentiation of hMSCs, specifically in dynamic culture condition showing its suitability for cartilage construct generation. On comparing expression profile of Col II with Col I (Figure 5.2.11F), a greater change was evident in spinner flask culture with significant difference ($p < 0.01$) on 21st day confirming the progress of chondrogenic differentiation.

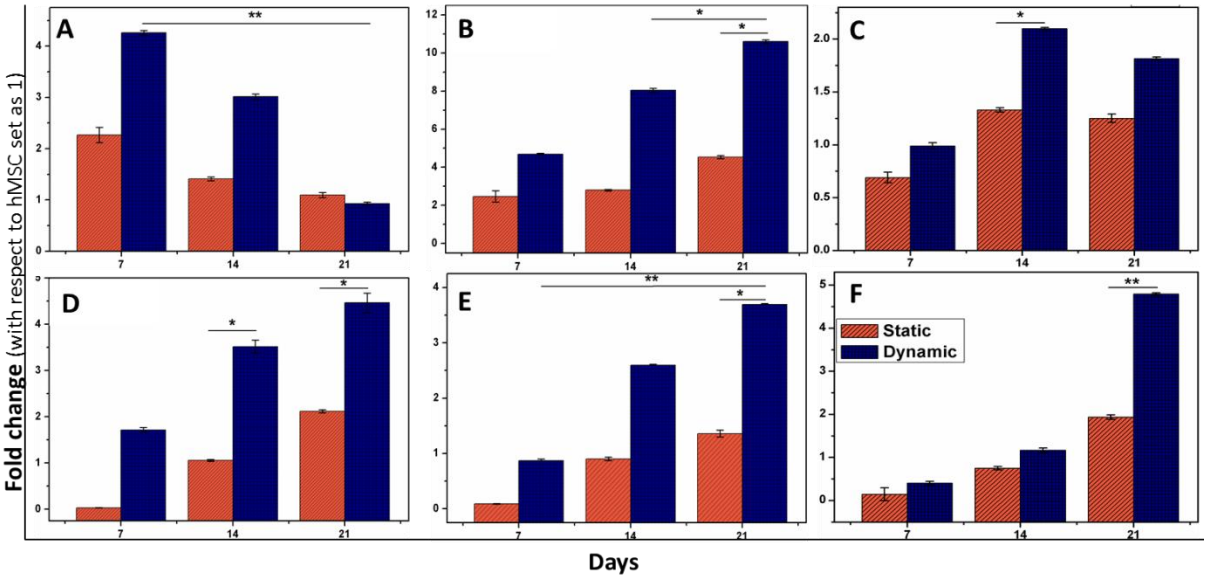

Figure 5.2.11 qPCR study representing expression of (A) Col I, (B) Sox9, (C) MATN3, (D) Col II and (E) Acan relative to hMSCs (Fold change set as 1) on 7th, 14th and 21st day of chondrogenic differentiation, under static and dynamic conditions. (F) Relative expression of Col II/Col I representing higher degree of chondrogenic progression in dynamic culture as compared to static culture (n=3, *p <0.05, **p < 0.01).

Conclusion

UCB-hMSCs were successfully cultured on SF/CS porous scaffolds under dynamic culture condition using spinner flask bioreactor. The mixing intensity of 60 rpm well supported cell viability and attachment to the scaffold surface. The dynamic culture environment also resulted in homogenous cell distribution into the scaffold, higher proliferation, and metabolic activity than static culture. The histological, sGAG synthesis, immunofluorescence and qPCR studies, demonstrated the superiority of dynamic culture condition in providing suitable microenvironment for chondrocyte ECM biosynthesis and gene expression thereby promoted chondrogenic differentiation of hMSCs cultured on SF/CS scaffold.

Chapter 5C

Development of cartilage construct by culturing and differentiating hMSCs over SF/CS- glucosamine scaffold

In the previous chapter, cartilage construct was developed by culturing and differentiating UCB-derived hMSCs over porous 3D SF/CS blend scaffold and demonstrated the efficiency of dynamic culture condition using spinner flask bioreactor. Cartilage tissue comprises of 30% by volume of chondrocytes, the rest is extracellular matrix (ECM) and water. The extensive ECM secreted by chondrocytes is composed of collagenous and proteoglycan (particularly GAG) components. Any damage to the integrity of cartilage tissue disturbs the tissue matrix that leads to progressive loss of GAG. Glucosamine (Gl), a basic component of disaccharide units of GAG, is reported to stimulate proteoglycan synthesis thereby it is used in cartilage damage treatment (Derfoul et al. 2007). Gl has been used in various oral formulations for cartilage treatment. However, the study for its use as a scaffold component is rare. Gl has been combined with gelatin, hyaluronic acid and poly(ethylene-glycol) gels, and their regulatory effect on the phenotype maintenance of chondrocytes obtained from rat and rabbit cartilage tissues were reported (Hwang et al. 2006; Chen et al. 2016a). The presence of Gl has improved the hydrophilicity of the scaffold developed previously in our laboratory (Vishwanath et al. 2017). The addition of Gl into SF/CS scaffolds may have beneficial effect to facilitate cartilage ECM production as reported earlier (Hwang et al. 2006; Chen et al. 2016a). However, the effect of Gl incorporated SF/CS scaffold on differentiation of hMSCs to chondrocytes is not yet investigated.

Keeping in view the beneficial effect of Gl loaded SF/CS scaffold in terms of enhanced chondrogenesis, the present research work was designed to develop cartilage construct by culture and differentiation of UCB-hMSCs on Gl incorporated SF/CS porous (SF/CS-Gl) scaffold in spinner flask bioreactor and analyzed against static culture condition. The effect of presence of Gl in SF/CS scaffold on chondrogenic matrix secretion was analyzed to determine the progression of chondrogenic differentiation. The result and discussion of these experimental studies are presented in this chapter.

5.3.1 Preparation of SF/CS-Gl scaffold and its physicochemical characterization

1 wt% Gl was added to the SF/CS (80:20 v/v) blend and SF/CS-Gl porous scaffold was prepared by freeze drying. The scaffold showed open pore structure with pore size 55–195 µm (Figure 5.3.1A and B), 79% porosity, 49˚ contact angle, and controlled biodegradation (24.03% weight loss in 28 days).

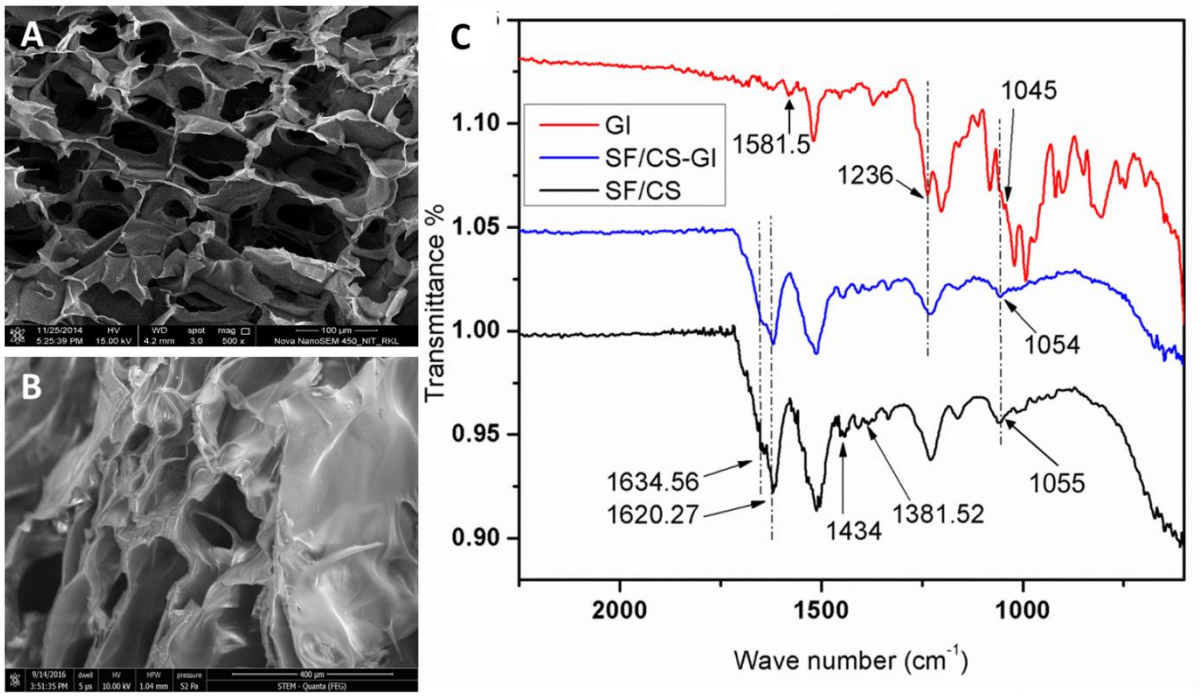

Figure 5.3.1 Physicochemical characterization of SF/CS-Gl scaffold. FESEM micrographs representing (A) transverse and (B) longitudinal sections of the scaffold. (C) FTIR spectra of Gl powder, SF/CS blend and SF/CS-Gl scaffold representing intermolecular interaction.

The interaction between the scaffold components was studied by FTIR analysis (Figure 5.3.1C). The characteristic peaks of –CH and $–CH_3$ deformation of CS were present at 1434 cm^{-1} and 1381.52 cm^{-1} in SF/CS scaffold and appeared as weak shoulders in the composite scaffold. The peaks at 1634.56 cm^{-1} and 1620 cm^{-1} representing amide I bond and β-sheet structure from SF were present in both SF/CS and SF/CS-Gl scaffolds. The characteristic band at 1236 cm^{-1} depicting S=O stretching was present in both Gl and SF/CS-Gl scaffolds, confirming the presence of sulfate group (Foot and Mulholland 2005). The peak for NH_3^+ bending was present at 1581.5 cm^{-1} in Gl and was absent in the SF/CS-Gl scaffold, which represents its involvement in amide bond formation with other components in the composite scaffold. Numerous small peaks between 1500 cm^{-1} to 1700 cm^{-1} in Gl and the scaffolds represented the presence of amine groups. The C-C vibration was depicted by small peaks at 1045 cm^{-1}, 1054 cm^{-1} and 1055 cm^{-1} in Gl, SF/CS-Gl and SF/CS scaffolds respectively.

5.3.2 Assessment of cell-scaffold constructs

5.3.2.1 Cell attachment, morphology and spreading

FESEM micrographs revealed that hMSCs were well uniformly spread over the scaffold and

exhibited elongated morphology on 14th day of culture under dynamic condition (Figure 5.3.2B), whereas the cells were round in morphology and growing in small colonies thereby confined to limited areas (Figure 5.3.2A) when cultured under static condition. The interconnected porous structure of the scaffolds (inset in Figure 5.3.2A), was adequate to support infiltration of hMSCs and chondrocytes having diameter of 15-50 µm (Ge et al. 2014). hMSCs appeared elongated with well-established interconnection that covered scaffold surface making its structure indistinguishable. Furthermore, the deposition of ECM was observed over SF/CS-Gl scaffolds, which was not shown by cell grown on SF/CS scaffold. The ECM deposition was partially due to the presence of Gl in SF/CS scaffold that provided biological cues for ECM secretion (Chen et al. 2016a).

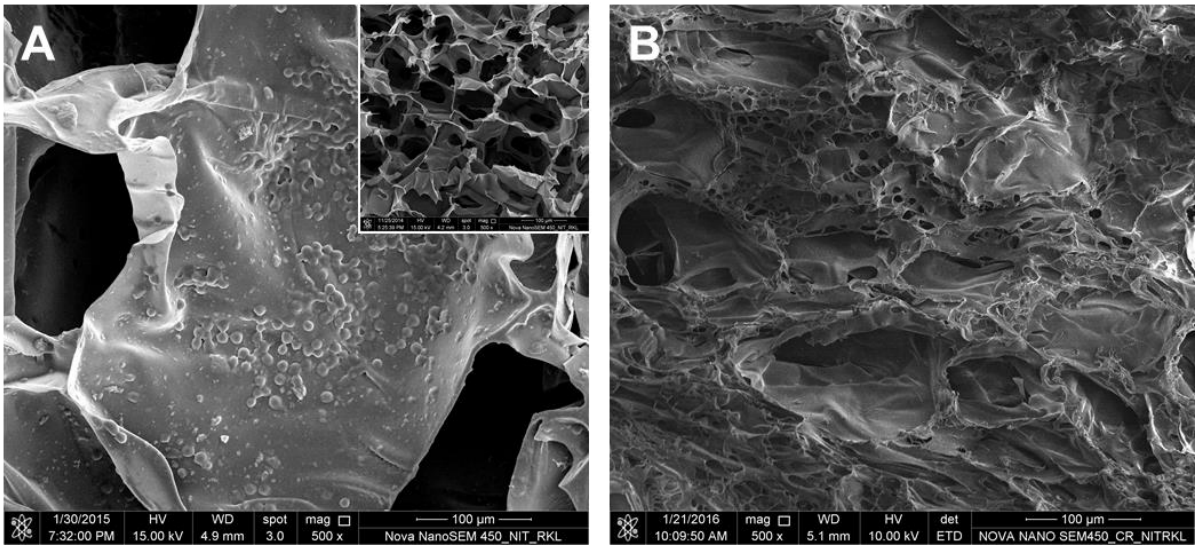

Figure 5.3.2 FESEM of hMSCs seeded SF/CS-Gl scaffold cultured under (A) static and (B) dynamic condition. Inset shows unseeded scaffold. The result represents cell attachment to SF/CS-Gl scaffold with uniform spreading and cellular interconnection on culturing under dynamic condition for 14 days.

5.3.2.2 Cell viability and distribution

The viability and distribution of hMSCs over SF/CS-Gl scaffolds were assessed by fluorescence analysis of confocal images. Figure 5.3.3 revealed well spreading of green fluorescent-viable hMSCs on scaffolds, and few red fluorescent- dead cells observed in both the culture conditions. The viable cells covered majority of the scaffold surface under dynamic culture condition (Figure 5.3.3B). The cross sectional view of construct revealed the cell infiltration to larger depths and uniform distribution throughout scaffold (Figure 5.3.3D), than static culture, in which most of the cells remained attached over the surface (Figure

5.3.3A and C). An increase in live cells with increase in culture period was evident, but with a varying degree (Figure 5.3.3E). The % live cell was steadily increasing from 1st day to 14th day of culture. The corresponding cell viability was measured to be 82.45±2.6%, which was significantly higher ($p < 0.05$) than the viability shown in control (62±3.3%) and the cells cultured over SF/CS-Gl scaffold under static condition (56.45±3%).

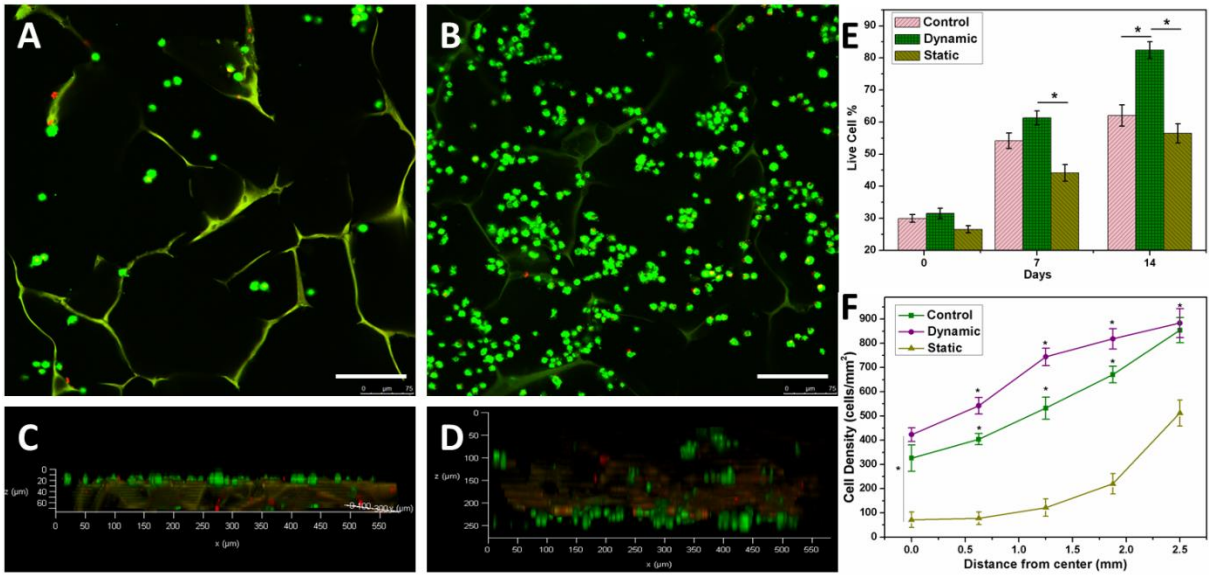

Figure 5.3.3 Fluorescence images of hMSCs seeded SF/CS-Gl scaffolds showing live cells stained green and dead cells stained red on 14th day of culture in (A and C) static and (B and D) dynamic system (Scale bar= 100 µm). (C and D) Side view of the images A and B showing cell infiltration. (E) Bar graph showing live cell percentage by intensity analysis (n=3, *$p < 0.05$). (F) Cell distribution as a function of distance from centre of construct. Dynamic culture maintained cell viability and facilitated infiltration into SF/CS-Gl scaffolds.

As expected, the cell distribution (Figure 5.3.3F) in dynamic culture depicted superior result in terms of number of cell penetration into the interior of the scaffold (587.5% more cells at the centre) than static culture where 72.9% cells were found within 1.25 mm depth. The cell distribution for the scaffolds cultured in spinner flask bioreactor showed similar trend, with higher density in SF/CS-Gl scaffolds at every point of observation than the SF/CS scaffold (control). These results represent that the culture condition has a predominant role in regulating cell viability and uniform cell distribution. The presence of Gl in the scaffold also showed beneficial effect in terms of improved hydrophilicity that resulted in better cell attachment and distribution as compared to control (Oh et al. 2003; Vishwanath et al. 2017).

5.3.2.3 Metabolic activity

The metabolic activity of cells over scaffolds was well maintained with a steady increase in optical density during the progress of culture. The increase in metabolic activity of cells on SF/CS-Gl scaffolds with culture duration was observed in both the culture conditions and was higher than that in control. This observation suggested the positive role of Gl in triggering chondrogenic characteristic during initial stages of culture (Hwang et al. 2006). Furthermore, improved pore interconnectivity on incorporation of Gl to SF/CS scaffolds as compared to control facilitated cell infiltration, nutrient and metabolites diffusion that might have resulted in higher metabolic activity of cells (Bruzauskaite et al. 2016). However, a significantly higher ($p < 0.05$) value was observed from 7th to 21st day in dynamic culture condition as compared to the static (Figure 5.3.4A).

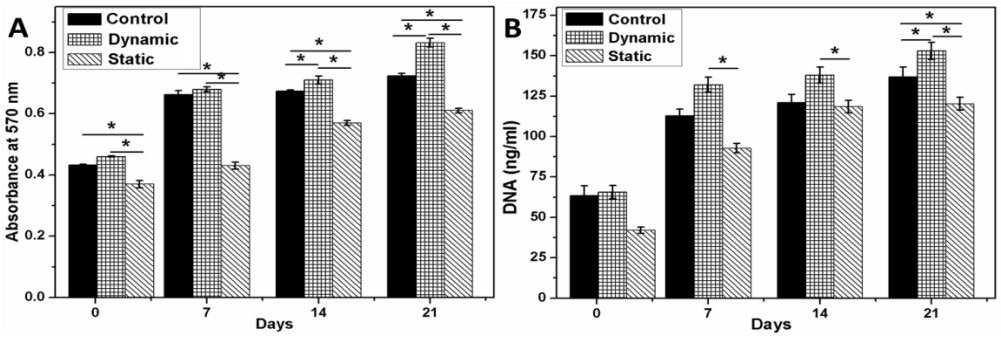

Figure 5.3.4 (A) Cell metabolic activity assessment by MTT assay on SF/CS-Gl scaffolds under static and dynamic conditions. (B) DNA quantification of hMSCs growing on the scaffolds for 21 days (n=3, *$p < 0.05$). The dynamic condition was superior in supporting metabolic activity and proliferation of hMSCs on SF/CS-Gl scaffolds.

5.3.2.4 DNA quantification

Cell proliferation was assessed by measuring DNA content of hMSCs in the scaffolds during the 21 days of culture. The cell proliferation was observed to be steadily increasing with culture duration (Figure 5.3.4B) and became double in 7 days. The DNA content representing the level of cell proliferation of 153±5.2 ng/ml was obtained on 21st day, which was significantly higher ($p < 0.05$) than the result obtained in static culture (120.24±4 ng/ml). Within similar culture condition, the cell proliferation in SF/CS-Gl scaffolds was higher than control at all the time points. The DNA content was also significantly higher in control than static culture. This phenomena may be due to the mass transfer limitation that affected the removal of metabolic waste resulting into a decrease in cell proliferation in static culture (Song et al. 2015). This result corroborates with the study, which reported an accelerated

proliferation of rat MSCs cultured on polymeric scaffold in dynamic culture for bone TE application (Sikavitsas et al. 2002). Thus, it demonstrated the advantage of the presence of Gl in the SF/CS scaffolds in terms of improving cell viability and metabolic activity that lead to enhanced proliferation (Chen et al. 2016a).

5.3.3 Assessment of chondrogenic differentiation

To determine the synergistic effect of the addition of Gl to SF/CS scaffold and dynamic culture environment on chondrogenic differentiation, particularly, cartilaginous matrix production, total sGAG content, histological, immunofluorescence of Col II and Acan in ECM and qPCR study for Col I, Sox9, MATN3, Col II and Acan genes expression were assessed.

5.3.3.1 Total sGAG estimation

The synthesis of sGAG, an important chondrocyte proteoglycan matrix component, was studied during 21 days of culture. The sGAG deposition was increased with culture duration in all the culture conditions, representing the synthesis of cartilage specific ECM by the hMSCs upon differentiation. The sGAG synthesis was higher in constructs cultured in dynamic condition than control under dynamic culture as well as static culture, at all the time points (Figure 5.3.5A). A significant difference in sGAG content was observed on 14^{th} and 21^{st} day among the three culture groups. On 14^{th} day, the constructs developed using SF/CS-Gl scaffolds deposited 80±10 µg/mg (dynamic culture) and 66±4 µg/mg (static culture) sGAG that was significantly higher than control achieving 45.9±10 µg/mg sGAG content. On 21^{st} day, the maximum of 130±6 µg/mg sGAG was deposited by construct developed in dynamic culture. A significantly lower sGAG deposition of 95±2 µg/mg ($p < 0.05$) was obtained using static culture condition and 83.2±7 µg/mg in control ($p < 0.01$). The sGAG synthesized by cells under non-induced conditions was too less to detect, thus the results were not presented.

Normalization of sGAG synthesis with DNA content showed progressive chondrogenic differentiation of cells in scaffolds under both dynamic and static culture conditions, with statistically non-significant difference between the two during each observation (Figure 5.3.5B). Furthermore, the constructs comprising of SF/CS-Gl scaffolds demonstrated a

significantly higher ($p < 0.05$) degree of difference in sGAG synthesis with respect to proliferation than control. This suggests that the presence of Gl in SF/CS scaffolds might have triggered chondrogenic matrix production resulting in an enhanced differentiation, irrespective of culture condition. Moreover, higher degradation rate of SF/CS-Gl scaffold than control resulted in increased availability of bioactive component (Gl) to the cells (Lam et al. 2009). A higher sGAG secretion obtained in constructs with Gl loaded SF/CS scaffolds is due to the metabolic role of Gl that upregulates hexosamine pathway for biosynthesis of GAG components (Hwang et al. 2006).

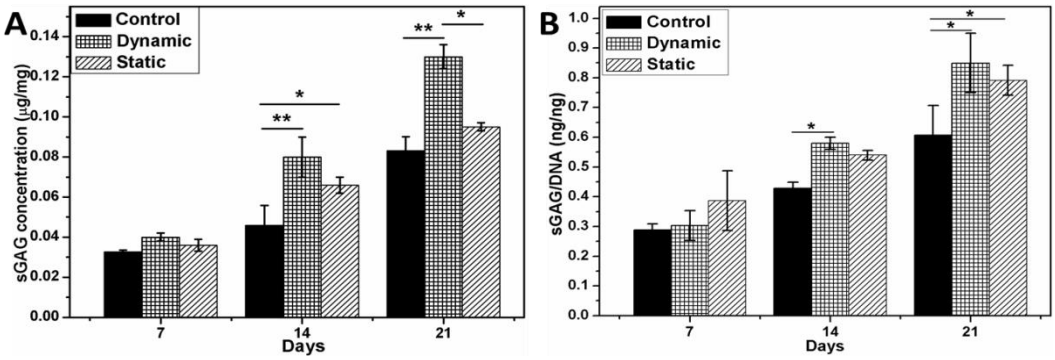

Figure 5.3.5 (A) Total sGAG secretion assessment by chondrocytes on SF/CS-Gl scaffolds cultured in static and spinner flask (dynamic) systems (n=3, *$p < 0.05$, **$p < 0.01$). (B) Normalised sGAG content with respect to DNA quantification of hMSCs growing on scaffolds for 21 days, representing the progressive chondrogenesis of hMSCs in SF/CS-Gl scaffolds in both the culture conditions.

5.3.3.2 Histological evaluation

Histology study using alcian blue dye is used to detect the presence of proteoglycans in the cell matrix, which are mainly secreted by chondrocytes that indicates the attainment of chondrogenic phenotype by the cells (Terry et al. 2000). On 21st day of histology, the chondrogenic phenotype was found prominent in the cells cultured over SF/CS-Gl scaffolds, where blue matrix of cells revealed proteoglycan synthesis in both the culture conditions (Figure 5.3.6). Cell aggregates were denser in chondrogenic induced SF/CS-Gl scaffold cultured in dynamic condition (Figure 5.3.6B) and proteoglycan matrix staining was spread to a greater distance as compared to control (Figure 5.3.6A), static culture (Figure 5.3.6C) and non-induced cultures (Figure 5.3.6E and F). Quantitatively, proteoglycan synthesis was the highest in constructs developed in induced SF/CS-Gl scaffold cultured in dynamic condition with a significant difference ($p < 0.05$) with control (Figure 5.3.6D). The staining of proteoglycan matrix observed in non-induced culture showed the positive effect of Gl in

SF/CS scaffolds in inducing chondrocyte type proteoglycan matrix synthesis. Furthermore, there was no staining observed in non-induced control, which represents that no proteoglycan matrix was formed (inset in figure 5.3.6A). Although due to the presence of Gl in scaffolds, some effect on proteoglycan matrix synthesis was evident, but it was not sufficient enough for the progression of chondrogenic differentiation in absence of other triggering factors like induction medium and dynamic culture condition (Hwang et al. 2006).

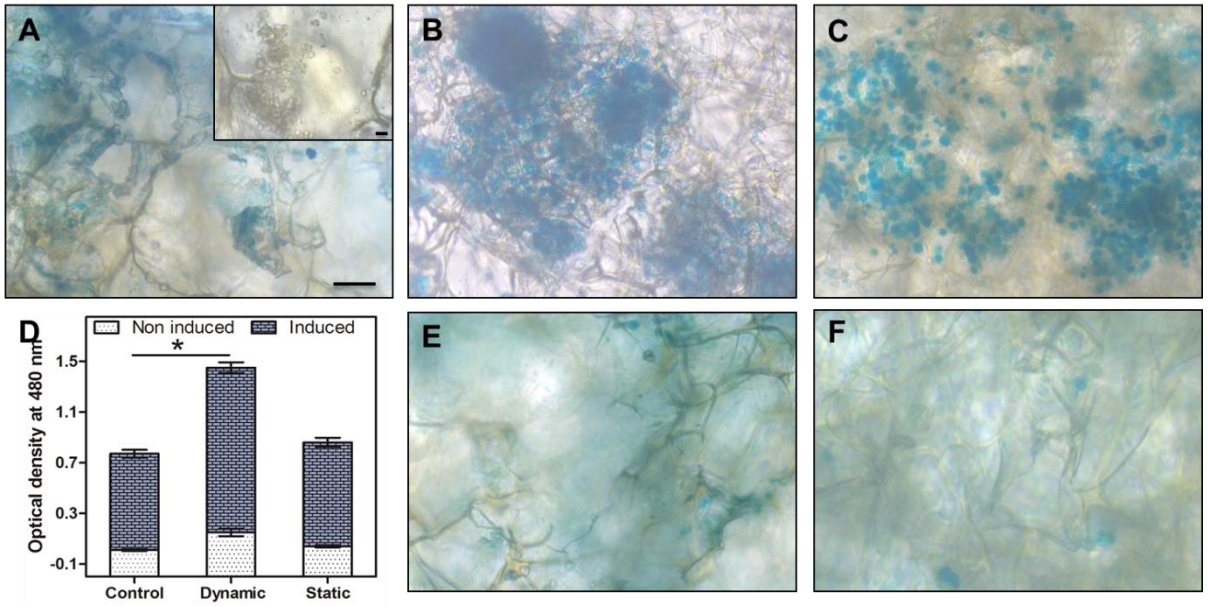

Figure 5.3.6 Histology staining for (A) control (B and E) spinner flask (dynamic) culture and (C and F) static systems showing proteoglycan matrix stained blue by alcian blue after 21 days of chondrogenic differentiation. E and F show lower matrix coloration in non-induced cultures. Scale bar= 50 µm. (D) Bar graph showing the difference in optical density for alcian blue staining between the static and dynamic culture condition (n=3, $*p < 0.05$). The results represent the hMSCs seeded SF/CS-Gl scaffolds support chondrogenic phenotype development by cells.

5.3.3.3 Immunofluorescence study

The different components of cells namely nucleus, cytoskeleton and chondrocyte specific ECM were tagged with their respective fluorescent dyes and studied by immunofluorescence analysis. The chondrocyte specific antibodies Col II and Acan were observed under confocal microscopy on 21st day of differentiation initiation. The constructs showed positive staining for Col II as indicated in figure 5.3.7A and D, but with varying degree of red coloration in ECM. Immunofluorescence of Acan was also observed in and around cytoplasm of the cells in SF/CS-Gl scaffolds (Figure 5.3.7B and E) with more fluorescence observed in dynamic culture. The staining of ECM components was quantified by measuring the intensity of red

fluorescence, and data was represented in terms of integrated density analysis with respect to the control samples, as shown in figure 5.2.9 (chapter 5B). Integrated density analysis confirmed a significantly higher ($p < 0.05$) degree of production of collagenous and proteoglycan matrix components by cells cultured with SF/CS-Gl scaffolds under dynamic condition as compared to static as well as control (Figure 5.3.7C). Gl incorporated SF/CS scaffolds provided biological signal that promoted differentiation of cells, leading to higher chondrocyte type ECM synthesis (Lippiello 2003; Marshall et al. 2004). In another study, an increased Col II and GAG synthesis was observed by chondrocytes when cultured under the effect of hydrodynamic force, as compared to static condition that resulted in redifferentiation of dedifferentiated chondrocytes (Heyland et al. 2006). The beneficial effect of mechanical stimulation provided by applying shear stress on chondrogenic phenotype by the cells has been reported earlier that expanded the study on different kinds of bioreactors for their application in cartilage tissue engineering (Vunjak-Novakovic et al. 1996; Temenoff and Mikos 2000).

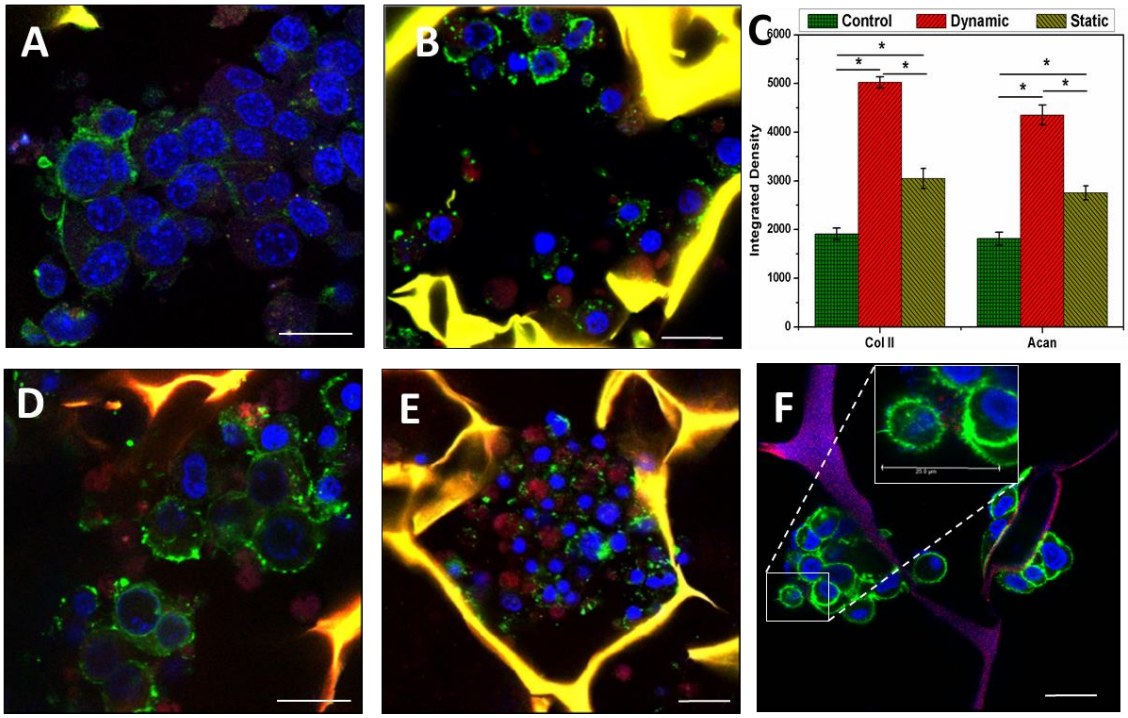

Figure 5.3.7 Immunofluorescence staining of Col II (A, D and F) and Acan (B and E) in chondrocytes ECM cultured under (A and B) static and (D, E and F) spinner flask (dynamic) culture systems. (C) Representing integrated density analysis of the ECM staining (n=3, *$p < 0.05$). (F) Col II staining in non-induced culture. Cell nucleus is stained blue and cytoskeleton in green. Scale bar= 25 µm. The results show efficiency of Gl loaded SF/CS scaffolds in inducing the synthesis of chondrocyte specific ECM components, however, differentiation promoting factors and dynamic culture environment promoted attainment of chondrogenic phenotype.

In non-induced cultures, the staining for Acan was not observed, while Col II appeared very faint and at very few places (Figure 5.3.7F). However, the cells in non-induced culture showed round morphology, similar to those observed in the induced culture (Li et al. 2003; Ko et al. 2009). These observations confirm that the presence of Gl in SF/CS scaffolds triggers hMSCs towards chondrogenic lineage. However, the chondrogenic differentiation promoting or inducing factors (provided by differentiation media) are required to accelerate the differentiation process and maintain differentiated state of chondrocytes (Hwang et al. 2006). Furthermore, among the induced culture groups, chondrocyte ECM production in dynamic environment maintained in spinner flask bioreactor was faster than static culture, representing the superior performance of dynamic culture condition for cartilage construct development. Thus, the significantly higher matrix staining by the cells cultured on SF/CS-Gl scaffold in spinner flask bioreactor is due to the combined effect of the presence of Gl as an ECM stimulatory component and dynamic culture condition.

5.3.3.4 qPCR analysis

The progress of chondrogenic differentiation was further confirmed by qPCR study by analysing the expression of Col I, Sox9, MATN3, Col II and Acan genes in differentiated cells in 3D constructs during the 21 days of culture (Figure 5.3.8). Col I, a marker for dedifferentiation of chondrocytes, was down-regulated in all the culture conditions, however with a rapid decline in dynamic culture (Figure 5.3.8A). On 21st day, the expression of Sox9 was increased by 21.23±0.51 fold, representing its faster differentiation in dynamic culture, which was almost double than static (12.13±0.6) and control (10.59±0.09) (Figure 5.3.8B). The expression of MATN3 was shown to be increased with culture time and stabilized after 14 days (Figure 5.3.8C). A significantly higher expression of MATN3 was observed in dynamic culture on 14th day (7.21±0.3 fold) than control and static culture achieving 2.1±0.1 and 5.23±0.41 fold change respectively. The expression profile of Col II and Acan were observed to be similar, exhibiting an increase in trend with culture duration, and higher fold change was obtained with Gl containing SF/CS scaffold cultured under dynamic condition (Figure 5.3.8D and E). The comparison of expression profile of chondrogenic gene Col II with respect to Col I (Figure 5.3.8F), revealed that on 7th day, there was not much difference in differentiation among the two culture groups having SF/CS-Gl scaffolds. However, the chondrogenic progression of hMSCs on SF/CS-Gl scaffolds significantly increased in dynamic culture with time, whereas there was a steady increase in static culture. This

observation was in accordance with the previous reports that demonstrated the stimulating effects of dynamic culture environment on chondrogenic differentiation and phenotype maintenance (Temenoff and Mikos 2000; Heyland et al. 2006).

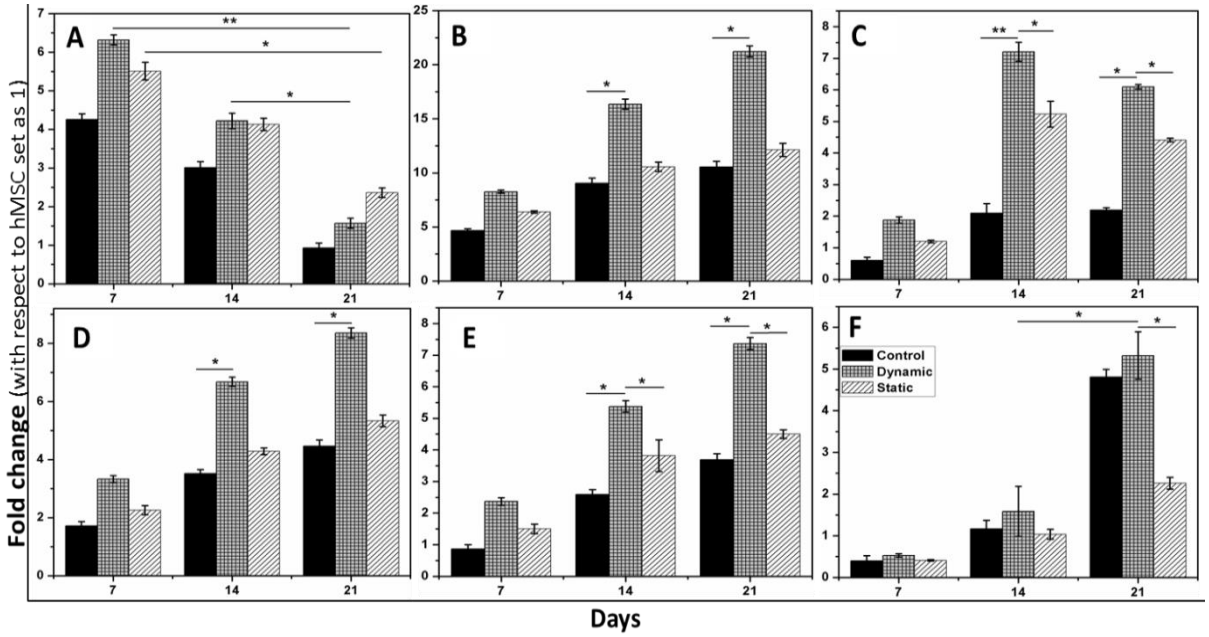

Figure 5.3.8 qPCR study representing expression of (A) Col I, (B) Sox9, (C) MATN3, (D) Col II and (E) Acan relative to hMSCs (Fold change set as 1) on 7th, 14th and 21st day of chondrogenic differentiation, under static and dynamic conditions for control and SF/CS-Gl scaffold constructs. (F) Relative expression of Col II/Col I representing higher degree of chondrogenic progression in dynamic system in comparison to control and static culture (n=3, *$p < 0.05$, **$p < 0.01$).

The expression profile of chondrogenic genes, Col I (early stage marker associated with mesenchymal phenotype), Sox9 (transcription factor), MATN3 (mid-stage marker), and genes associated with chondrogenic ECM production namely Col II and Acan (late stage markers) (Zaucke et al. 2001; Pei et al. 2008) were significantly up-regulated in their respective stages in Gl containing scaffolds under the same culture condition as control. Similar observation was reported earlier where upregulation of Acan and col II genes was shown by culturing hMSCs and chondrocytes in Gl containing media (Derfoul et al. 2007). Thus, in this study, the presence of Gl as an integral component of scaffold was demonstrated to be beneficial in promoting chondrogenic differentiation of hMSCs, owing to its regulatory role in chondrocyte matrix synthesis (Marshall et al. 2004; Hwang et al. 2006; Shikhman et al. 2009).

Conclusion

The addition of Gl to SF/CS scaffold was demonstrated to be beneficial in enhancing differentiation of hMSCs to chondrocytes thereby cartilage ECM synthesis was promoted. Though, SF/CS-Gl scaffolds did not stimulate cell viability to a great extent, the cartilage specific ECM secretion was remarkably increased, implying the positive role of Gl in triggering chondrogenic characteristic during initial stages. Furthermore, the histological, immunofluorescence, sGAG synthesis and qPCR analyses confirmed that hMSCs differentiated on SF/CS-Gl scaffolds developed chondrocyte specific phenotype. As in previous chapter, the use of dynamic culture was found to be effective in promoting cell proliferation and homogenous cell distribution, which further facilitated chondrogenic differentiation. Thus, the generation of cartilage construct was successfully demonstrated by utilizing the combined benefits of glucosamine incorporated SF/CS scaffolds and dynamic culture condition provided by spinner flask bioreactor, with improved biological properties as compared to the construct generated using pure SF/CS scaffold.

Chapter 5D

Development of cartilage construct by culturing and differentiating hMSCs over SF/CS-chondroitin sulphate scaffold

In previous chapter, the inclusion of glucosamine as a GAG component to SF/CS scaffold has improved the chondrogenic potential of UCB-hMSCs and thereby, an enhanced cartilage specific matrix formation was achieved. Chondroitin sulfate (Ch) is another prominent chondrocyte ECM component that protects cartilage degeneration along with promoting chondrocyte matrix synthesis, when it is dispensed for cartilage disease or damage treatment (Hammad et al. 2015). Ch has been used as a key component in the matrices combining with collagen, hyaluronic acid, poly(l-lactide), and other polymers, for chondrocytes culture (Gong et al. 2007; Zhang et al. 2011). Therefore, it was hypothesised that the addition of Ch might improve cell attachment due to enhanced hydrophilicity of the scaffold and cartilage ECM formation by the cells.

Thus, in this part of the research study, effort has been given to evaluate the biocompatibility of Ch loaded SF/CS (SF/CS-Ch) composite scaffold by assessing UCB-hMSCs attachment, viability, metabolic activity and proliferation. Furthermore, the effect of Ch on the cartilage ECM production by chondrogenic differentiation of hMSCs was investigated by assessing its potentiality of proteoglycan synthesis, protein and gene expression. The result and discussion of these experimental studies are presented in this chapter.

5.4.1 Preparation of SF/CS-Ch scaffold and physicochemical characterization

The SF/CS-Ch composite scaffold containing 0.8% (w/v) Ch was prepared by freeze drying. The scaffold possessed desired physicochemical property like pore size of 57-210 μm with interconnected pore network as evident by transverse and longitudinal section by SEM study (Figure 5.4.1A and B), 85% porosity, contact angle of 45.93 degree and controlled biodegradation (28.06% weight loss in 28 days).

FTIR analysis of the scaffolds was performed to understand the intermolecular interaction between the components upon blending and scaffold formation. The peaks in the resulted spectra were identified for functional groups of the components in SF/CS scaffold, Ch powder and SF/CS-$Ch_{1.0}$ scaffold, where similar observation was made for all the Ch containing scaffolds (Figure 5.4.1C). The characteristic β-sheet structure of SF was observed at 1620.27 cm^{-1} and 1634.56 cm^{-1} representing amide I bond present in both SF/CS and SF/CS-Ch scaffolds (Nazrov et al. 2004; Wang and Li 2007). The bands at 1425 cm^{-1} and

1381 cm^{-1} are characteristic bands for –CH deformation and $–CH_3$ symmetric deformation, respectively as found in CS. These bands were also observed in SF/CS scaffolds with a slight shift at 1434 cm^{-1} and 1381.52 cm^{-1}. Whereas the band for –CH deformation was seen at 1444.78 cm^{-1} in the composite scaffold (Wang and Li 2007). The peaks of SF in the region around 1400-1700 cm^{-1} are very strong that overlaid the peaks for CS making them appear as weak shoulders in the blend as well as composite scaffolds. The peak at 855.03 cm^{-1} was identified for chondroitin-4-sulfate in Ch powder which was slightly shifted to 846.87 cm^{-1} in SF/CS-Ch scaffold (Garnjanagoonchorn et al. 2007). The characteristic band of Ch at 1246 cm^{-1} corresponding to S==O stretching was observed in both Ch powder and composite scaffold, confirming the presence of Ch in the scaffolds (Anisha et al. 2013).

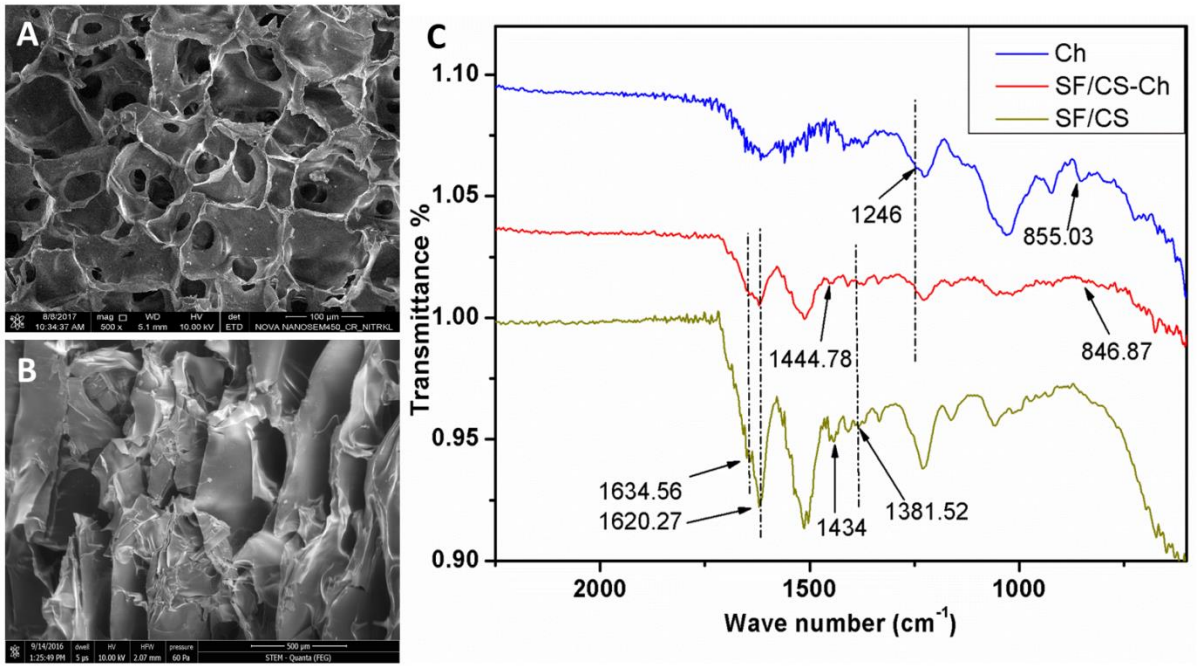

Figure 5.4.1 Physicochemical characterization of SF/CS-Ch scaffold. FESEM micrographs representing (A) transverse and (B) longitudinal sections of the scaffold. (C) FTIR spectra of Ch powder, SF/CS blend and SF/CS-Ch scaffold representing intermolecular interaction.

5.4.2 Assessment of cell-scaffold construct

5.4.2.1 Cell attachment, morphology and spreading

As in the previous chapter, hMSCs seeded SF/CS-Ch scaffolds were cultured for 14 days to observe the change in cell morphology and spreading over the scaffold surface by FESEM analysis. As depicted in figure 5.4.2, the cultured hMSCs were attached to the SF/CS-Ch scaffolds and elongated in morphology with well-connected cellular network formation

representing the biocompatibility of the scaffold. Cell spreading was relatively more homogeneous in the SF/CS-Ch constructs (Figure 5.4.2B) than pure SF/CS and SF/CS-Gl constructs (shown in previous chapters, figure 5.2.3C and 5.3.2B). The results also revealed that the dynamic culture condition well supported cell attachment and cell spreading. Furthermore, a varying amount of ECM production was also observed in both the culture condition (Figure 5.4.2A), which might be due to stimulatory effect of Ch on ECM production (Deal and Moskowitz 1999).

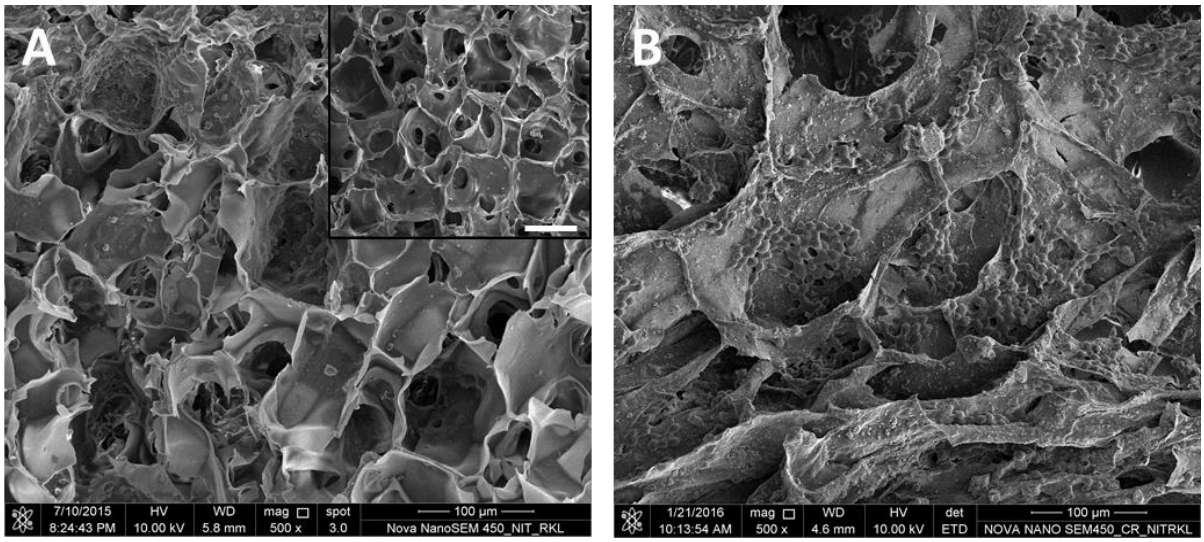

Figure 5.4.2 FESEM of hMSCs seeded SF/CS-Ch scaffold cultured under (A) static and (B) dynamic condition representing better spreading and ECM production by cells in the construct cultured in dynamic condition. Inset shows unseeded scaffold (Scale bar= 100 µm).

5.4.2.2 Cell viability and distribution

Attaining cell population with adequate viability and proper distribution throughout the scaffold are important, because during chondrogenic differentiation, hMSCs start losing division capability, which can affect the homogeneity of generated 3D construct (Solchaga et al. 2006). The viability of hMSCs on SF/CS-Ch scaffolds was assessed by calcein-AM and EthD-1 staining. The 3D view of the constructs (Figure 5.4.3A and B) confirmed a uniform cell distribution and infiltration into the scaffolds. Figure 5.4.3C shows on 14^{th} day, the cell viability of 91.53±2.1% was obtained in constructs developed under dynamic culture, which is significantly higher ($p < 0.05$) than the cell viability obtained in static culture (58±1.2%) and control (62±3.3%). The observed effect may be due to the increasing acidic environment that resulted from the accumulation of scaffold degradation products and cell metabolites,

which might not be properly dispersed in static culture due to the absence of dynamic flow (Sung et al. 2004).

The cell distribution assessed by confocal study at different depth of scaffolds has revealed a higher penetration and better occupancy of the cells in dynamic culture systems than the static one (Figure 5.4.3D). At the centre of the scaffolds, 472±38 cells/mm^2 was found, which is quite higher than 87±22 cells/mm^2 shown in static culture system. Similar observation was made in our earlier chapters, where the dynamic culture using spinner flask bioreactor was proven to be superior to static culture in promoting cell attachment, proliferation and distribution on scaffolds. However, in this part of the study, hMSCs seeded SF/CS-Ch scaffold was also assessed under static culture to investigate the role of Ch towards the cell behaviour in different culture conditions. Ch was added to SF/CS scaffold to promote chondrogenesis of hMSCs. However, the higher cell viability and distribution in SF/CS-Ch scaffolds as compared to control, which may be due to increased availability of growth factors for cells that was facilitated by the presence of Ch in the scaffolds (Ko et al. 2009).

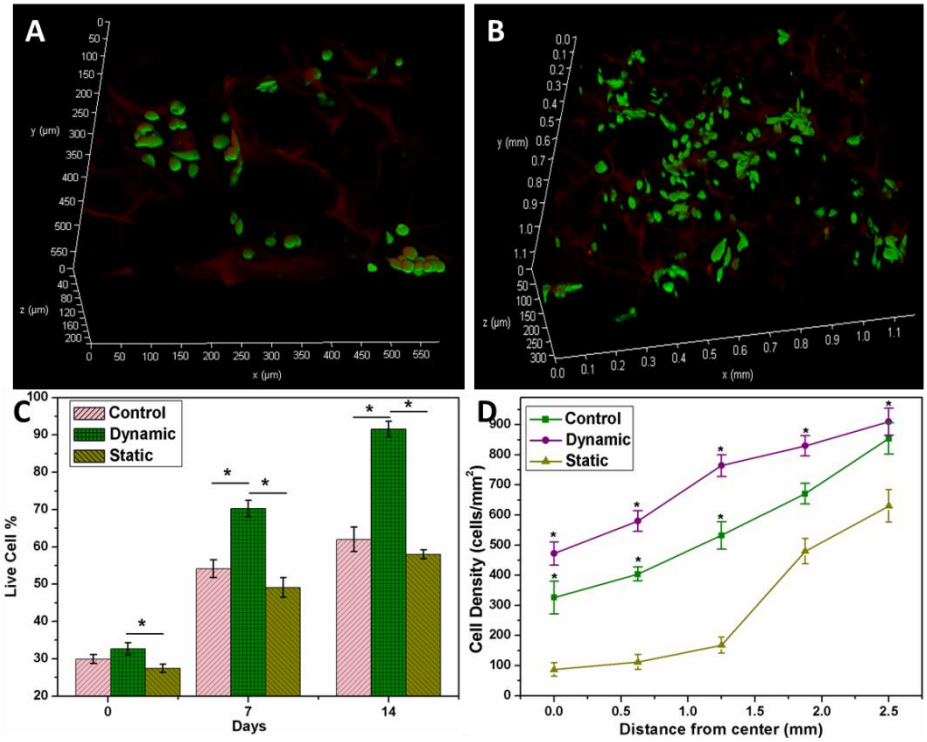

Figure 5.4.3 Fluorescence images of hMSCs seeded SF/CS-Ch scaffolds showing live cells stained green and dead cells stained red on 14th day cultured in (A) static and (B) dynamic condition. (C) Bar graph showing % live cell by intensity analysis. (D) Cell distribution as a function of distance from centre of construct (n=3, *p < 0.05). The results represent higher cell viability and homogenous distribution in dynamic culture compared to control and static culture.

The viability and distribution of hMSCs in SF/CS-Ch scaffolds were improved with respect to control (SF/CS scaffolds), however the results were comparable to the SF/CS-Gl scaffolds. FESEM results of SF/CS scaffolds incorporated with Gl or Ch showed ECM secretion by cells, even in the absence of differentiation media, representing positive effect of Gl and Ch, whereas culture condition was found to play a dominant role in promoting cell viability and distribution. In another study, it has been demonstrated that static seeding is able to provide uniform cell distribution only in thin scaffolds (≤ 2 mm), however, for spatial uniform distribution of cells into thick scaffolds (2-5 mm) spinner flask or other aid is necessary (Vunjak-Novakovic et al. 1998). The above findings are in accordance with this observation, as the scaffold thickness of 5-10 mm was used, and in all the cases dynamic culture was observed to be providing homogenous cell distribution throughout the scaffold as compared to static culture condition. On comparing, the results of SF/CS-Gl and SF/CS-Ch scaffolds with hMSCs seeded SF/CS scaffold (control), cultured under spinner flask, reveal that the culture condition was more effective in terms of promoting cell viability and distribution than the composition of the scaffold.

5.4.2.3 Metabolic activity

The population of metabolically active cells in the scaffold during culture as determined by calorimetric measurement using MTT assay, is depicted in figure 5.4.4A. The results revealed an increasing trend in absorbance representing increase in metabolically active cell population with the culture period. The constructs developed in dynamic culture showed a higher metabolic activity of cells with a statistically significant difference with static culture ($p < 0.05$) from 7^{th} day to 21^{st} day. This represents an increase in cell metabolic activity in dynamic culture system, providing superior microenvironment for cell culture. Furthermore, cells in SF/CS-Ch scaffolds demonstrated higher metabolic activity than control representing the beneficial effect of Ch in regulating metabolic activity of the cells (Hammad et al. 2015). Similar observation was made in earlier study where metabolic activity of fibroblast cells was reported to increase in the SF/Ch-hyaluronic acid scaffold, which may be attributed to the increased nutrient receptors on the scaffold due to the presence of Ch (Yan et al. 2013). The higher metabolic activity shown by cells cultured in SF/CS-Ch scaffold as compared to SF/CS and SF/CS-Gl scaffolds, may also be attributed to the increased hydrophilicity of SF/CS-Ch scaffold that facilitated cell attachment and dissolution of nutrients required for maintaining cell metabolism (Oh et al. 2003).

5.4.2.4 DNA quantification

The hMSCs proliferation was further measured by DNA quantification. As indicated in figure 5.4.4B, the cells were observed to be proliferating at a rapid rate in SF/CS-Ch scaffolds and the DNA content of hMSCs was increasing over a period of 21 days. In comparison to control, DNA content of cells in SF/CS-Ch scaffolds cultured under dynamic condition was shown to be higher at all the time points, representing the positive role of Ch in supporting cell proliferation. The presence of Ch in the scaffold improved water binding capacity and provided the receptors for interaction with cytokines and growth factors available in the media that resulted into an overall increase in cell proliferation (Yan et al. 2013; Hammad et al. 2015).

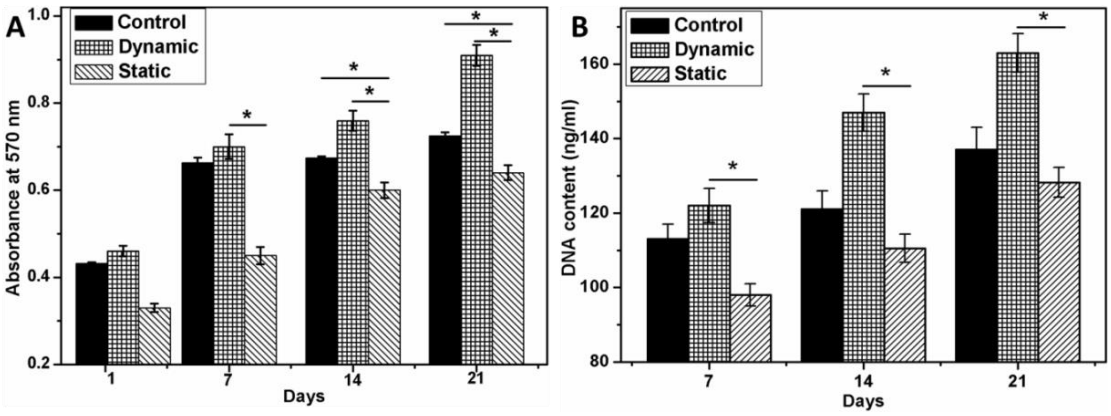

Figure 5.4.4 (A) Cell metabolic activity assessment by MTT assay on SF/CS-Ch scaffolds cultured under static and dynamic condition. (B) DNA quantification of hMSCs growing on the scaffolds for 21 days (n=3, *p < 0.05). The results represent higher metabolic activity and proliferation on the SF/CS-Ch scaffold cultured under dynamic condition than static and control.

5.4.3 Assessment of chondrogenic differentiation

5.4.3.1 Total sGAG estimation

The DMMB dye assay showed a gradual increase of sGAG content when hMSCs was cultured over SF/CS-Ch scaffolds for 21 days (Figure 5.4.5A). A prominent increase in sGAG content from 118±10 µg/mg on 14th day to 247±20 µg/mg was observed on 21st day when construct was cultured under dynamic condition. Furthermore, sGAG synthesis was significantly higher ($p < 0.05$) in comparison to pure SF/CS (83.2±7 µg/mg) and SF/CS-Gl (130±6 µg/mg) scaffold. Noticeably, although the cell number was lesser in static culture, the sGAG content in Ch containing scaffold cultured in static condition on 14th day was almost

same to that of control on 21st day, indicating the positive effect of Ch in stimulating sGAG synthesis by the cells.

On normalizing sGAG synthesis with the amount of DNA, a significantly higher ($p < 0.05$) value of these components were shown in constructs cultured in SF/CS-Ch scaffolds than the control on 14th and 21st day (Figure 5.4.5B). A significant increase in sGAG content was observed in the constructs developed using SF/CS-Ch scaffold as compared to SF/CS (control) and SF/CS-Gl scaffolds, which may be due to the presence of Ch in scaffold acting as a triggering factor for proteoglycan synthesis (Deal and Moskowitz 1999). The other possible reason may be the increase in degradation rate of scaffolds upon incorporation of Ch to SF/CS blend, which increased the availability of Ch to the cells, and accelerated chondrogenesis (Bruzauskaite et al. 2016). This result signifies that the chondrogenic differentiation and proliferation are occurring in parallel in the constructs consisting SF/CS-Ch scaffolds.

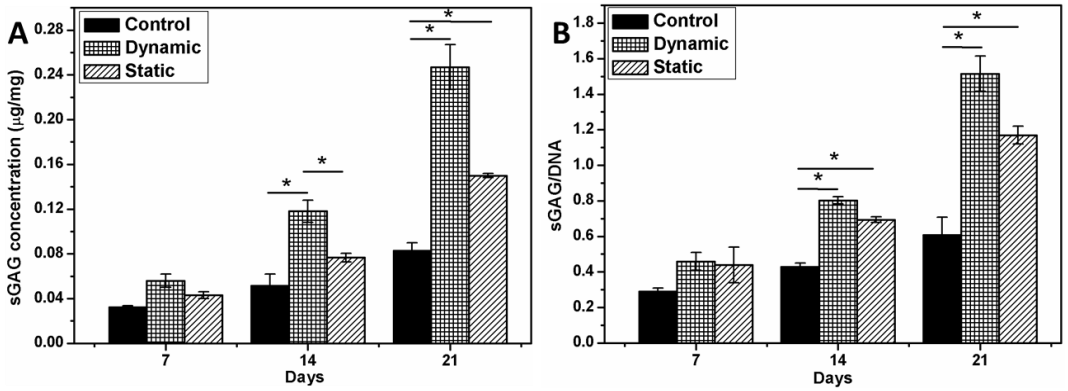

Figure 5.4.5 (A) Total sGAG secretion assessment by chondrocytes on SF/CS-Ch scaffolds cultured under static and dynamic conditions as compared to SF/CS scaffold (control). (B) Normalised sGAG content with respect to DNA quantification of hMSCs growing on the scaffolds for 21 days (n=3, *$p < 0.05$), demonstrating higher degree of chondrogenic differentiation occurring in SF/CS-Ch containing constructs.

5.4.3.2 Histological evaluation

At the end of 21 days of culture in chondrogenic media, the constructs generated from hMSCs seeded scaffolds containing Ch showed positive staining for alcian blue. The staining appeared denser and colony formation of chondrocytes was evident in the construct cultured in spinner flask bioreactor (Figure 5.4.6B). In static culture, all the cells showed blue colored ECM production, however, cell colony was smaller than that observed in dynamic culture

(Figure 5.4.6C). The cells in non-induced culture also showed blue coloration when stained for proteoglycan matrix (Figure 5.4.6E and F), although the number of cells showing blue colored matrix was very much lower than their respective induced cultures, with significant difference ($p < 0.05$) in optical density (Figure 5.4.6D). The optical density of alcian blue, representing the quantification of proteoglycan matrix staining, was higher in the constructs developed in spinner flask bioreactor. The result demonstrated chondrocyte like ECM deposition, and shifting of cells phenotype from MSCs to chondrocytes under the influence of Ch. This observation is in accordance with earlier study that showed the stimulatory effect of Ch on production of chondrocyte matrix components specifically demonstrating large amount of proteoglycan staining using alcian blue in the scaffolds containing col II-Ch-hyaluronic acid (Ko et al. 2009).

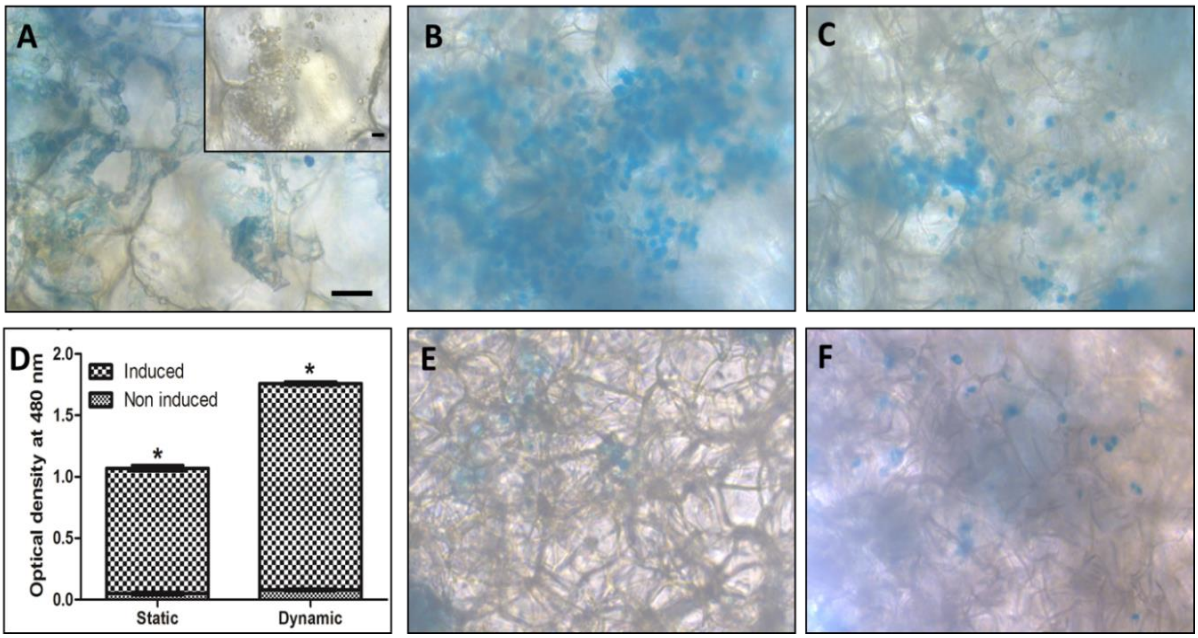

Figure 5.4.6 Histology staining for constructs developed containig (A) SF/CS (control) and SF/CS-Ch scaffolds in (B and E) dynamic and (C and F) static culture condition showing proteoglycan matrix stained blue by alcian blue after 21 days of chondrogenic differentiation. E, F and inset in A show non-induced cultures. Scale bar= 50 µm (D) Bar graph showing difference in optical density for alcian blue staining between the static and spinner flask culture systems, with significant difference between induced and non-induced cultures (n=3, *$p < 0.05$).

5.4.3.3 Immunofluorescence study

Chondrocyte differentiation of hMSCs was evaluated by studying the fluorescence of Col II and Acan, the predominant chondrocyte matrix proteins. Cartilage tissue mainly contains Col II in its matrix, and its expression by differentiating hMSCs indicates successful

chondrogenesis (Lee et al. 2006). On the other hand, Acan is responsible for compressive strength of tissue by forming macromolecular aggregates in cartilage matrix (Poole et al. 2002). The expression of Col II and Acan in cell ECM was observed in the cells cultured in SF/CS-Ch scaffolds (Figure 5.4.7). The study of Col II expression in non-induced culture (Figure 5.4.7C), demonstrated that the presence of Ch enhanced the expression of the matrix components, indicating its role in promoting chondrogenic differentiation of hMSCs. The expression of these markers, as indicated by integrated density analysis, was higher in the constructs developed in SF/CS-Ch scaffolds than control ($p < 0.05$, Figure 5.4.7F). The immunofluorescence analysis of cells in SF/CS-Ch scaffolds also showed aggregate formation.

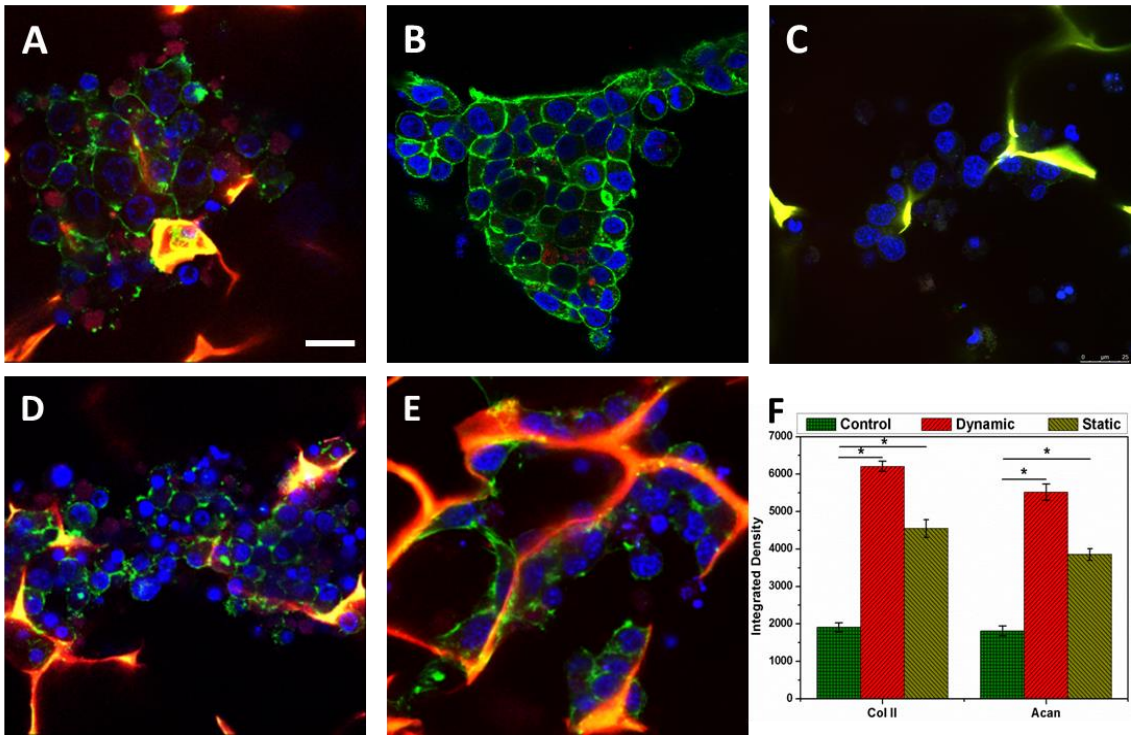

Figure 5.4.7 Immunofluorescence staining of Col II (A, C and D) and Acan (B and E), shown in red in chondrocytes ECM cultured under (A-C) dynamic and (D and E) static condition. (C) Col II staining in non-induced culture. Cell nucleus is stained blue and cytoskeleton in green. Scale bar= 25 µm. (E) Representing integrated density analysis of ECM staining (n=3, *$p < 0.05$). The results show efficiency of SF/CS-Ch scaffolds in promoting synthesis of chondrocyte specific ECM components, in the presence of induction media and dynamic culture environment.

The typical chondrogenic phenotype includes spherical morphology, with ample ECM secretion that majorly comprises of Acan and Col II, and cell aggregation leading to diffused cytoskeleton (Bhardwaj and Kundu 2012). From confocal microscopy study, it is evident that

the cells in constructs exhibited chondrocyte phenotype indicating successful chondrogenic differentiation.

The histological, sGAG quantification and immunofluorescence studies show enhanced accumulation of cartilaginous ECM by hMSCs differentiated on SF/CS-Ch scaffolds as compared to SF/CS scaffolds. These studies confirmed that the hMSCs cultured on SF/CS-Ch scaffold acquired chondrocyte phenotype, in terms of morphology, aggregation and deposition of proteoglycan and collagenous matrix (Dominici et al. 2006; Somoza et al. 2014).

5.4.3.4 qPCR analysis

The induction of chondrogenesis of hMSCs over the SF/CS-Ch scaffold was confirmed by qPCR analysis assessing the expression of chondrocyte specific genes such as Sox9, MATN3, Col II and Acan, and Col I, which is usually down-regulated in chondrocytes (Ko et al. 2009; Sawatjui et al. 2015). As observed from Figure 5.4.8A, the expression of Col I was decreasing throughout the culture period with significant difference ($p < 0.05$) among subsequent observations. However, in control and static system, the reduction in Col I expression was insignificant throughout the culture period. The expression of Sox9 was up-regulated during the differentiation period and the highest expression of 24.12±0.61 fold was observed in SF/CS-Ch on 21st day (Figure 5.4.8B). A significant increase in MATN3 expression was also seen on 14th day which is higher as compared to 7th day in constructs containing SF/CS-Ch scaffolds, with a slight decrease on 21st day as expected (Figure 5.4.8C). The expression pattern of Col II and Acan confirmed the immunofluorescence findings, and was observed to be highly expressed in Ch containing SF/CS scaffolds (Figure 5.4.8D and E). However, the increase in expression for chondrogenic markers Sox9, Col II and Acan, was not very prominent in the static culture system. The lower expression in static culture may be due to the insufficient availability of required nutrients that affected the removal of metabolites necessary for the progression of chondrogenesis during *in vitro* incubation (Wang et al. 2008).

The increase in Col II expression versus a decline in Col I gene expression with culture period (Figure 5.4.8F), is in accordance with the literature that confirms the phenotype shift

of cells from hMSCs to chondrocytes at gene level (Gigout et al. 2009; Bhardwaj and Kundu 2012). The differentiation of hMSCs in Ch containing SF/CS scaffolds was evident by up-regulation of mRNAs for cartilage-related genes (Sox9, MATN3, Col II and Acan). A similar observation was reported in another study where cells cultured on Ch containing Collagen-Hyaluronic acid scaffolds showed upregulation of Sox9, Acan and Col II genes, with decreased expression of Col I, in comparison to pure collagen scaffolds. The observed result was speculated to be due to the stimulatory effect of Ch on cell metabolism that increased the interaction between ligands present in ECM and cells, ultimately leading to gene upregulation (Ko et al. 2009; Yan et al. 2013). Thus, the presence of Ch was proven to be beneficial for accelerating chondrogenesis of hMSCs seeded onto the scaffolds as well as maintaining their characteristic phenotype.

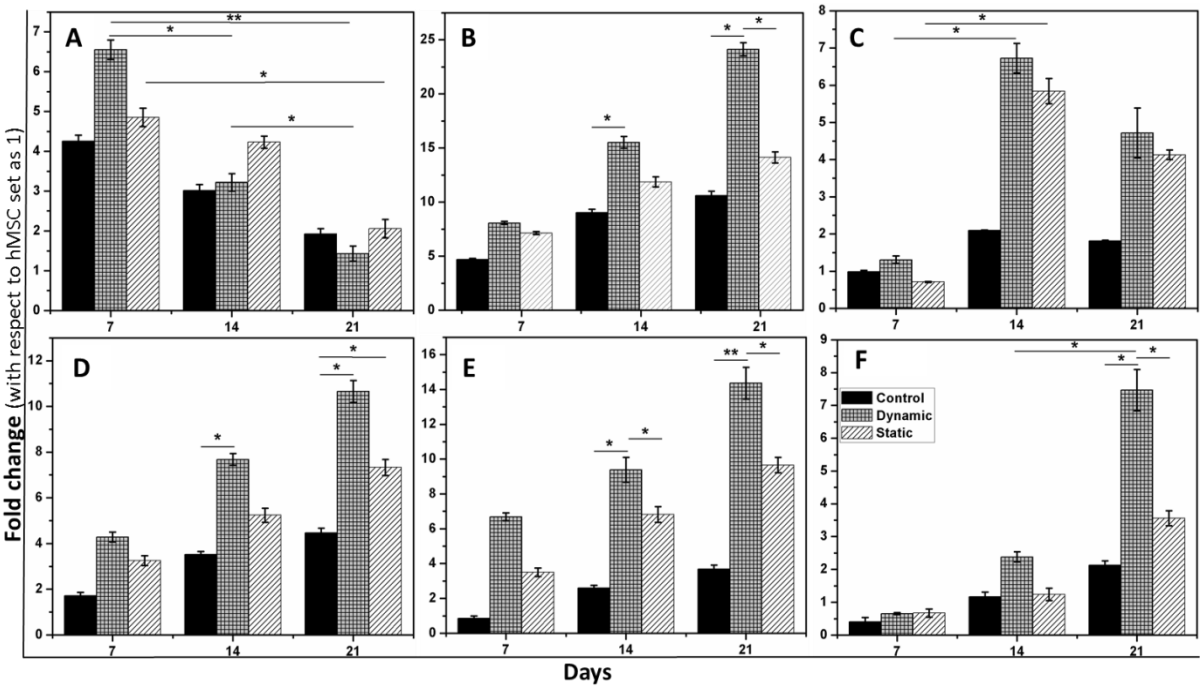

Figure 5.4.8 qPCR study representing expression of (A) Col I, (B) Sox9, (C) MATN3, (D) Col II and (E) Acan relative to hMSCs (Fold change set as 1) on 7th, 14th and 21st day of chondrogenic differentiation, for control and SF/CS-Ch scaffolds cultured under static and dynamic conditions. (F) Relative expression of Col II/Col I representing higher degree of chondrogenic progression in dynamic condition (n=3, $^{**}p < 0.01$, $^{*}p < 0.05$).

Conclusion

SF/CS-Ch scaffolds showed an overall improvement in cell attachment, distribution and proliferation in dynamic culture condition. Keeping culture conditions same, the results of *in*

vitro differentiation showed a greater extent of chondrogenesis of hMSCs in SF/CS-Ch scaffolds as compared to SF/CS and SF/CS-Gl scaffolds as demonstrated in earlier chapters. The histology assessment for proteoglycan matrix synthesis, sGAG quantification, immunofluorescence and gene expression of Col II, Acan and other chondrogenic markers, namely MATN3 and Sox9, were improved in SF/CS-Ch scaffold. The presence of Ch has shown to have positive impact thereby stimulating the synthesis of proteoglycans. Thus, it was demonstrated that the additive effect of the presence of Ch in SF/CS scaffolds and dynamic culture environment resulted in cartilage construct generation, which has potentiality to promote cartilage tissue regeneration.

Chapter 5E

Development of cartilage construct by culturing and differentiating hMSCs over SF/CS-Glucosamine-Chondroitin sulfate scaffold

In earlier chapters, the addition of Gl and Ch in the SF/CS scaffold was demonstrated to be beneficial for maintenance of chondrogenic phenotype of hMSCs upon differentiation. It is reported that no single drug is able to perform all the required functions, and studies on orally administered Gl and Ch in combination has shown that their long term use retards OA progression (Lippiello et al. 2000; Pavelka et al. 2002). These components were also studied individually in different scaffold formulations (Zhang et al. 2011; Anisha et al. 2013; Huang et al. 2015; Chen et al. 2016a). However their effect on chondrogenesis of stem cells in combination is unexplored so far. Therefore, this part of study has been designed to assess the combined effect of Gl and Ch in the SF/CS porous scaffold with the aim of further enhancing the attachment, proliferation and differentiation of UCB-hMSCs and thereby generation of cartilage construct.

The chondrogenic differentiation of hMSCs involves four major stages, cell proliferation followed by aggregation, gene regulation and finally ECM deposition (Xu et al. 2014). Among these, aggregation of cells acts as an initiator for expression of genes that drive the cells to later stages of differentiation. Thus, pellet culture method, which is a conventional method of cell aggregation commonly used for chondrocytes culture, was also studied in this part (Zhang et al. 2010b). Cartilage construct generation was further studied by culturing hMSCs on SF/CS-Gl-Ch scaffolds under dynamic condition in a spinner flask bioreactor. This chapter describes the result and discussion of these experimental studies.

5.5.1 Fabrication and physicochemical characterization of SF/CS-Gl-Ch scaffold

1 wt% Gl containing SF/CS blend (80:20 v/v) was modified by adding Ch in 0.5, 1.0 and 1.5 wt% and thus SF/CS-Gl-$Ch_{0.5}$, SF/CS-Gl-$Ch_{1.0}$ and SF/CS-Gl-$Ch_{1.5}$ composite scaffolds were prepared. The scaffolds were fabricated by freeze drying method and physicochemical characterization (Table 5.2) showed their suitability for TE applications. Well interconnected open pore structure of the scaffolds was evident from the transverse and longitudinal sections of SEM study (Figure 5.5.1A-F). The pore size slightly decreased with increase in Ch content (Figure 5.5.1A-C) in the SF/CS-Gl-Ch scaffolds that also contributed in overall increase in porosity. The decrease in contact angle and increase in biodegradation of SF/CS-Gl-$Ch_{1.5}$ scaffold, compared to SF/CS-Gl-$Ch_{0.5}$ and SF/CS-Gl-$Ch_{1.0}$ scaffolds, was owing to the hydrophilic nature of Ch (Yan et al. 2013).

Table 5.2 Physicochemical properties of SF/CS-Gl-Ch scaffolds

Scaffold composition	Pore size (µm)	Porosity (%)	Contact angle (Degree)	Biodegradation in 28 days (%)
SF/CS-Gl-$Ch_{0.5}$	76.8-196.5	86.7±2.1	49.6±0.1	32
SF/CS-Gl-$Ch_{1.0}$	62.8-193	89.6±1.6	46.8±0.8	38
SF/CS-Gl-$Ch_{1.5}$	56.5-168.1	90.3±1.3	40.86±0.4	39.4

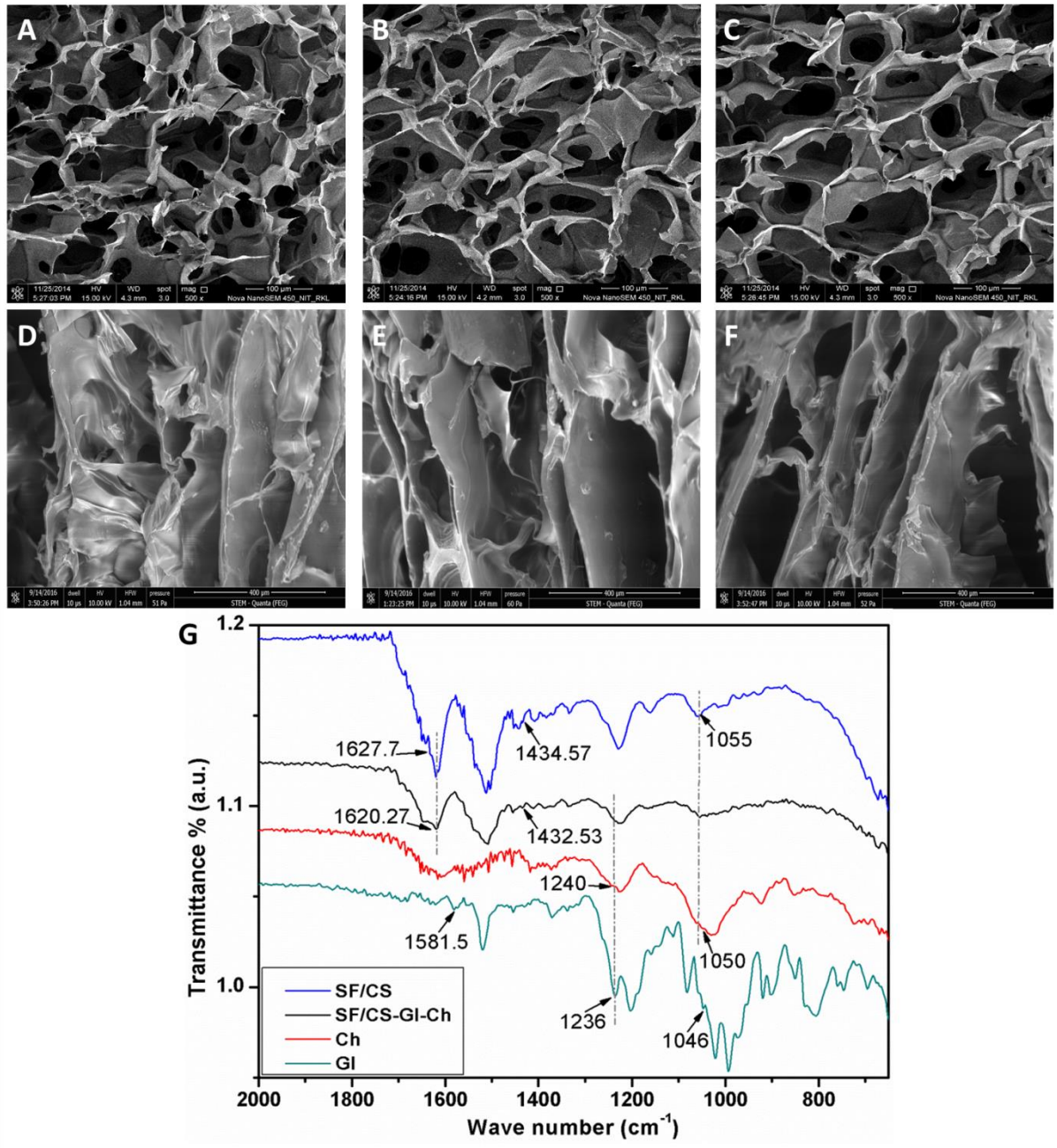

Figure 5.5.1 Physicochemical characterization of SF/CS-Gl-Ch scaffold. (A-F) FESEM micrographs representing (A-C) transverse and (D-F) longitudinal sections of (A and D) SF/CS-Gl-$Ch_{0.5}$, (B and E) SF/CS-Gl-$Ch_{1.0}$ and (C and F) SF/CS-Gl-$Ch_{1.5}$ scaffolds, showing interconnected pore network. (G) FTIR spectra of Gl and Ch powder, SF/CS blend and SF/CS-Gl-Ch scaffold representing intermolecular interaction.

As indicated in FTIR spectroscopy (Figure 5.5.1G), the characteristic -CH deformation peak of CS is present at 1434.57 cm^{-1} in SF/CS blend and with a slight shift to 1432.53 cm^{-1} in SF/CS-Gl-Ch scaffold (Wang and Li 2007). Numerous small peaks between 1500 cm^{-1} to 1700 cm^{-1} observed in Gl depicting amine group, were broadened in the composite scaffold and appeared as a single prominent peak at 1620.27 cm^{-1}. The characteristic peak for asymmetric NH_3^+ bending found in Gl at 1581.5 cm^{-1} was completely absent in composite scaffold (Foot and Mulholland 2005). The peak for amide bond appeared as a weak shoulder at 1627.7 cm^{-1} that corresponds to β-sheet structure of SF in the blend scaffold (Nazrov et al. 2004). Whereas, the band at 1236 cm^{-1} depicting S=O stretching was found in both Gl and SF/CS-Gl-Ch scaffolds, and with a slight shift to 1240 cm^{-1} in Ch, confirming the presence of sulfate group. Characteristic peak for C-O-S vibration was present in Ch powder at 850 cm^{-1}, which was not shown in the scaffold. The vibration of C-C bond was common in all the compounds, and was observed at 1046 cm^{-1} in Gl, 1050 cm^{-1} in Ch and 1055 cm^{-1} in SF/CS and SF/CS-Gl-Ch scaffolds (Foot and Mulholland 2005).

5.5.2 Assessment of cell-scaffold construct

5.5.2.1 Cell attachment, morphology and spreading

The FESEM micrographs depicted in Figure 5.5.2A-C revealed uniform spreading of hMSCs on SF/CS-Gl-Ch scaffolds, and insets show the unseeded scaffolds. As indicated, hMSCs appeared elongated, though the clear morphology could not be observed, which is due to the excessive deposition of ECM. Cell to cell interconnection was noticed to be well established and cells were homogenously distributed on the scaffolds surface. The secretion of ECM was more prominent in scaffolds containing 1.0% and 1.5% Ch (Figure 5.5.2B and C). In SF/CS-Gl-$Ch_{1.5,}$ the ECM secreted by cells was completely covered the scaffold surface reflecting the beneficial effect of presence of Ch in higher amount that leads to higher ECM production. A gradual increase in ECM synthesis with Ch content is due to the regulatory effects on matrix production (Varghese et al. 2008).

The cells in pellet culture were elongated with interconnected network as evident from FESEM micrographs (Figure 5.5.2D). The aggregates formed by pellet culture were spherical in shape, with a diameter range from 1675-1875 µm, the average of which is 1808.33 µm (Figure 5.5.2E).

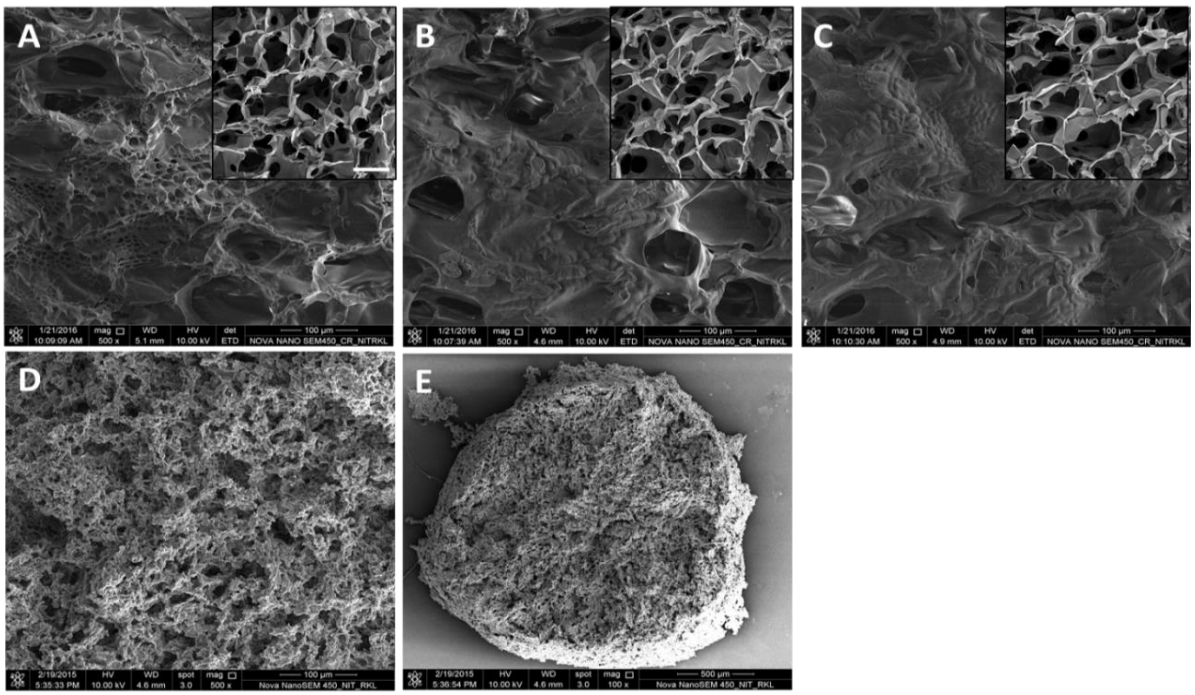

Figure 5.5.2 FESEM micrograph representing hMSCs attachment and spreading on SF/CS-Gl-Ch scaffolds with (A) 0.5%, (B) 1.0% and (C) 1.5% Ch. Insets represent the unseeded scaffolds, scale bar= 100 µm. (D) FESEM of cell aggregate and (E) lower magnification image showing shape and size of the aggregate formed by pellet culture. The results reflect suitability of scaffolds for cell attachment, and substantial amount of ECM secretion was observed by cells cultured in SF/CS-Gl-$Ch_{1.0}$ and SF/CS-Gl-$Ch_{1.5}$ scaffolds.

5.5.2.2 Cell viability and distribution

The live-dead analysis demonstrated the localization of live and dead hMSCs in the scaffolds on 14th day of culture. As observed in Figure 5.5.3A-F, the green fluorescent live cells were evenly distributed throughout the scaffolds, with a fewer red fluorescent dead cells. The formation of small cell aggregates was observed in the scaffolds containing Ch in 1.0% or greater amount. The viable cell population was increasing with increase in Ch content with significantly higher ($p < 0.05$) difference in 1.0 and 1.5% Ch in comparison to 0.5% Ch containing scaffold on 14th day (Figure 5.5.3G). The amount of cell penetrated into the core of scaffolds was lesser in SF/CS-Gl-$Ch_{0.5}$ scaffolds, though their distribution throughout the scaffold structure was uniform (Figure 5.5.3H). At the core, a significantly higher ($p < 0.05$) number of cells were present in SF/CS-Gl-$Ch_{1.0}$ (470 ± 35 cell/mm^2) and SF/CS-Gl-$Ch_{1.5}$ (550 ± 42 cell/mm^2) scaffolds, than SF/CS-Gl-$Ch_{0.5}$ (342 ± 26 cell/mm^2). The cell distribution analysis showed that all the three scaffolds supported cell penetration throughout its structure, which may also be due to the directional fluid flow driven by dynamic culture environment. Notably, the cell distribution in the SF/CS-Gl-$Ch_{1.5}$ scaffolds was more even

that may be attributed to the uniform pore morphology and higher porosity in these scaffolds.

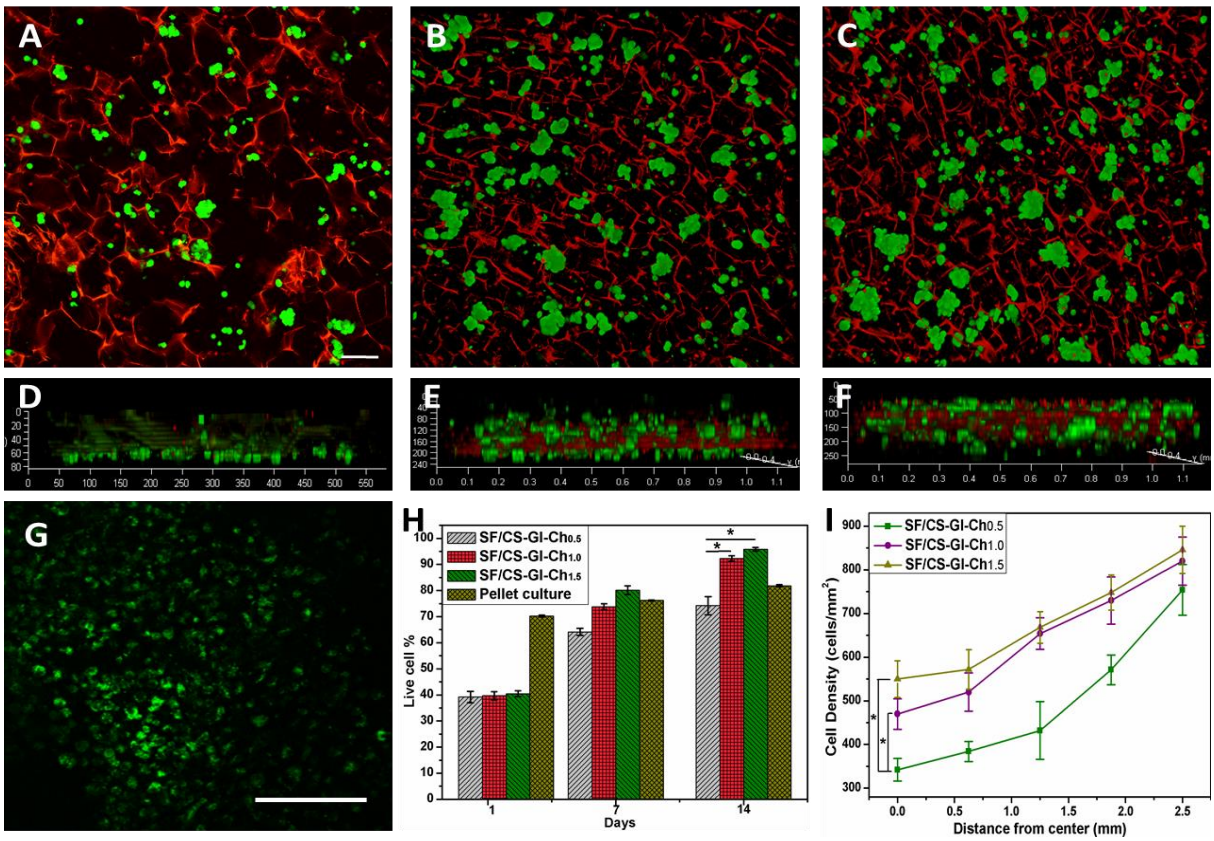

Figure 5.5.3 Fluorescent assay for hMSCs seeded SF/CS-Gl-Ch scaffolds with (A and D) 0.5%, (B and E) 1% and (C and F) 1.5% Ch, showing green live and red stained dead cell population on 14th day. Scale bar= 100 µm. (G) hMSCs aggregates by pellet culture showing green stained live cell population. Scale bar= 50 µm. (H) Live cell % on scaffolds and pellet culture with increase in culture duration. (I) Cell distribution with scaffold depth (n=3, $*p < 0.05$). The results demonstrate even distribution of cells in all the scaffolds, with significantly higher viability and distribution in SF/CS-Gl-Ch$_{1.5}$ scaffold as compared to other scaffolds.

The cells in aggregates formed by pellet culture have shown green fluorescence depicting the presence of live cells throughout the aggregate (Figure 5.5.3G). The intensity analysis revealed an increase in live cell population with increase in culture duration, with significant change from 1st to 14th day in the aggregate culture (Figure 5.5.3H). Furthermore, there was a gradual increase in live cell population in pellet culture with increase in culture period, and the highest viable cell population of 81.85±0.45% was obtained on 14th day of culture. The cell population was lesser than those observed with cell cultured on SF/CS scaffolds loaded with 1% (92.3±1.1%) and 1.5% Ch (95.8±0.7%) as shown in Figure 5.5.3G. Since the aggregates formed by this method were comprised of cells only, the in-depth cell distribution analysis was not performed.

5.5.2.3 Metabolic Activity

Figure 5.5.4A shows the metabolic activity of hMSCs over the scaffolds on 1st, 7th and 14th day of culture. There was an increase in absorbance, representing the increase in cell metabolic activity for all the constructs with increase in culture period. On 14th day, the metabolic activity of the cells was significantly higher ($p < 0.05$) in SF/CS-Gl-Ch$_{1.5}$ than SF/CS-Gl-Ch$_{0.5}$ scaffold. The activity was also more than SF/CS-Gl-Ch$_{1.0}$ though the difference was statistically non-significant. This observation may be attributed to the stimulatory effect of Ch in increasing the interaction between growth factors and cells, leading to increased metabolic activity of cells (Yan et al. 2013). The difference in Ch content is greater among SF/CS-Gl-Ch$_{1.5}$ and SF/CS-Gl-Ch$_{0.5}$ scaffold that resulted in a significant difference in the metabolic activity of cultured cells.

The metabolic activity of cells also increased in aggregate during 14 days culture time. Surprisingly, although the cell number was higher in cell aggregates, the metabolic activity of cells in pellet culture was comparable to the activity shown by cell-seeded scaffolds on 7th and 14th day. ECM production can be considered as one of the prime functions representing metabolic activity, this observation co-relates with the FESEM result, where lesser or no ECM secretion was observed by cells in pellet culture as compared to the cells cultured in scaffolds.

5.5.2.4 DNA quantification

The cell proliferation studied by DNA content analysis (Figure 5.5.4B) followed a similar trend as measured by MTT study. The DNA content of cells in scaffolds almost became double on 14th day, and thereafter, the change in DNA content was insignificant. The proliferating cell population was higher in SF/CS-Gl-Ch$_{1.5}$ at all the time points with significantly higher difference than SF/CS-Gl-Ch$_{0.5}$ on 14th ($p < 0.05$) and 21st day ($p < 0.01$). The DNA content of SF/CS-Gl-Ch$_{1.0}$ was also significantly higher ($p < 0.05$) than SF/CS-Gl-Ch$_{0.5}$ on 21st day. Furthermore, there was a significant rise ($p < 0.05$) in DNA content for the cell aggregates formed by pellet culture, from 7th to 14th and 21st day, though the difference was not significant between 14th and 21st day of culture. The amount of DNA in scaffolds remained significantly lower than those in cell aggregate, which may be owing to the structural and composition differences in the scaffolds.

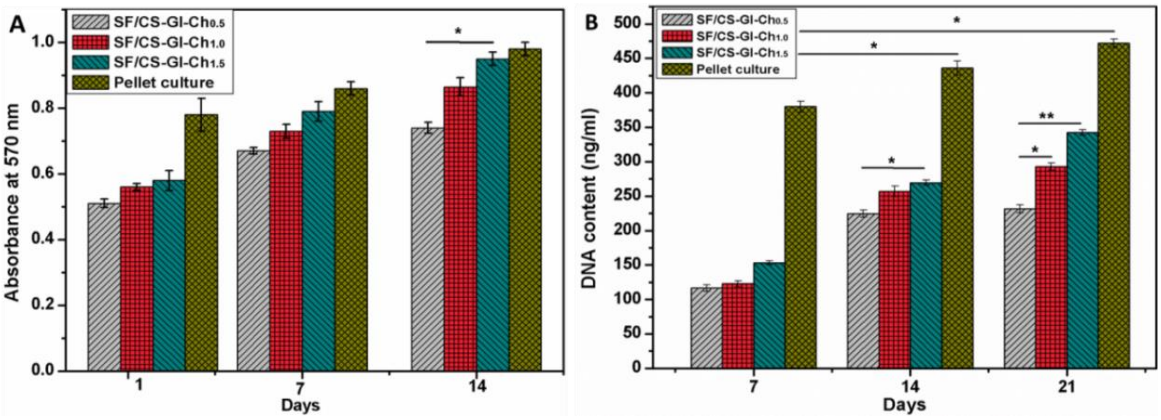

Figure 5.5.4 (A) Cell metabolic activity assessment by MTT assay and (B) DNA quantification on SF/CS-Gl-Ch scaffolds and cell aggregate formed by pellet culture for 21 days (n=3, *$p < 0.05$, **$p < 0.01$). SF/CS-Gl-$Ch_{1.5}$ scaffold supported cell metabolic activity and promoted cell proliferation to a greater extent than other scaffolds.

Based on MTT assay and DNA content study, the initial rapid increase observed in metabolic activity and cell proliferation rate indicates the quick adaptation of cells to the 3D environment provided by the scaffolds. Similar observation was also reported on using 2D expanded rat chondrocytes in alginate beads and culturing in spinner flask for 28 days (Xu et al. 2014). However, in this study, the higher rate of cell proliferation obtained with SF/CS-Gl-$Ch_{1.5}$ scaffolds than SF/CS-Gl-$Ch_{1.0}$ and SF/CS-Gl-$Ch_{0.5}$ scaffolds or SF/CS, SF/CS-Gl and SF/CS-Ch scaffolds, studied in earlier chapters, may be due to the structural differences in terms of increase in pore interconnectivity and decrease in average pore size. This led to higher porosity and greater hydrophilicity that supported cell attachment, infiltration and proliferation in a favourable manner (Oh et al. 2003; Naeimi et al. 2014; Bruzauskaite et al. 2016). Thus, based on the *in vitro* study, SF/CS-Gl-Ch scaffold consisting of 1.5% Ch was considered as the most suitable scaffold for further study.

5.5.3 Assessment of chondrogenic differentiation

5.5.3.1 Total sGAG estimation

Figure 5.5.5A shows the deposition of sGAG by chondrocytes in scaffolds and in pellet culture with time. Although, there was no difference in sGAG synthesis at initial stage (7^{th} day) of culture, a significantly higher ($p < 0.05$) sGAG deposition was obtained with cell seeded scaffold (construct) than that obtained in pellet culture on 14^{th} and 21^{st} day. On 21^{st} day, sGAG deposited by cells in the construct using SF/CS-Gl-Ch scaffolds was 383 µg/mg,

which was higher than that observed in SF/CS scaffolds loaded with these components individually, 130 µg/mg with glucosamine and 247 µg/mg with chondroitin sulfate. In native cartilage tissue, Gl and Ch show regulatory role in sGAG synthesis pathway, thus enhancing proteoglycan deposition by the chondrocytes (Vangsness et al. 2009). In this study, their combination in scaffold showed synergistic effect on sGAG synthesis, representing their potentiality in prevention of cartilage tissue degeneration along with enhancing regeneration capability. The observed results correlate with the earlier study where *in vitro* combination of Gl and Ch was shown to stimulate sGAG synthesis to a greater extent than their use individually as an oral supplement in to rabbit model suffering with osteoarthritis (Lippiello et al. 2000).

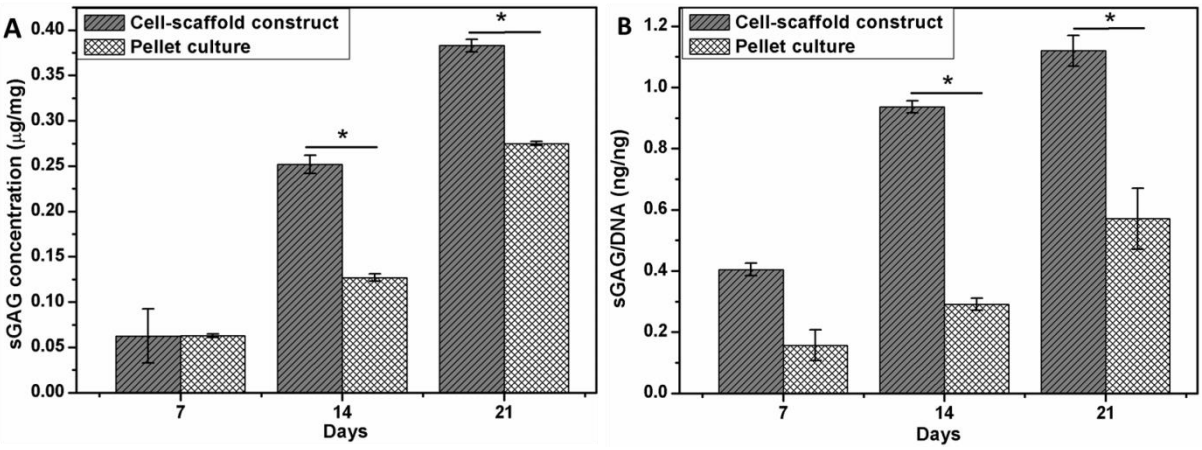

Figure 5.5.5 (A) Total sGAG secretion by chondrocytes on SF/CS-Gl-Ch scaffolds (construct) and pellet system (n=3, $*p < 0.05$). (B) Normalised sGAG content with respect to DNA quantification for 21 days, representing superiority of constructs in chondrocyte ECM secretion.

Furthermore, to study the relation between differentiation and proliferation phenomenon occurring in the cells, the obtained results for sGAG content was normalized to DNA content, and the result is represented as sGAG/DNA (Figure 5.5.5B). The cells in scaffolds showed a higher value for sGAG/DNA than pellet culture system at all the time points, with significant difference ($p < 0.05$) on 14^{th} and 21^{st} day. The results represent that in cell-scaffold construct, a higher rate of cell differentiation was shown with respect to proliferation. Gl and Ch are the molecules that possess carboxylic acid and sulfate moieties that make their polarity highly negative, this in turn attracts positively charged growth factors (Sawatjui et al. 2015). Thus the presence of Gl and Ch in the scaffold facilitated the adsorption of growth factors and made them available for the cells cultured on them resulting into improving their attachment, ECM secretion and differentiation.

5.5.3.2 Histological evaluation

The histology study by alcian blue staining showed chondrocyte type matrix component in ECM of hMSCs when cultured on SF/CS-Gl-$Ch_{1.5}$ scaffolds (Figure 5.5.6A and B), and aggregate formation by pellet culture for 21 days (Figure 5.5.6C). A plenty of proteoglycan matrix was observed in cytoplasm and ECM in blue color. ECM staining in pellet culture was more prominent at aggregate boundary and lighter towards the core, indicating the presence of cells that are inferior in phenotype at the centre of aggregate (Zhang et al. 2010b). All the cells in scaffold showed uniform staining with alcian blue that represents the homogeneity of constructs in maintaining stable chondrocyte phenotype. The quantification of proteoglycan matrix staining using alcian blue was performed by optical density analysis that showed a significant difference ($p < 0.05$) between induced and non-induced cultures (constructs cultured without differentiation media) (Figure 5.5.6D). The results demonstrated the requirement of inducing factors for initiating the chondrogenic differentiation as well as the efficiency of construct in developing chondrogenic phenotype.

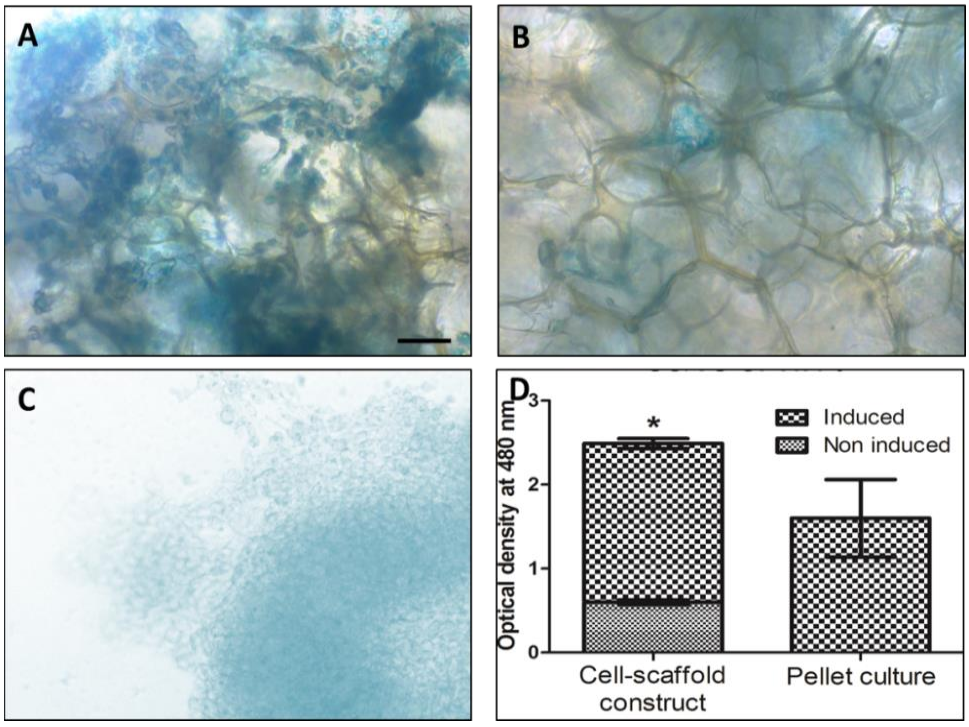

Figure 5.5.6 Histology staining for cell seeded SF/CS-Gl-Ch scaffold cultured under (A) induced and (B) non-induced medium, and (C) pellet culture showing proteoglycan matrix staining by alcian blue after 21 days of chondrogenic differentiation (Scale bar= 50 µm). (D) Bar graph showing difference in optical density for alcian blue staining between the culture systems, with significant difference between induced and non-induced cultures (n=3, *$p < 0.05$). The constructs showed higher degree of proteoglycan matrix staining and development of chondrogenic phenotype.

These result confirmed the result of sGAG deposition study where proteoglycan matrix productivity was higher in construct than pellet culture. This observation is in accordance with the earlier study that demonstrated enhanced proteoglycan synthesis by the chondrocytes cultured *in vitro* in the medium supplemented with Gl and Ch (Lippiello 2003). The presence of GAG stimulating components, Gl and Ch in scaffolds, might have stimulated differentiation process and helped in acquiring and maintaining chondrogenic phenotype of cells in a better manner as compared to the scaffold-free culture (Lippiello et al. 2000).

5.5.3.3 Immunofluorescence study

The cartilage specific ECM production was further examined by immunofluorescence staining using Col II and Acan (both represented in red colour in Figure 5.5.7) after 21 days of chondrogenic initiation. The developed construct showed uniform immunofluorescence for both the markers in cytoplasm and ECM, among the studied culture groups (Figure 5.5.7A and C). While cells in pellet culture showed greater staining for Acan (Figure 5.5.7D), the staining for Col II was not observed (Figure 5.5.7B).

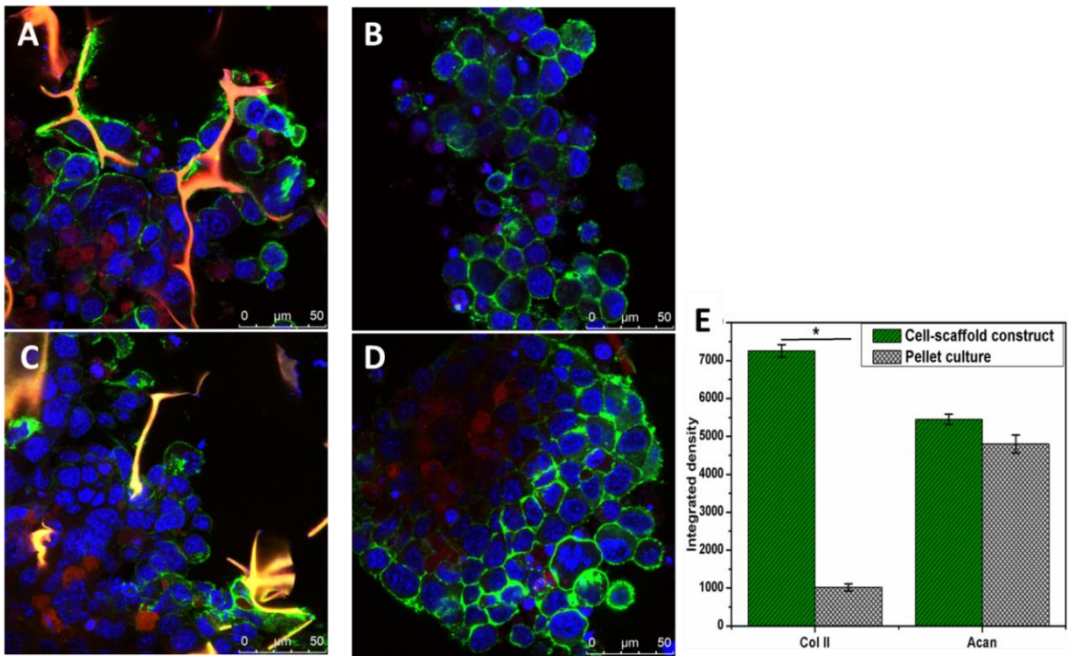

Figure 5.5.7 Confocal microscopy images of chondrogenic differentiated hMSCs on (A and C) SF/CS-Gl-Ch scaffolds and (B and D) pellet culture, where red represent immunofluorescence of Col II in A-B and Acan in C-D. Green fluorescence represents β-actin stained by phalloidin and blue corresponds to nucleus stained by Hoechst 33258. (E) Integrated density analysis of the ECM staining (n=3, *$p < 0.05$), showing significantly higher expression of cartilagenous matrix components (Col II and Acan) in the constructs compared to pellet culture.

Integrated density analysis, performed to quantify the fluorescence on ECM components, supported microscopic observation, and Col II expression was observed to be significantly higher ($p < 0.05$) in construct than pellet culture, though the intensity of Acan was comparable among the culture groups (Figure 5.5.7E). The results reflected the higher degree of non-collagenous (proteoglycan) matrix production in pellet culture as compared to the collagenous matrix. This may be attributed to poor distribution of nutrients and growth factors at the central region of the aggregates that resulted into inconsistency in metabolic activity of cells, leading to difference in ECM production ability (Zhang et al. 2010b). However, the ability of producing both types of cartilage ECM components, as shown by the cells in constructs, increases the possibility of a wider application of constructs, i.e. generation all types of cartilage, for cartilage tissue engineering. As evident by fluorescence staining of cytoskeleton component (β-actin), represented by green color, depicted that cells in both the culture groups attained characteristic chondrocyte like round morphology.

5.5.3.4 qPCR analysis

The qPCR analysis showed the expression of Col I, Sox9, MATN3, Col II and Acan chondrogenic markers at gene level on 7^{th}, 14^{th} and 21^{st} day of chondrogenic initiation. The expression profiles of these genes are represented as fold change with respect to undifferentiated hMSCs (Figure 5.5.8). The expression of Col I, the marker usually present in hMSCs and supressed in chondrocytes, was observed to be decreasing with culture period in all the culture systems, with a significant change ($p < 0.05$) in construct with respect to pellet culture on 14^{th} and 21^{st} day (Figure 5.5.8A). A significant down-regulation ($p < 0.05$) in Col I expression was also evident from 7^{th} to 21^{st} day in cell scaffold construct. The relative expression in Col I gene in pellet culture was 6.57 fold on 21^{st} day, which represents the inferiority in phenotype of cells present in aggregate. Sox9, a transcription factor, was highly expressed on 14^{th} day in construct, which showed a decrease on 21^{st} day (Figure 5.5.8B). The expression of Sox9 in pellet culture was significantly lower than cell-scaffold construct ($p < 0.01$) on 14^{th} and 21^{st} day. MATN3 is a non-collagen cartilage ECM component. Its expression profile was similar to Sox9, showing the highest expression on 14^{th} day and declined beyond this period in both the culture condition (Figure 5.5.8C). The fold change in both culture systems was comparable for MATN3 at all the time points. Col II is the most abundant matrix component of hyaline cartilage. The expression of Col II was increasing with increase in culture time, and was significantly up-regulated in cell-scaffold construct on

14th ($p < 0.05$) and 21st day ($p < 0.01$) as compared to 7th day (Figure 5.5.8D). The expression of Acan, the most abundant proteoglycan for chondrocytes, followed a similar trend of Col II (Figure 5.5.8E). For the late chondrogenic markers (Col II and Acan), pellet culture offered lower expression level than construct on 21st day. The difference in Acan expression was significantly higher ($p < 0.05$) in construct compared to pellet culture on 21st day.

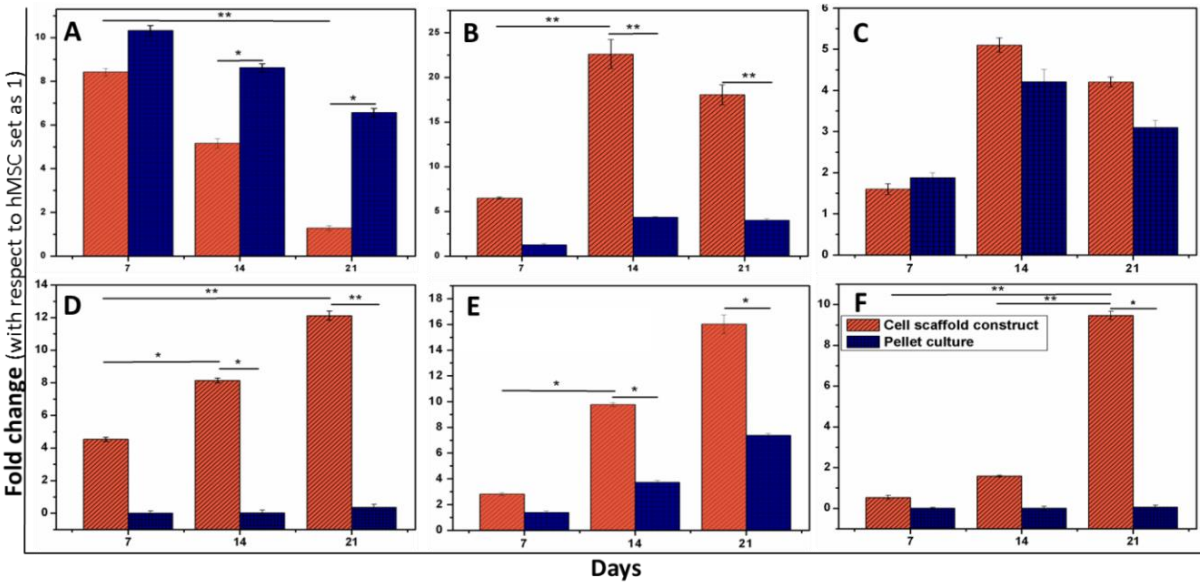

Figure 5.5.8 qPCR study representing expression of (A) Col I, (B) Sox9, (C) MATN3, (D) Col II and (E) Acan relative to hMSCs (Fold change set as 1) on 7th, 14th and 21st day of chondrogenic differentiation, under cell seeded SF/CS-Gl-Ch scaffold and pellet culture systems. (F) Relative expression of Col II/Col I representing higher degree of chondrogenic progression in cell-scaffold construct (n=3, *$p < 0.05$, **$p < 0.01$).

To determine the degree of progression of chondrogenesis, the expression of Col II was compared with Col I (Figure 5.5.8F). The higher Col II/Col I ratio for constructs at all the time points, prove that the cells present in constructs were active in differentiation right from the 7th day, with significant rise on 21st day. However, there was no apparent change in cell aggregate, representing that the rate of chondrogenic differentiation was slower in the pellet culture. The observed upregulation of chondrogenic genes in their respective stages may be attributed to the presence of Gl and Ch in combination in the SF/CS scaffold that provided required biological signals by attracting the differentiation promoting factors present in the culture environment to enhance the differentiation process (Yan et al. 2013). Similarly, Sawatjui et al. demonstrated an upregulation of Col II and Acan with down regulation of Col I in BM-MSCs cultured on Ch containing SF-gelatin-hyaluronic acid scaffolds as compared to cell pellet. On comparing the results with non-Ch containing scaffold, it was concluded

that the presence of Ch is the major regulator of improving chondrogenic differentiation of BM-MSCs (Sawatjui et al. 2015).

The results of pellet culture demonstrated a comparatively stronger proteoglycan matrix production and up-regulation of associated gene as compared to the collagenous matrix, suggesting their inefficiency for application in hyaline cartilage. Although Sox9 plays a regulator for expression of other ECM components in chondrocytes, its expression in pellet culture did not induce the secretion of col II, as evident from qPCR and immunofluorescence analysis. A high cell density is desirable for initiation and enhancement of chondrogenesis of hMSCs (Zhang et al. 2010b; Xu et al. 2014), but in the present study, it was observed that high density cell aggregate led to poor distribution of nutrients and factors responsible for differentiation that resulted into inferior phenotype cells in the central region of the pellet. Similar observation was made by Zhang et al, when they compared micromass culture with pellet culture, and determined the heterogeneity in Col II production (Zhang et al. 2010b). However, in this study, the developed cell-scaffold constructs provided an optimal cell density and cell to cell interconnection that resulted into uniformity in cell phenotype as compared to pellet culture. Additionally, the aid of dynamic culture is speculated to facilitate sufficient nutrient distribution resulting into a homogenous cartilage construct generation.

5.5.4 Comparison among the cartilage constructs developed in this thesis work and with the published report

A comparison was done among the cartilage tissue constructs developed in this thesis work using pure SF/CS scaffold and its composites prepared by the addition of glucosamine and chondroitin sulfate individually and also incombination as the key GAG stimulating agents, as shown in table 5.3. It is observed that the physicochemical properties, cell viability, proliferation, metabolic activity and ultimately cartilage ECM formation were improved when SF/CS scaffold was improvised with Gl, Ch and their combination. This observation is due to the beneficial regulatory effect of Gl and Ch on matrix synthesis. The general trend followed by the constructs is- SF/CS-Gl-Ch > SF/CS-Ch ≥ SF/CS-Gl > SF/CS

All scaffolds showed open pore morphology with distinct pore walls and interconnected pore network as revealed by SEM study. The incorporation of Gl and Ch as bioactive components

to SF/CS blends showed a slight variation in their microstructure. The pore size of the scaffolds was apparently within similar range though the average pore size of SF/CS and SF/CS-Gl scaffolds was higher than SF/CS-Ch and SF/CS-Gl-Ch scaffold (Table 5.3). This can be attributed to enhanced hydrophilicity of the scaffolds upon incorporation of Ch that led to the occurrence of more solvent molecules within the composite solution, thus increasing number of pores per unit area resulting into formation of smaller pores upon freeze drying (Yan et al. 2013; Naeimi et al. 2014). The pore interconnectivity in SF/CS scaffolds was lesser than the composite scaffolds, while SF/CS-Gl and SF/CS-Ch scaffolds showed an increase in interconnectivity between the pores, with thinner but intact pore walls. The SF/CS-Gl-Ch showed highest degree of pore interconnectivity that might be due to the combined effect of the presence of hydrophilic molecules (SF, Gl and Ch) in scaffolds. The addition of Ch to SF/CS and SF/CS-Gl scaffolds led to the formation of numerous small pores and thus enhanced its overall porosity. Similar observation was made by other researchers on adding Ch to SF containing scaffolds that decreased mean pore diameter and increased the porosity on increasing Ch content (Yan et al. 2013; Naeimi et al. 2014).

The improvements in physicochemical property of scaffolds, upon addition of Gl and Ch to SF/CS blend, led to improved biological outcomes, with most favorable features possessed by SF/CS-Gl-Ch scaffolds. The size of MSCs and chondrocytes is in the range 15-50 μm (Ge et al. 2014). The morphology assessment of transverse section of scaffolds (FESEM study) showed that the average pore size was higher even than the maximum cell size, which signifies the suitability of the scaffolds to support cell infiltration. Moreover, the longitudinal sections of scaffolds revealed elongated pores running through the depth that is expected to provide space for cell aggregation, thereby facilitates chondrogenic differentiation and tissue formation at later stages. In addition to improved porosity, well interconnected porous network was observed in SF/CS-Gl, SF/CS-Ch and SF/CS-Gl-Ch scaffolds, which plays important role in cell infiltration, nutrient diffusion and removal of biodegradation products and metabolites (Bruzauskaite et al. 2016). Previous studies have reported that hydrophilic scaffolds enhance cellular attachment (Oh et al. 2003). A hydrophilic environment also ensures better dissolution of nutrients required for cell metabolism, proliferation and chondrogenic differentiation. The same was observed in the present study where the most hydrophilic scaffold (SF/CS-Gl-Ch) showed significant improvement in cell attachment,

viability, metabolism, proliferation and chondrocyte like ECM production, as evident from various in vitro analyses.

Application of a scaffold requires proper balance between regeneration rate of tissue at the defect site and biodegradation rate of the scaffold, as the scaffold is anticipated to provide the required structural support until the host tissue regenerates (Lam et al. 2009). Among all the scaffolds, SF/CS-Gl-Ch scaffolds showed highest yet synchronized rate of biodegradation. During biodegradation, the scaffold components are released into the media by leaching or depolymerisation that increases the availability of bioactive components (Gl and Ch, in present case) to the cells (Lam et al. 2009). This increases metabolic activity of the cells which in turn results in an increase in cell proliferation and chondrogenic differentiation, as observed in the present study. Some studies performed with different polymeric scaffolds have reported their complete *in vitro* degradation in 16-18 weeks, whereas in another research the scaffold stability was maintained for 6 weeks, after which the distortion in morphology appeared (Holy et al. 2000). In a study demonstrating ear-shaped auricular cartilage development by tissue engineering approach, complete cartilage tissue was regenerated in 12-20 weeks (Pomerantseva et al. 2016). The present study demonstrates biodegradation study of scaffolds for 28 days (4 weeks) where 13%-40% weight loss was observed for scaffolds, which is in accordance with the cartilage tissue regeneration rate as demonstrated in different research. Moreover, the hMSCs cultured on these scaffolds, exhibited successful chondrogenic differentiation in 21 days, and it is expected to proceed further to cartilage tissue formation, along with continuous biodegradation of the scaffold, thus generating a cartilage construct. Furthermore, the rate of cartilage tissue regeneration can vary depending upon species, type of cartilage tissue, or depth of cartilage tissue damage (Tiku and Sabaawy 2015). As observed in the present study, rate of scaffold biodegradation can be easily optimised to synchronize with the required rate of cartilage regeneration by adjusting the amount of Gl and Ch incorporation to SF/CS blend. Thus, it is evident from different physicochemical analysis that scaffold constituents, Gl, Ch, SF and CS together determine physical property of the scaffolds that influences biological outcome, assessed in terms of hMSCs attachment, metabolic activity, proliferation and chondrogenic differentiation.

Further in comparison with respect to culture condition, superiority of dynamic environment provided by spinner flask was proven over static culture, in promoting infiltration of cells

into the porous scaffolds leading to homogeneity in construct development. The use of dynamic culture also facilitated better mass transfer that improved cell viability, metabolic activity and chondrogenic phenotype development by the cells. Another set of experiment performed using cell aggregates formed by pellet culture, was shown to be capable of maintaining comparable cell viability and proliferation with the constructs. However, collagenous matrix production and chondrocyte gene upregulation were significantly lower than the cell-scaffold constructs. The trend observed was- Dynamic culture > Static culture > Pellet culture

Table 5.3 Comparison among the cell-scaffold constructs developed in present study

Assessment	**SF/CS**	**SF/CS-Gl**	**SF/CS-Ch**	**SF/CS-Gl-Ch**	**Pellet culture**
Pore size (µm)	64-190	55-195	57-210	56.5-168.1	
Porosity (%)	84.28	79	85	90.3	
Contact angle	49.9º	49º	45.93º	40.86º	
Biodegradation 28 days (%)	13.36	24.03	28.06	39.4	
Viability %*	48 ± 2.2	56.45±3	58±1.2		81.85±0.45
	62±3.3	82.45±2.6	91.53±2.1	95.8±0.7	
Distribution at the centre* (cells/mm^2)	60±28	72±32	87±22		--
	326±54	423±28	472±38	550±42	
Metabolic activity*	0.54±0.012	0.61±0.007	0.64±0.017		0.98±0.02
	0.73±0.008	0.83±0.014	0.91±0.024	0.93±0.02	
Proliferation* (ng/ml)	82±8	120.24±4	128.2±4		482±7
	137±6	153±5.2	163±5	344.24±4	
sGAG (µg/mg)	35±4	95±2	150±12		275±2
	83.2±7	130±6	247±20	383±7	
Col I (Fold change)	1.09±0.03	2.36±0.12	2.06±0.23		6.57±0.19
	0.9±0.13	1.57±0.13	1.42±0.19	1.2±0.11	
Sox9 (Fold change)	4.53±0.08	12.13±0.6	14.13±0.51		4.36±0.09
	10.59±0.09	21.23±0.51	24.12±0.61	22.59±1.62*	
MATN3* (Fold change)	1.33±0.2	5.23±0.41	5.84±0.34		4.21±0.3
	2.1±0.1	7.21±0.3	6.73±0.4	5.1±0.17	
Col II (Fold change)	2.12±0.04	5.33±0.2	7.33±0.35		0.36±0.18
	4.46±0.21	8.36±0.18	10.66±0.48	12.12±0.28	
Acan (Fold change)	1.36±0.06	4.5±0.14	9.65±0.44		7.37±0.15
	3.69±0.22	7.37±0.19	14.37±0.91	16.0±0.72	
Col II/ col I (qPCR)	1.93	2.26	3.56		0.06
	4.79	5.32	7.45	9.47	

*Result of 14th day, values in white cells represent results of static culture and shaded cells are dynamic culture.

So, the corresponding values of the UCB-hMSCs seeded SF/CS-Gl-Ch scaffold construct in terms of viability is 95.8±0.7%, 344.24±4 ng/ml DNA content, 383±7 µg/mg sGAG synthesis, 22.59±1.62, 12.12±0.28 and 16.0±0.72 fold increase in Sox9, Col II and Acan gene expression respectively, with respect to hMSCs.

In addition to above, the best result of cartilage construct formation, obtained in the present work was also compared with the published literature as shown in Table 5.4. It is clearly seen that the cell proliferation and sGAG formation by the cells cultured on SF/CS-Gl-Ch scaffolds was much higher than the other cell-scaffold combinations studied earlier. This may be due to the beneficial effect of the presence of GAG stimulatory components combined with dynamic culture environment used in the present study. Moreover, the cell source used by others comprised of bone marrow, adipose tissue or chondrocytes that involved invasive isolation procedure. In present study, UCB was used as a non-invasive and inexpensive cell source that provided continuous proliferation and ease of differentiation to chondrogenic lineage. Furthermore, in most of the cases, detail study for the characterization of the cartilage construct is not performed.

Table 5.4 A comparison of the generated cartilage constructs with the cartilage construct reported in literature

Scaffold	**SF/CS-Gl-Ch**	**SF/gelatin –Ch–HA**	**Gelatin**	**Alginate**	**Gl-gelatin-HA**	**Gelatin/PCL**
Cells	UCB-hMSCs	BM-hMSCs	hADSCs	Rabbit chondrocytes	Rabbit chondrocytes	Bovine chondrocytes
DNA content*	342.24±4 ng/ml	58 ± 5.6 µg/sample	6.5 mg/ scaffold	0.35 µg/sample	2.2 µg/sample	n.a.
sGAG	383±7 µg/mg	11 µg/sample	19 ± 2 µg/ scaffold	40 µg/sample	n.a.	90 mg/g
Col I	1.28±0.11	n.a.	n.a.	0.1 (38 days)	n.a.	n.a.
Sox9	22.6±1.6*	1.5	n.a.	n.a.	14±5	n.a.
Col II	12.12±0.8	2.8	n.a.	0.5	15±4	7 ±0.2 mg/g
Acan	16±0.72	1.9	n.a.	n.a.	16±5	n.a.
Reference	Present study	(Sawatjui et al. 2015)	(Awad et al. 2004)	(Xu et al. 2014)	(Chen et al. 2016a)	(Zheng et al. 2014)

n.a.- not available, *Result of 14th day, all other values represent the results obtained at 21st day unless specified.

Thus, in the present study, a systematic development and characterization of the cartilage

construct using UCB-hMSCs and SF/CS-Gl-Ch scaffolds. Moreover, the use of Gl and Ch in combination was reported to have profound influence in cartilage ECM formation as compared to other scaffolds reported earlier. Therefore, it is demonstrated that the developed construct may pave the way for developing cartilage tissue graft for future clinical application.

Human articular cartilage is 3-4 mm thick, in order to fill a partial or full thickness defect, a tissue-engineered construct of maximum 4 mm thickness is required (Nöth et al. 2002). Following cell seeding on SF/CS based scaffolds and culturing in spinner flask bioreactor a cartilage construct of upto 5 mm thickness was prepared, which is comparable with the thickness of healthy articular cartilage. This approach provides a scope of controlling the dimension of constructs by using the scaffold size and architecture mimicking the defect area and also provides a simple option for scale-up.

The research for generating cartilage construct is ongoing since decades. Despite a large number of preclinical data, the damaged articular cartilage tissue has not yet been completely restored to a healthy structure and function (Vinatier and Guicheux 2016). In this regard, various clinical practices are applied at various levels, from treatment of focal lesions in cartilage to treating osteoarthritis (Mollon et al. 2013). The most common clinically used matrix component is collagen that is employed in autologous chondrocyte implantation (ACI) kits, commercially known as MACI® (Matrix associated chondrocyte implantation, Germany), Chondro-Gide® (Switzerland), Atelocollagen® (Tokyo) and Maix® (Gernamy). Other polymer based matrices, namely Hyalograft® (hyaluronic acid, Italy) and BST-CarGel® (CS and β-glycerophosphate, Canada), were not successful in in vivo studies. Other products like Bioseed®-C (polyglycolic acid, polylactic acid and polydioxanone, Germany), and MaioRegen® (equine collagen and Mg-Hydroxyapatite, Italy), have shown promising results in hyaline cartilage formation but are not yet applied clinically. On the other hand, cell based system Carticel® has been applied for repair of femoral condyle but not for OA. All these are chondrocyte based systems that suffer from various limitations like availability, expansion and instability of cells phenotype in long term maintenance in vitro. Cartisem® is an UCB-MSCs developed for treating OA, however its clinical results are not reported till date (Vinatier and Guicheux 2016; Liu et al. 2017).

The cartilage tissue graft developed in present study is advantageous in terms of biomaterials used for scaffold generation, which are derived from natural biopolymers and thus are less immunogenic to cells and host. Moreover, the cell source used in this study is UCB-hMSCs that has shown to exhibit continuous division ability as well as stable phenotype in long term in vitro cultures. Furthermore, the presence of chondroinductive molecules (Gl and Ch) in the scaffold promotes the differentiation of MSCs to chondrocytes. Thus, the developed tissue construct might be promising for the treatment of cartilage lesions and OA in future clinically.

Conclusion

In the present study, porous scaffolds acted as a physical support for hosting cells, whereas, the presence of Gl and Ch in the scaffold had an added advantage of stimulating gene and protein expression, which triggered sGAG synthesis. The use of Gl and Ch in combination in SF/CS scaffold showed higher metabolic activity, proliferation, sGAG deposition and expression of chondrogenic genes by hMSCs, as compared to the SF/CS-Gl and SF/CS-Ch scaffolds. The conventional pellet culture favoured cell aggregation and matrix formation, but were less efficient in long term maintenance of cell phenotype that limits their application in cartilage tissue engineering. These findings suggest that hMSCs seeded SF/C-Gl-$Ch_{1.5}$ scaffold cultured in spinner flask, is capable of providing a promising cartilage construct for tissue engineering application.

Chapter 6

Summary and Conclusion

In the last decade, cartilage tissue engineering has been evolved as a promising technique to develop cartilage tissue construct from a suitable cell of mesenchymal in nature and scaffold derived from biomaterial with desired properties for the treatment of cartilage tissue defects. This is because, the currently used cartilage treatment methods have several drawbacks such as poor integration, limited mobility and longevity of implants, thereby normal cartilage function is not restored. Silk fibroin/chitosan based scaffold improvised with bioactive molecules is suitable for cartilage TE application and can be used as a platform for cartilage construct generation using a suitable cell source. In this context, the umbilical cord blood derived hMSC is attractive because of its easy availability, inexpensive and non-invasive isolation procedure that involves minimal ethical concern. Furthermore, the maintenance of a suitable microenvironment during culture is vital for the *in vitro* tissue regeneration that can be achieved by dynamic culture condition using a suitable bioreactor.

Keeping the above aspects in mind, the present research has focused on the development of tissue-engineered cartilage construct from UCB-derived hMSCs and SF/CS scaffold and its composites using a simple and economic spinner flask bioreactor. The most significant research outcome from this present study is summarized as follows-

I. In this part of the study, MNCs were successfully isolated from UCB by Ficoll-Hypaque mediated density gradient centrifugation, and cultured upto 4^{th} to 5^{th} passage to obtain MSCs for use in cartilage construct generation. The cultured cells exhibited hMSCs phenotype in terms of morphology and expression of surface markers CD73, CD90, CD105, CD34 and CD45. The >95% expression of CD73, CD90 and CD105 as positive markers and <2% expression of CD34 and CD45 as negative markers confirmed the pure population of hMSCs. The UCB-hMSCs shows the trilineage differentiation potency including chondrogenic differentiation as confirmed by histological analysis. Furthermore, since the cells obtained at 4^{th} and 5^{th} passage showed similar characteristics, hMSCs of 4^{th} passage were used for further experiment.

II. In this part of work, attempt has been made to develop cartilage construct by the culture and differentiation of UCB-hMSCs over SF/CS scaffolds. To this end, freeze dried porous SF/CS (80:20 v/v) scaffold was fabricated and characterized. The

scaffold possessed open pore microstructure with desired pore size (64-190 μm), porosity (84±3%), hydrophilicity (50.2˚ contact angle) and biodegradation. The hMSCs were seeded on the SF/CS scaffolds and cultured under dynamic condition in a spinner flask bioreactor for a period of 14day. From the study of the effect of rotation speed, 60 rpm was found to be the most favourable speed in supporting cell attachment and viability as assessed by FESEM, MTT and DNA quantification analysis. The histological, sGAG synthesis, immunofluorescence and qPCR studies, demonstrated the superiority of dynamic culture condition over static culture in providing microenvironment for ECM production (83.2 μg/mg sGAG) and expression of chondocyte specific genes such as Sox9, MATN3, Col II, and Acan.

III. Glucosamine a basic component of GAG, is reported to stimulate proteoglycan synthesis thereby facilitates cartilage ECM production. Therefore, in this part of research, it was attempted to achieve improved cartilage construct generation by culturing and differentiating hMSCs over glucosamine loaded SF/CS scaffold. The presence of Gl in the scaffold did not show any significant improvement in cell viability, proliferation and metabolic activity of hMSCs during 14 days of culture. However, the sGAG synthesis, thereby cartilage specific ECM deposition was remarkably enhanced, implying the positive influence of Gl in triggering chondrogenic differentiation of hMSCs over SF/CS-Gl composite scaffold. Furthermore, the histological, immunofluorescence, sGAG synthesis and qPCR analyses confirmed that hMSCs differentiated on SF/CS-Gl scaffolds developed chondrocyte specific phenotype. Furthermore, as in the previous part of work, the dynamic culture environment in spinner flask bioreactor has shown advantageous in promoting cell proliferation and homogenous cell distribution in 3D culture that facilitated construct generation. The sGAG production in dynamic culture was 130±6 μg/mg, which was significantly higher than static culture 95±2 μg/mg.

IV. Like glucosamine, chondroitin sulfate is another prominent chondrocyte ECM component that not only protects cartilage degeneration, but also promotes chondrocyte ECM synthesis. So, it was hypothesised that, the presence of Ch in SF/CS scaffold would facilitate cartilage tissue construct formation. Therefore, an effort was given to develop cartilage construct by culturing and differentiating hMSCs

on SF/CS scaffolds improvised with Ch. As evident from experimental result, the viability, distribution, proliferation and metabolic activity of hMSCs over SF/CS-Ch were increased due to the presence of Ch. The chondrogenic differentiation studied for 21 days demonstrated a remarkably higher sGAG production (247 µg/mg) and hence ECM deposition than SF/CS-Gl scaffolds. The increment in synthesis of proteoglycan as well as the expression of collagenous protein and genes further proved the beneficial effect of Ch on chondrogenic differentiation of hMSCs. The use of dynamic culture was also demonstrated to be acting synergistically in promoting the differentiation process, providing an overall benefit on cartilage construct development.

V. This part of the study was designed considering the beneficial effects of the addition of GAG components, Gl and Ch in combination in improving cartilage ECM secretion, thereby promoting chondrogenic differentiation of hMSCs. Thus, SF/CS-Gl-Ch composite scaffold was fabricated and used as a platform for the recruitment and differentiation of hMSCs to develop cartilage construct. Among the scaffolds with varied concentration of Ch (0.5-1.5 wt%), SF/CS-Gl loaded with 1.5% Ch showed superiority in promoting cell attachment, viability, and proliferation. The SF/CS-Gl-$Ch_{1.5}$ scaffolds showed significantly higher cell proliferation (342.24±4 ng/ml) as compared to SF/CS-Gl (153±5.2 ng/ml) and SF/CS-Ch (163±5 ng/ml) scaffolds. The hMSCs seeded SF/CS-Gl-Ch scaffold augmented the chondrogenic differentiation as evident from the production of proteoglycan matrix as studied by sGAG deposition (383±7 µg/mg) and histology analysis. The immunofluorescence staining for Col II and Acan were more prominent than other constructs generated with hMSCs seeded SF/CS-Gl and SF/CS-Ch scaffolds. Moreover, the significant upregulation of Col II, Sox9 and Acan genes in their respective stages confirmed the synchronised chondrogenic differentiation of cells cultured in SF/CS-Gl-Ch scaffolds.

Overall, cartilage constructs were successfully developed by culturing and differentiating UCB derived hMSCs over SF/CS and its composite scaffolds. Among the various scaffolds, SF/CS-Gl-Ch scaffold was demonstrated to be the most promising for construct generation, by promoting proliferation and differentiation of hMSCs eventually leading to an enhanced cartilage specific ECM generation. The overall trend of ECM production was SF/CS-Gl-Ch >

SF/CS-Ch > SF/CS-Gl > SF/CS. It was further demonstrated that the dynamic culture condition maintained by using spinner flask bioreactor played a prominent role in improving the attachment, viability, distribution, proliferation and ultimately ECM formation by hMSCs. The cartilage construct generated from hMSCs and SF/CS-Gl-Ch composite scaffold in a dynamic bioreactor may lead to the production of cartilage tissue construct for future clinical application.

Suggested future work

The following research work are suggested for further study with the developed cartilage constructs-

- The constructs can be incorporated into the cartilage defect site in a suitable animal model to assess their performance *in vivo*, evaluating them for future clinical use.
- A more dedicated and sophisticated culture system could be employed, like perfusion bioreactor, and using the studied components (hMSCs and SF/CS-Gl-Ch scaffolds), cartilage construct can be generated.
- The efficiency of the developed cartilage constructs can be tested after cryopreservation to ensure their long term viability.

References

Abreu SC, Antunes MA, de Castro JC, et al (2013) Bone marrow-derived mononuclear cells vs. mesenchymal stromal cells in experimental allergic asthma. Respir Physiol Neurobiol 187:190–198. doi: 10.1016/j.resp.2013.03.014

Akhter E, Bilal S, Haque U (2011) Prevalence of arthritis in India and Pakistan: A review. Rheumatol Int 31:849–855. doi: 10.1007/s00296-011-1820-3

Altman AM, Gupta V, Ríos CN, et al (2010) Adhesion, migration and mechanics of human adipose-tissue-derived stem cells on silk fibroin-chitosan matrix. Acta Biomater 6:1388–1397. doi: 10.1016/j.actbio.2009.10.034

Altman G, Horan R, Martin I, et al (2002) Cell differentiation by mechanical stress. Faseb J 16:270–272. doi: 10.1096/fj.01

Altman GH, Diaz F, Jakuba C, et al (2003) Silk-based biomaterials. Biomaterials 24:401–416. doi: 10.1016/S0142-9612(02)00353-8

Alvarez-Viejo M, Menendez-Menendez Y, Blanco-Gelaz MA, et al (2013) Quantifying mesenchymal stem cells in the mononuclear cell fraction of bone marrow samples obtained for cell therapy. Transplant Proc 45:434–439. doi: 10.1016/j.transproceed.2012.05.091

Amini AR, Laurencin CT, Nukavarapu SP (2012) Bone tissue engineering: recent advances and challenges. Crit Rev Biomed Eng 40:363–408. doi: 10.1615/CritRevBiomedEng.v40.i5.10

Anisha BS, Sankar D, Mohandas A, et al (2013) Chitosan-hyaluronan/nano chondroitin sulfate ternary composite sponges for medical use. Carbohydr Polym 92:1470–1476. doi: 10.1016/j.carbpol.2012.10.058

Awad HA, Wickham MQ, Leddy HA, et al (2004) Chondrogenic differentiation of adipose-derived adult stem cells in agarose, alginate, and gelatin scaffolds. Biomaterials 25:3211–3222. doi: 10.1016/j.biomaterials.2003.10.045

Baici A, Hörler D, Moser B, et al (1992) Analysis of glycosaminoglycans in human serum after oral administration of chondroitin sulfate. Rheumatol Int 12:81–88. doi: 10.1007/BF00290259

Bartholomew A, Sturgeon C, Siatskas M, et al (2002) Mesenchymal stem cells suppress lymphocyte proliferation in vitro and prolong skin graft survival in vivo. Exp Hematol 30:42–48. doi: 10.1016/S0301-472X(01)00769-X

Bassleer C, Malaise M (1997) Chondroitin sulfate: Its in vitro effects on human articular chondrocytes cultivated in clusters. Osteoarthr Cartil 5:68–72

Beddoes CM, Whitehouse MR, Briscoe WH, Su B (2016) Hydrogels as a replacement material for damaged articular hyaline cartilage. Materials (Basel) 9:. doi: 10.3390/ma9060443

Behrens AM, Casey BJ, Sikorski MJ, et al (2014) In situ deposition of PLGA nanofibers via solution blow spinning. ACS Macro Lett 3:249–254. doi: 10.1021/mz500049x

Berry CC, Charles S, Wells S, et al (2004) The influence of transferrin stabilised magnetic nanoparticles on human dermal fibroblasts in culture. Int J Pharm 269:211–225. doi: https://doi.org/10.1016/j.ijpharm.2003.09.042

Bhardwaj N, Kundu SC (2012) Chondrogenic differentiation of rat MSCs on porous scaffolds of silk fibroin/chitosan blends. Biomaterials 33:2848–2857

Bhardwaj N, Kundu SC (2011) Silk fibroin protein and chitosan polyelectrolyte complex porous scaffolds for tissue engineering applications. Carbohydr Polym 85:325–333. doi: 10.1016/j.carbpol.2011.02.027

Bhardwaj N, Nguyen QT, Chen AC, et al (2011) Potential of 3-D tissue constructs engineered from

bovine chondrocytes/silk fibroin-chitosan for in vitro cartilage tissue engineering. Biomaterials 32:5773–5781. doi: 10.1016/j.biomaterials.2011.04.061

Bhat S, Tripathi A, Kumar A (2011) Supermacroprous chitosan-agarose-gelatin cryogels: in vitro characterization and in vivo assessment for cartilage tissue engineering. J R Soc Interface 8:540–554. doi: 10.1098/rsif.2010.0455

Bi L, Cao Z, Hu Y, et al (2011) Effects of different cross-linking conditions on the properties of genipin-cross-linked chitosan/collagen scaffolds for cartilage tissue engineering. J Mater Sci Mater Med 22:51–62. doi: 10.1007/s10856-010-4177-3

Bieback K, Kern S, Klüter H, Eichler H (2004) Critical Parameters for the Isolation of Mesenchymal Stem Cells from Umbilical Cord Blood. Stem Cells 22:625–634

Bissoyi A, Pramanik K (2013) Effects of non-toxic cryoprotective agents on the viability of cord blood derived MNCs. Cryo-Letters 34:453–465

Bruzauskaite I, Bironait D, Bagdonas E, Bernotiene E (2016) Scaffolds and cells for tissue regeneration : different scaffold pore sizes — different cell effects. Cytotechnology 68:355–369. doi: 10.1007/s10616-015-9895-4

Buschmann MD, Gluzband YA, Grodzinsky AJ, et al (1992) Chondrocytes in agarose culture synthesize a mechanically functional extracellular matrix. J Orthop Res 10:745–758. doi: 10.1002/jor.1100100602

Cai R, Nakamoto T, Kawazoe N, Chen G (2015) Influence of stepwise chondrogenesis-mimicking 3D extracellular matrix on chondrogenic differentiation of mesenchymal stem cells. Biomaterials 52:199–207. doi: 10.1016/j.biomaterials.2015.02.033

Cajander S, Tina E, Bäckman A, et al (2016) Quantitative Real-Time Polymerase Chain Reaction Measurement of HLA-DRA Gene Expression in Whole Blood Is Highly Reproducible and Shows Changes That Reflect Dynamic Shifts in Monocyte Surface HLA-DR Expression during the Course of Sepsis. PLoS One 11:e0154690. doi: 10.1371/journal.pone.0154690

Campbell CJ (1969) The healing of cartilage defects. Clin Orthop 64:45–63

Campbell D, Pei M (2012) Surface Markers for Chondrogenic Determination: A Highlight of Synovium-Derived Stem Cells. Cells 1:1107–1120. doi: 10.3390/cells1041107

Cancedda R, Dozin B, Giannoni P, Quarto R (2003) Tissue engineering and cell therapy of cartilage and bone. Matrix Biol 22:81–91

Chameettachal S, Murab S, Vaid R, et al (2015) Effect of visco-elastic silk–chitosan microcomposite scaffolds on matrix deposition and biomechanical functionality for cartilage tissue engineering. J Tissue Eng Regen Med 11:1212–1229. doi: 10.1002/term

Chan KOW, Ng GYF (2011) A review on the effects of glucosamine for knee osteoarthritis based on human and animal studies. Hong Kong Physiother J 29:42–52. doi: 10.1016/j.hkpj.2011.06.004

Chandy T, Sharma CP (1990) Chitosan-as a Biomaterial. Biomater Artif Cells Artif Organs 18:1–24. doi: 10.3109/10731199009117286

Chang C-Y, Chen P-H, Li C-J, et al (2016) Isolation and characterization of mesenchymal stem cells derived from umbilical cord blood mononuclear cells. E-Da Med J 3:1–13

Chen CH, Kuo CY, Wang YJ, Chen JP (2016a) Dual Function of Glucosamine in Gelatin/Hyaluronic Acid Cryogel to Modulate Scaffold Mechanical Properties and to Maintain Chondrogenic Phenotype for Cartilage Tissue Engineering. Int J Mol Sci 17:1957. doi: 10.3390/ijms17111957

Chen F, Yu S, Liu B, et al (2016b) An Injectable Enzymatically Crosslinked Carboxymethylated Pullulan/Chondroitin Sulfate Hydrogel for Cartilage Tissue Engineering. Sci Rep 6:20014. doi: 10.1038/srep20014

Chen G, Yue A, Ruan Z, et al (2014) Monitoring the biology stability of human umbilical cord-

derived mesenchymal stem cells during long-term culture in serum-free medium. Cell Tissue Bank 15:513–521. doi: 10.1007/s10561-014-9420-6

Chung C, Burdick JA (2008) Engineering cartilage tissue. Adv Drug Deliv Rev 60:243–262. doi: 10.1016/j.addr.2007.08.027

Dai W, Dong J, Chen G, Uemura T (2009) Application of low-pressure cell seeding system in tissue engineering. Biosci Trends 3:216–219

Dar A, Shachar M, Leor J, Cohen S (2002) Optimization of cardiac cell seeding and distribution in 3D porous alginate scaffolds. Biotechnol Bioeng 80:305–312. doi: 10.1002/bit.10372

Darling EM, Athanasiou KA (2003) Articular cartilage bioreactors and bioprocesses. Tissue Eng 9:9–26

Deal CL, Moskowitz RW (1999) Nutraceuticals As Therapeutic Agents in Osteoarthritis. Rheum Dis Clin North Am 25:379–395. doi: 10.1016/S0889-857X(05)70074-0

Decker RS, Koyama E, Pacifici M (2014) Genesis and morphogenesis of limb synovial joints and articular cartilage. Matrix Biol 39:5–10. doi: 10.1016/j.matbio.2014.08.006

Deng J, She R, Huang W, et al (2013) A silk fibroin/chitosan scaffold in combination with bone marrow-derived mesenchymal stem cells to repair cartilage defects in the rabbit knee. J Mater Sci Mater Med 24:2037–2046. doi: 10.1007/s10856-013-4944-z

Derfoul A, Miyoshi AD, Freeman DE, Tuan RS (2007) Glucosamine promotes chondrogenic phenotype in both chondrocytes and mesenchymal stem cells and inhibits MMP-13 expression and matrix degradation. Osteoarthiritis Cartil 15:646–655. doi: 10.1016/j.joca.2007.01.014

Dodge GR, Jimenez SA (2003) Glucosamine sulfate modulates the levels of aggrecan and matrix metalloproteinase-3 synthesized by cultured human osteoarthritis articular chondrocytes. Osteoarthiritis Cartil 11:424–432. doi: 10.1016/S1063-4584(03)00052-9

Dominici M, Blanc K Le, Mueller I, et al (2006) Minimal criteria for defining multipotent mesenchymal stromal cells . The International Society for Cellular Therapy position statement. Cytotherapy 8:315–317

Drovanti A, Bignamini A, Rovati A (1980) Therapeuitc Activity of Oral Glucosamine Sulfate in Osteoarthosis: A Placebo-Controlled Double-Blind Investigation. Clin Ther 3:260–272

Elliott HC (1936) Studies on articular cartilage. I. Growth mechanisms. Am J Anat 58:127–145. doi: 10.1002/aja.1000580109

Erices A, Conget P, Minguell JJ (2000) Mesenchymal progenitor cells in human umbilical cord blood. Br J Haematol 109:235–242

Ficat RP, Ficat C, Gedeon P, Toussaint JB (1979) Spongialization: a new treatment for diseased patellae. Clin Orthop Relat Res 74–83

Foot M, Mulholland M (2005) Classification of chondroitin sulfate A, chondroitin sulfate C, glucosamine hydrochloride and glucosamine 6 sulfate using chemometric techniques. J Pharm Biomed Anal 38:397–407. doi: 10.1016/j.jpba.2005.01.026

Francis Suh J-K, Matthew HW. (2000) Application of chitosan-based polysaccharide biomaterials in cartilage tissue engineering: a review. Biomaterials 21:2589–2598. doi: 10.1016/S0142-9612(00)00126-5

Fransen M, BRIDGETT L, MARCH L, et al (2011) The epidemiology of osteoarthritis. Best Pract Res Clin Rheumatol 14:113–121. doi: 10.1016/j.berh.2014.01.004

Freed LE, Marquis JC, Langer R, et al (1994) Composition of cell-polymer cartilage implants. Biotechnol Bioeng 43:605–614. doi: 10.1002/bit.260430710

Freed LE, Marquis JC, Nohria A, et al (1993) Neocartilage formation *in vitro* and *in vivo* using cells

cultured on synthetic biodegradable polymers. J Biomed Mater Res 27:11–23

Freed LE, Vunjak-Novakovic G (1997) Microgravity tissue engineering. In Vitro Cell Dev Biol Anim 33:381–5. doi: 10.1007/s11626-997-0009-2

Freyria AM, Cortial D, Ronzière MC, et al (2004) Influence of medium composition, static and stirred conditions on the proliferation of and matrix protein expression of bovine articular chondrocytes cultured in a 3-D collagen scaffold. Biomaterials 25:687–697. doi: 10.1016/S0142-9612(03)00568-4

Friedenstein AJ, Gorskaja JF, Kulagina NN (1976) Fibroblast precursors in normal and irradiated mouse hematopoietic organs. Exp Hematol 4:267—274

Fuller JA, Ghadially FN (1972) Ultrastructural observations on surgically produced partial-thickness defects in articular cartilage. Clin Orthop Relat Res 86:193–205

Gan L, Kandel RA (2007) In Vitro Cartilage Tissue Formation by Co-culture of Primary and Passaged Chondrocytes. Tissue Eng 13:10–15

Garnjanagoonchorn W, Wongekalak L, Engkagul A (2007) Determination of chondroitin sulfate from different sources of cartilage. Chem Eng Process Process Intensif 46:465–471. doi: 10.1016/j.cep.2006.05.019

Ge J, Guo L, Wang S, et al (2014) The Size of Mesenchymal Stem Cells is a Significant Cause of Vascular Obstructions and Stroke. Stem Cell Rev Reports 10:295–303. doi: 10.1007/s12015-013-9492-x

Ghosh P, Wells C, Smith M, Hutadilok N (1990) Chondroprotection, myth or reality: An experimental approach. Semin Arthritis Rheum 19:3–9. doi: 10.1016/0049-0172(90)90078-T

Gigout A, Buschmann MD, Jolicoeur M (2009) Chondrocytes cultured in stirred suspension with serum-free medium containing pluronic-68 aggregate and proliferate while maintaining their differentiated phenotype. Tissue Eng Part A 15:2237–2248. doi: 10.1089/ten.tea.2008.0256

Gimble J, Guilak F (2003) Adipose-derived adult stem cells: isolation, characterization, and differentiation potential. Cytotherapy 5:362–369. doi: 10.1080/14653240310003026

Gini EJ, Sivakumar T, Kuppuswamy S (2016) Preliminary phytochemical screening, evaluation and comparison of anticancer activity of Ficus gibbosa blume by MTT assay method. Int J Res Pharm Sci 7:190–194

Gobin AS, Froude VE, Mathur AB (2005) Structural and mechanical characteristics of silk fibroin and chitosan blend scaffolds for tissue regeneration. J Biomed Mater Res - Part A 74:465–473. doi: 10.1002/jbm.a.30382

Godbey WT, Stacey Hindy BS, Sherman ME, Atala A (2004) A novel use of centrifugal force for cell seeding into porous scaffolds. Biomaterials 25:2799–2805. doi: 10.1016/j.biomaterials.2003.09.056

Goessler UR, Bieback K, Bugert P, et al (2006a) In vitro analysis of integrin expression during chondrogenic differentiation of mesenchymal stem cells and chondrocytes upon dedifferentiation in cell culture. Int J Mol Med 17:301–307. doi: 10.3892/ijmm.17.2.301

Goessler UR, Bugert P, Bieback K, et al (2006b) In vitro analysis of differential expression of collagens, integrins, and growth factors in cultured human chondrocytes. Otolaryngol - Head Neck Surg 134:510–515. doi: 10.1016/j.otohns.2005.10.026

Goldenberg IS (1959) Catgut, silk, and silver--the story of surgical sutures. Surgery 46:908--912

Gong Y, Zhu Y, Liu Y, et al (2007) Layer-by-layer assembly of chondroitin sulfate and collagen on aminolyzed poly(l-lactic acid) porous scaffolds to enhance their chondrogenesis. Acta Biomater 3:677–685. doi: 10.1016/j.actbio.2007.04.007

Gooch KJ, Kwon JH, Blunk T, et al (2001) Effects of mixing intensity on tissue-engineered cartilage.

Biotechnol Bioeng 72:402–407. doi: 10.1002/1097-0290(20000220)72:4<402::AID-BIT1002>3.0.CO;2-Q

Grassel S, Ahmed N (2007) Influence of cellular microenvironment and paracrine signals on chondrogenic differentiation. Front Biosci 12:4946. doi: 10.2741/2440

Grogan SP, Sovani S, Pauli C, et al (2012) Effects of Perfusion and Dynamic Loading on Human Neocartilage Formation in Alginate Hydrogels. Tissue Eng Part A 18:1784–1792. doi: 10.1089/ten.tea.2011.0506

Hammad YH, Magid HR, Sobhy MM (2015) Clinical and biochemical study of the comparative efficacy of topical versus oral glucosamine/chondroitin sulfate on osteoarthritis of the knee. Egypt Rheumatol 37:85–91. doi: 10.1016/j.ejr.2014.06.007

Hanson RR, Lowell RS, Huff GK, et al (1997) Oral treatment with a glucosamine-chondroitin sulfate compound for degenerative joint disease in horses: 25 cases. Equine Pract 19:16–22

Hass R, Kasper C, Böhm S, Jacobs R (2011) Different populations and sources of human mesenchymal stem cells (MSC): A comparison of adult and neonatal tissue-derived MSC. Cell Commun Signal 9:12. doi: 10.1186/1478-811X-9-12

Haugland RP, MacCoubrey IC, Moore PL (1994) Dual-fluorescence cell viability assay using ethidium homodimer and calcein AM. United States patent US 5,314,805.

Herlofsen SR, Küchler AM, Melvik JE, Brinchmann JE (2011) Chondrogenic differentiation of human bone marrow-derived mesenchymal stem cells in self-gelling alginate discs reveals novel chondrogenic signature gene clusters. Tissue Eng Part A 17:1003–1013. doi: 10.1089/ten.TEA.2010.0499

Heyland J, Wiegandt K, Goepfert C, et al (2006) Redifferentiation of chondrocytes and cartilage formation under intermittent hydrostatic pressure. Biotechnol Lett 28:1641–1648. doi: 10.1007/s10529-006-9144-1

Hjelle K, Solheim E, Strand T, et al (2002) Articular cartilage defects in 1,000 knee arthroscopies. Arthroscopy 18:730–734. doi: 10.1053/jars.2002.32839

Hofmann S, Wong Po Foo CT, Rossetti F, et al (2006) Silk fibroin as an organic polymer for controlled drug delivery. J Control Release 111:219–227. doi: 10.1016/j.jconrel.2005.12.009

Holy CE, Shoichet MS, Davies JE (2000) Engineering three-dimensional bone tissue in vitro using biodegradable scaffolds: Investigating initial cell-seeding density and culture period. J Biomed Mater Res 51:376–382. doi: 10.1002/1097-4636(20000905)51:3<376::AID-JBM11>3.0.CO;2-G

Homayoni H, Ravandi SAH, Valizadeh M (2009) Electrospinning of chitosan nanofibers: Processing optimization. Carbohydr Polym 77:656–661. doi: 10.1016/j.carbpol.2009.02.008

Howell D, Altman R (1993) Cartilage repair and conservation in osteoarthritis. A brief review of some experimental approaches to chondroprotection. Rheum Dis Clin North Am 19:713–724

Hu L, Hu J, Zhao J, et al (2013) Side-by-Side Comparison of the Biological Characteristics of Human Umbilical Cord and Adipose Tissue-Derived Mesenchymal Stem Cells. Biomed Res Int 2013:1–12. doi: 10.1155/2013/438243

Hu SG, Jou CH, Yang MC (2003) Protein adsorption, fibroblast activity and antibacterial properties of poly(3-hydroxybutyric acid-co-3-hydroxyvaleric acid) grafted with chitosan and chitooligosaccharide after immobilized with hyaluronic acid. Biomaterials 24:2685–2693. doi: 10.1016/S0142-9612(03)00079-6

Huang XP, Sun Z, Miyagi Y, et al (2010) Differentiation of allogeneic mesenchymal stem cells induces immunogenicity and limits their long-term benefits for myocardial repair. Circulation 122:2419–2429. doi: 10.1161/CIRCULATIONAHA.110.955971

Huang Z, Nooeaid P, Kohl B, et al (2015) Chondrogenesis of human bone marrow mesenchymal

stromal cells in highly porous alginate-foams supplemented with chondroitin sulfate. Mater Sci Eng C 50:160–172. doi: 10.1016/j.msec.2015.01.082

Hunziker EB (1999) Articular cartilage repair: Are the intrinsic biological constraints undermining this process insuperable? Osteoarthr Cartil 7:15–28. doi: 10.1053/joca.1998.0159

Hutmacher DW (2000) Scaffolds in tissue engineering bone and cartilage. Biomaterials 21:2529–2543. doi: 10.1016/s0142-9612(00)00121-6

Hwang NS, Varghese S, Theprungsirikul P, et al (2006) Enhanced chondrogenic differentiation of murine embryonic stem cells in hydrogels with glucosamine. Biomaterials 27:6015–6023. doi: 10.1016/j.biomaterials.2006.06.033

Inouye K, Kurokawa M, Nishikawa S, Tsukada M (1998) Use of Bombyx mori silk fibroin as a substratum for cultivation of animal cells. J Biochem Biophys Methods 37:159–164. doi: 10.1016/S0165-022X(98)00024-4

Izadifar Z, Chen X, Kulyk W (2012) Strategic Design and Fabrication of Engineered Scaffolds for Articular Cartilage Repair. J Funct Biomater 3:799–838. doi: 10.3390/jfb3040799

Jin H, Bae Y, Kim M, et al (2013) Comparative Analysis of Human Mesenchymal Stem Cells from Bone Marrow, Adipose Tissue, and Umbilical Cord Blood as Sources of Cell Therapy. Int J Mol Sci 14:17986–18001. doi: 10.3390/ijms140917986

Johnson KA, Hulse DA, Hart RC, et al (2001) Effects of an orally administered mixture of chondroitin sulfate, glucosamine hydrochloride and manganese ascorbate on synovial fluid chondroitin sulfate 3B3 and 7D4 epitope in a canine cruciate ligament transection model of osteoarthritis. Osteoarthr Cartil 9:14–21. doi: 10.1053/joca.2000.0345

Kern S, Eichler H, Stoeve J, et al (2006) Comparative analysis of mesenchymal stem cells from bone marrow, umbilical cord blood, or adipose tissue. Stem Cells 24:1294–301. doi: 10.1634/stemcells.2005-0342

Kim SE, Park JH, Cho YW, et al (2003) Porous chitosan scaffold containing microspheres loaded with transforming growth factor-β1: Implications for cartilage tissue engineering. J Control Release 91:365–374. doi: 10.1016/S0168-3659(03)00274-8

Kim UJ, Park J, Joo Kim H, et al (2005) Three-dimensional aqueous-derived biomaterial scaffolds from silk fibroin. Biomaterials 26:2775–2785. doi: 10.1016/j.biomaterials.2004.07.044

Knutsen AP, Wall DA (1999) Kinetics of T-cell development of umbilical cord blood transplantation in severe T-cell immunodeficiency disorders. J Allergy Clin Immunol 103:823–832. doi: 10.1016/S0091-6749(99)70426-4

Ko CS, Huang JP, Huang CW, Chu IM (2009) Type II collagen-chondroitin sulfate-hyaluronan scaffold cross-linked by genipin for cartilage tissue engineering. J Biosci Bioeng 107:177–182. doi: 10.1016/j.jbiosc.2008.09.020

Kock L, Van Donkelaar CC, Ito K (2012) Tissue engineering of functional articular cartilage: The current status. Cell Tissue Res 347:613–627. doi: 10.1007/s00441-011-1243-1

Kraan PM Van Der, Vries BJ De, Vitters EL, et al (1988) Inhibition of glycosaminoglycan synthesis in anatomically intact rat patellar cartilage by paracetamol-induced serum sulfate depletion. Biochem Pharmacol 37:3683–3690. doi: http://dx.doi.org/10.1016/0006-2952(88)90401-7

Kundu B, Rajkhowa R, Kundu SC, Wang X (2013) Silk fibroin biomaterials for tissue regenerations ☆. Adv Drug Deliv Rev 65:457–470. doi: 10.1016/j.addr.2012.09.043

Kuo YC, Chung CY (2012) Chondrogenesis in scaffolds with surface modification of elastin and poly-l-lysine. Colloids Surfaces B Biointerfaces 93:85–91. doi: 10.1016/j.colsurfb.2011.12.011

Lai R, Juco J, Lee SF, et al (2000) Flow cytometric detection of CD79a expression in T-cell acute lymphoblastic leukemias. Am J Clin Pathol 113:823–830. doi: 10.1309/391R-93YF-DB4D-

1L35

Lal MRLP, Suraishkumar GK, Nair PD (2017) Chitosan-agarose scaffolds supports chondrogenesis of Human Wharton's Jelly mesenchymal stem cells. J Biomed Mater Res - Part A 105:1845–1855. doi: 10.1002/jbm.a.36054

Lam CXF, Hutmacher DW, Schantz J-T, et al (2009) Evaluation of polycaprolactone scaffold degradation for 6 months in vitro and in vivo. J Biomed Mater Res A 90:906–919. doi: 10.1002/jbm.a.32052

Lee C, Huang C, Lee Y (2006) Biomimetic Porous Scaffolds Made from Poly(l-lactide)-g-chondroitin Sulfate Blend with Poly(l-lactide) for Cartilage Tissue Engineering. Biomacromolecules 7:2200–2209. doi: 10.1021/bm060451x

Lee OK, Kuo TK, Chen W, et al (2004) Isolation of multipotent mesenchymal stem cells from umbilical cord blood. Blood 103:1669–1675. doi: 10.1182/blood-2003-05-1670.Supported

Lee TJ, Bhang SH, La WG, et al (2011) Spinner-flask culture induces redifferentiation of de-differentiated chondrocytes. Biotechnol Lett 33:829–836. doi: 10.1007/s10529-010-0488-1

Lefebvre R, Huang W, Harley VR, et al (1997) SOX9 Is a Potent Activator of the Chondrocyte-Specific Enhancer of the Pro α1 (II) Collagen Gene. Mol Cell Biol 17:2336–2346

Li DW, Lei X, He FL, et al (2017) Silk fibroin/chitosan scaffold with tunable properties and low inflammatory response assists the differentiation of bone marrow mesenchymal stem cells. Int J Biol Macromol 105:584–597. doi: 10.1016/j.ijbiomac.2017.07.080

Li W-J, Danielson KG, Alexander PG, Tuan RS (2003) Biological response of chondrocytes cultured in three-dimensional nanofibrous poly(ε-caprolactone) scaffolds. J Biomed Mater Res A 67:1105–1114. doi: 10.1002/jbm.a.10101

Lippiello L (2003) Glucosamine and chondroitin sulfate: Biological response modifiers of chondrocytes under simulated conditions of joint stress. Osteoarthr Cartil 11:335–342. doi: 10.1016/S1063-4584(03)00026-8

Lippiello L, Woodward J, Karpman R, Hammad TA (2000) In vivo chondroprotection and metabolic synergy of glucosamine and chondroitin sulfate. Clin Orthop Relat Res 381:229–240. doi: 10.1097/00003086-200012000-00027

Liu L, Wu W, Tuo X, et al (2010) Novel strategy to engineer trachea cartilage graft with marrow mesenchymal stem cell macroaggregate and hydrolyzable scaffold. Artif Organs 34:426–433. doi: 10.1111/j.1525-1594.2009.00884.x

Liu Y, Zhou G, Cao Y (2017) Recent Progress in Cartilage Tissue Engineering—Our Experience and Future Directions. Engineering 3:28–35. doi: 10.1016/J.ENG.2017.01.010

Lo Surdo J, Bauer SR (2012) Quantitative Approaches to Detect Donor and Passage Differences in Adipogenic Potential and Clonogenicity in Human Bone Marrow-Derived Mesenchymal Stem Cells. Tissue Eng Part C Methods 18:877–889. doi: 10.1089/ten.tec.2011.0736

Lu YH, Lin H, Chen YY, et al (2007) Structure and performance of Bombyx mori silk modified with nano-TiO2 and chitosan. Fibers Polym 8:1–6. doi: 10.1007/bf02908152

Madihally S V., Matthew HWT (1999) Porous chitosan scaffolds for tissue engineering. Biomaterials 20:1133–1142. doi: 10.1016/S0142-9612(99)00011-3

Mahmoudifar N, Doran PM (2005) Tissue engineering of human cartilage in bioreactors using single and composite cell-seeded Scaffolds. Biotechnol Bioeng 91:338–355. doi: 10.1002/bit.20490

Majumdar MK, Banks V, Peluso DP, Morris E (2000) Isolation, characterization, and chondrogenic potential of human bone marrow-derived multipotential stromal cells. J Cell Physiol 185:98–106

Malda J, Woodfield TBF, Van Der Vloodt F, et al (2005) The effect of PEGT/PBT scaffold architecture on the composition of tissue engineered cartilage. Biomaterials 26:63–72. doi:

10.1016/j.biomaterials.2004.02.046

Mandal BB, Kundu SC (2008) Non-bioengineered silk fibroin protein 3D scaffolds for potential biotechnological and tissue engineering applications. Macromol Biosci 8:807–818. doi: 10.1002/mabi.200800113

Mankin HJ, Lippiello L (1971) The glycosaminoglycans of normal and arthritic cartilage. J Clin Invest 50:1712–1719. doi: 10.1172/JCI106660

Marolt D, Augst A, Freed LE, et al (2006) Bone and cartilage tissue constructs grown using human bone marrow stromal cells, silk scaffolds and rotating bioreactors. Biomaterials 27:6138–6149. doi: 10.1016/j.biomaterials.2006.07.015

Marshall S, Nadeau O, Yamasaki K (2004) Dynamic actions of glucose and glucosamine on hexosamine biosynthesis in isolated adipocytes: Differential effects on glucosamine 6-phosphate, UDP-N-acetylglucosamine, and ATP levels. J Biol Chem 279:35313–35319. doi: 10.1074/jbc.M404133200

Martin I, Vunjak-Novakovic G, Yang J, et al (1999) Mammalian chondrocytes expanded in the presence of fibroblast growth factor 2 maintain the ability to differentiate and regenerate three-dimensional cartilaginous tissue. Exp Cell Res 253:681–688. doi: 10.1006/excr.1999.4708

Martino A Di, Sittinger M, V RM (2005) Chitosan: a versatile biopolymer for orthopaedic tissue-engineering. Biomaterials 26:5983–5990

Mauck RL, Byers BA, Yuan X, Tuan RS (2007) Regulation of cartilaginous ECM gene transcription by chondrocytes and MSCs in 3D culture in response to dynamic loading. Biomech Model Mechanobiol 6:113–125. doi: 10.1007/s10237-006-0042-1

McCarthy G, O'Donovan J, Jones B, et al (2007) Randomised double-blind, positive-controlled trial to assess the efficacy of glucosamine/chondroitin sulfate for the treatment of dogs with osteoarthritis. Vet J 174:54–61. doi: 10.1016/j.tvjl.2006.02.015

Meinel L, Hofmann S, Karageorgiou V, et al (2004) Engineering cartilage-like tissue using human mesenchymal stem cells and silk protein scaffolds. Biotechnol Bioeng 88:379–391. doi: 10.1002/bit.20252

Messier SP, Mihalko S, Loeser RF, et al (2007) Glucosamine/chondroitin combined with exercise for the treatment of knee osteoarthritis: a preliminary study. Osteoarthr Cartil 15:1256–1266. doi: 10.1016/j.joca.2007.04.016

Minoura N, Aiba S, Gotoh Y, et al (1995) Attachment and growth of cultured fibroblast cells on silk protein matrices. J Biomed Mater Res 29:1215–1221. doi: 10.1002/jbm.820291008

Mirahmadi F, Tafazzoli-Shadpour M, Shokrgozar MA, Bonakdar S (2013) Enhanced mechanical properties of thermosensitive chitosan hydrogel by silk fibers for cartilage tissue engineering. Mater Sci Eng C 33:4786–4794. doi: 10.1016/j.msec.2013.07.043

Mollon B, Kandel R, Chahal J, Theodoropoulos J (2013) The clinical status of cartilage tissue regeneration in humans. Osteoarthritis Cartilage 21:1824–33. doi: 10.1016/j.joca.2013.08.024

Muzzarelli RAA, Greco F, Busilacchi A, et al (2012) Chitosan, hyaluronan and chondroitin sulfate in tissue engineering for cartilage regeneration: A review. Carbohydr Polym 89:723–739. doi: 10.1016/j.carbpol.2012.04.057

Naeimi M, Fathi M, Rafienia M, Bonakdar S (2014) Silk fibroin-chondroitin sulfate-alginate porous scaffolds: Structural properties and in vitro studies. J Appl Polym Sci 131:1–9. doi: 10.1002/app.41048

Nazrov R, Jin H-J, Kaplan DL (2004) Porous 3-D scaffolds from regenerated silk fibroin. Biomacromolecules 5:718–726. doi: 10.1002/pat.998

Nöth U, Tuli R, Osyczka AM, et al (2002) In Vitro Engineered Cartilage Constructs Produced by

Press-Coating Biodegradable Polymer with Human Mesenchymal Stem Cells. Tissue Eng 8:131–144. doi: 10.1089/107632702753503126

O'Brien TA, Tiedemann K, Vowels MR (2006) No longer a biological waste product: Umbilical cord blood. Med J Aust 184:407–410. doi: obr10569_fm [pii]

Oh SH, Kang SG, Kim ES, et al (2003) Fabrication and characterization of hydrophilic poly(lactic-co-glycolic acid)/poly(vinyl alcohol) blend cell scaffolds by melt-molding particulate-leaching method. Biomaterials 24:4011–4021. doi: 10.1016/S0142-9612(03)00284-9

Patil H, Chandel IS, Rastogi AK, Srivastava P (2013) Studies on a Novel Bioreactor Design for Chondrocyte Culture. Int J Tissue Eng 2013:7. doi: 10.1155/2013/976894

Pavelka K, Gatterova J, Olejarova M, et al (2002) Glucosamine Sulfate Use and Delay of Progression of Knee Osteoarthritis: A 3-Year, Randomized, Placebo-Controlled, Double-blind Study. Arch Intern Med 162:2113–2123. doi: 10.1001/archinte.162.18.2113

Pazzano D, Mercier KA, Moran JM, et al (2000) Comparison of chondrogensis in static and perfused bioreactor culture. Biotechnol Prog 16:893–896. doi: 10.1021/bp000082v

Pei M, Luo J, Chen Q (2008) Enhancing and maintaining chondrogenesis of synovial fibroblasts by cartilage extracellular matrix protein matrilins. Osteoarthr Cartil 16:1110–1117. doi: 10.1016/j.joca.2007.12.011

Peng L, Jia Z, Yin X, et al (2008) Comparative Analysis of Mesenchymal Stem Cells from Bone Marrow, Cartilage, and Adipose Tissue. Stem Cells Dev 17:761–774. doi: 10.1089/scd.2007.0217

Pomerantseva I, Bichara DA, Tseng A, et al (2016) Ear-Shaped Stable Auricular Cartilage Engineered from Extensively Expanded Chondrocytes in an Immunocompetent Experimental Animal Model. Tissue Eng Part A 22:197–207. doi: 10.1089/ten.tea.2015.0173

Poole AR, Kobayashi M, Yasuda T, et al (2002) Type II collagen degradation and its regulation in articular cartilage in osteoarthritis. Ann Rheum Dis 61:78–81

Rahman MM, Devi R, Megha PU (2017) In vitro screening of antioxidant and antiproliferative effect of Pogostemon quadrifolius extracts on cultured MCF-7 cell line. Int J Mod Biol Res 5:64–70

Rawal BR, Ribeiro R, Chouksey M, Tripathi K (2013) Biomaterials for cartilage repair: A review. J Med Sci 13:615–620. doi: 10.3923/jms.2013.615.620

Riesle J, Hollander AP, Langer R, et al (1998) Collagen in tissue-engineered cartilage: Types, structure, and crosslinks. J Cell Biochem 71:313–327. doi: 10.1002/(SICI)1097-4644(19981201)71:3<313::AID-JCB1>3.0.CO;2-C

Riss TL, Moravec RA, Niles AL, et al (2016) Cell Viability Assays. In: Assay guidance manual. Eli Lilly \& Company and the National Center for Advancing Translational Sciences, pp 1–31

Rojewski MT, Weber BM, Schrezenmeier H (2008) Phenotypic characterization of mesenchymal stem cells from various tissues. Transfus Med Hemotherapy 35:168–184. doi: 10.1159/000129013

Salter RB, Simmonds DF, Malcolm BW, et al (1980) The biological effect of continuous passive motion on the healing of full-thickness defects in articular cartilage. J Bone Jt Surg Am 62–A:1232–1251

Sasaki T, Iwasaki N, Kohno K, et al (2008) Magnetic nanoparticles for improving cell invasion in tissue engineering. J Biomed Mater Res - Part A 86:969–978. doi: 10.1002/jbm.a.31724

Sawatjui N, Damrongrungruang T, Leeanansaksiri W, et al (2015) Silk fibroin/gelatin-chondroitin sulfate-hyaluronic acid effectively enhances in vitro chondrogenesis of bone marrow mesenchymal stem cells. Mater Sci Eng C 52:90–96. doi: 10.1016/j.msec.2015.03.043

Sawitzke AD, Shi H, Finco MF, et al (2008) The effect of glucosamine and/or chondroitin sulfate on

the progression of knee osteoarthritis: A report from the glucosamine/chondroitin arthritis intervention trial. Arthritis Rheum 58:3183–3191. doi: 10.1002/art.23973

Schulze-Tanzil G, Mobasheri A, de Souza P, et al (2004) Loss of chondrogenic potential in dedifferentiated chondrocytes correlates with deficient Shc-Erk interaction and apoptosis. Osteoarthr Cartil 12:448–458. doi: 10.1016/j.joca.2004.02.007

Schuurman W, Levett PA, Pot MW, et al (2013) Gelatin-methacrylamide hydrogels as potential biomaterials for fabrication of tissue-engineered cartilage constructs. Macromol Biosci 13:551–561. doi: 10.1002/mabi.201200471

Schwarz RP, Goodwin TJ, Wolf DA (1992) Cell culture for three-dimensional modeling in rotating-wall vessels: An application of simulated microgravity. J Tissue Cult Methods 14:51–58. doi: 10.1007/BF01404744

Shahin K, Doran PM (2011) Strategies for Enhancing the Accumulation and Retention of Extracellular Matrix in Tissue-Engineered Cartilage Cultured in Bioreactors. PLoS One 6:e23119. doi: 10.1371/journal.pone.0023119

She Z, Jin C, Huang Z, et al (2008) Silk fibroin/chitosan scaffold: Preparation, characterization, and culture with HepG2 cell. J Mater Sci Mater Med 19:3545–3553. doi: 10.1007/s10856-008-3526-y

Sherwood JK, Riley SL, Palazzolo R, et al (2002) A three-dimensional osteochondral composite scaffold for articular cartilage repair. Biomaterials 23:4739–4751. doi: 10.1016/S0142-9612(02)00223-5

Shikhman AR, Brinson DC, Valbracht J, Lotz MK (2009) Differential metabolic effects of glucosamine and N-acetylglucosamine in human articular chondrocytes. Osteoarthr Cartil 17:1022–1028. doi: 10.1016/j.joca.2009.03.004

Shimizu K, Ito A, Honda H (2006) Enhanced cell-seeding into 3D porous scaffolds by use of magnetite nanoparticles. J Biomed Mater Res - Part B Appl Biomater 77:265–272. doi: 10.1002/jbm.b.30443

Sikavitsas VI, Bancroft GN, Mikos AG (2002) Formation of three-dimensional cell/polymer constructs for bone tissue engineering in a spinner flask and a rotating wall vessel bioreactor. J Biomed Mater Res 62:136–148. doi: 10.1002/jbm.10150

Simánek V, Kren V, Ulrichová J, Gallo J (2005) The efficacy of glucosamine and chondroitin sulfate in the treatment of osteoarthritis: are these saccharides drugs or nutraceuticals? Biomed Pap 149:51–56

Sofia S, McCarthy MB, Gronowicz G, Kaplan DL (2001) Functionalized silk-based biomaterials for bone formation. J Biomed Mater Res 54:139–148. doi: 10.1002/1097-4636(200101)54:1<139::AID-JBM17>3.0.CO;2-7

Solchaga LA, Tognana E, Penick K, et al (2006) A rapid seeding technique for the assembly of Large Cell / Scaffold Composite Constructs. Tissue Eng 12:1851–1863

Somoza RA, Welter JF, Correa D, Caplan AI (2014) Chondrogenic Differentiation of Mesenchymal Stem Cells: Challenges and Unfulfilled Expectations. Tissue Eng Part B Rev 20:596–608. doi: 10.1089/ten.teb.2013.0771

Song K, Li L, Li W, et al (2015) Three-dimensional dynamic fabrication of engineered cartilage based on chitosan/gelatin hybrid hydrogel scaffold in a spinner flask with a special designed steel frame. Mater Sci Eng C 55:384–392. doi: 10.1016/j.msec.2015.05.062

Stoddart MJ, Grad S, Eglin D, Alini M (2009) Cells and biomaterials in cartilage tissue engineering. Regen Med 4:81–98

Subia B, Kundu J, Kundu SC (2010) Biomaterial Scaffold Fabrication Techniques for Potential Tissue Engineering Applications. Tissue Eng 141–159. doi: 10.5772/8581

Sun K, Li H, Li R, et al (2014) Silk fibroin/collagen and silk fibroin/chitosan blended three-dimensional scaffolds for tissue engineering. Eur J Orthop Surg Traumatol 25:243–249. doi: 10.1007/s00590-014-1515-z

Sung H-J, Meredith C, Johnson C, Galis ZS (2004) The effect of scaffold degradation rate on three-dimensional cell growth and angiogenesis. Biomaterials 25:5735–5742. doi: 10.1016/j.biomaterials.2004.01.066

Takahashi K, Mizuarai S, Araki H, et al (2003) Adiposity Elevates Plasma MCP-1 Levels Leading to the Increased CD11b-positive Monocytes in Mice. J Biol Chem 278:46654–46660. doi: 10.1074/jbc.M309895200

Tan H, Chu CR, Payne KA, Marra KG (2009a) Injectable in situ forming biodegradable chitosan-hyaluronic acid based hydrogels for cartilage tissue engineering. Biomaterials 30:2499–2506. doi: 10.1016/j.biomaterials.2008.12.080

Tan H, Wu J, Lao L, Gao C (2009b) Gelatin / chitosan / hyaluronan scaffold integrated with PLGA microspheres for cartilage tissue engineering. Acta Biomater 5:328–337. doi: 10.1016/j.actbio.2008.07.030

Tandon N, Marolt D, Cimetta E, Vunjak-Novakovic G (2013) Bioreactor engineering of stem cell environments. Biotechnol Adv 31:1020–1031. doi: 10.1016/j.biotechadv.2013.03.007

Temenoff JS, Mikos AG (2000) Review : tissue engineering for regeneration of articular cartilage. Biomaterials 21:431–440. doi: 10.1016/S0142-9612(99)00213-6

Terry DE, Chopra RK, Ovenden J, Anastassiades TP (2000) Differential Use of Alcian Blue and Toluidine Blue Dyes for the Quantification and Isolation of Anionic Glycoconjugates from Cell Cultures : Application to Proteoglycans and a High-Molecular-Weight Glycoprotein Synthesized by Articular Chondrocytes. Anal Biochem 219:211–219. doi: 10.1006/abio.2000.4761

Theodosakis J, Adderly B FB (1997) The arthritis cure: the medical miracle that can halt, reverse, and may even cure osteoarthritis

Tiku ML, Sabaawy HE (2015) Cartilage regeneration for treatment of osteoarthritis: A paradigm for nonsurgical intervention. Ther Adv Musculoskelet Dis 7:76–87. doi: 10.1177/1759720X15576866

Tuan RS, Boland G, Tuli R (2003) Adult mesenchymal stem cells and cell-based tissue engineering. Arthritis Res Ther 5:32–45. doi: 10.1186/ar614

Tuli R, Li W, Tuan RS (2003) Current state of cartilage tissue engineering. Arthritis Res Ther 5:235–238. doi: 10.1186/ar991

Tutak W, Sarkar S, Lin-Gibson S, et al (2013) The support of bone marrow stromal cell differentiation by airbrushed nanofiber scaffolds. Biomaterials 34:2389–2398. doi: 10.1016/j.biomaterials.2012.12.020

Uebelhart D, J-MA Thonar E, D. Delmas P, et al (1998) Effects of oral chondroitin sulfate on the progression of knee osteoarthritis: a pilot study. Osteoarthr Cartil 6:39–46

Uebelhart D, Zhang J, Thonar E (1997) Acute degeneration of articular cartilage in the rabbit: Protective effect of chondroitin 4 and 6 sulfate. Osteoarthiritis Cartil 5:68–75

Ullah I, Subbarao RB, Rho GJ (2015) Human mesenchymal stem cells - current trends and future prospective. Biosci Rep 35:1–18. doi: 10.1042/BSR20150025

Vacanti JP, Langer R (1999) Tissue engineering: the design and fabrication of living replacement devices for surgical reconstruction and transplantation. Lancet 354:SI32-I34. doi: 10.1016/S0140-6736(99)90247-7

Vangsness CT, Spiker W, Erickson J (2009) A Review of Evidence-Based Medicine for Glucosamine and Chondroitin Sulfate Use in Knee Osteoarthritis. Arthrosc - J Arthrosc Relat Surg 25:86–94.

doi: 10.1016/j.arthro.2008.07.020

Varghese S, Hwang NS, Canver AC, et al (2008) Chondroitin sulfate based niches for chondrogenic differentiation of mesenchymal stem cells. Matrix Biol 27:12–21. doi: 10.1016/j.matbio.2007.07.002

Vinatier C, Guicheux J (2016) Cartilage tissue engineering: From biomaterials and stem cells to osteoarthritis treatments. Ann Phys Rehabil Med 59:139–144. doi: 10.1016/j.rehab.2016.03.002

Vishwanath V, Pramanik K, Biswas A (2016) Optimization and evaluation of silk fibroin-chitosan freeze-dried porous scaffolds for cartilage tissue engineering application. J Biomater Sci Polym Ed 27:657–674. doi: 10.1080/09205063.2016.1148303

Vishwanath V, Pramanik K, Biswas A (2017) Development of a novel glucosamine/silk fibroin–chitosan blend porous scaffold for cartilage tissue engineering applications. Iran Polym J 26:11–19. doi: 10.1007/s13726-016-0492-y

Vunjak-Novakovic G, Freed LE, Biron RJ, Langer R (1996) Effects of mixing on the composition and morphology of tissue-engineered cartilage. AIChE J 42:850–860. doi: 10.1002/aic.690420323

Vunjak-Novakovic G, Obradovic B, Martin I, et al (1998) Dynamic cell seeding of polymer scaffolds for cartilage tissue engineering. Biotechnol Prog 14:193–202. doi: 10.1021/bp970120j

Wang H-J, Bertrand-de Haas M, van Blitterswijk CA, Lamme EN (2003) Engineering of a dermal equivalent: seeding and culturing fibroblasts in PEGT/PBT copolymer scaffolds. Tissue Eng 9:909–917. doi: 10.1089/107632703322495556

Wang L, Li C (2007) Preparation and physicochemical properties of a novel hydroxyapatite/chitosan-silk fibroin composite. Carbohydr Polym 68:740–745. doi: 10.1016/j.carbpol.2006.08.010

Wang Y, Bian YZ, Wu Q, Chen GQ (2008) Evaluation of three-dimensional scaffolds prepared from poly(3-hydroxybutyrate-co-3-hydroxyhexanoate) for growth of allogeneic chondrocytes for cartilage repair in rabbits. Biomaterials 29:2858–2868. doi: 10.1016/j.biomaterials.2008.03.021

Wang Y, Kim UJ, Blasioli DJ, et al (2005) In vitro cartilage tissue engineering with 3D porous aqueous-derived silk scaffolds and mesenchymal stem cells. Biomaterials 26:7082–7094. doi: 10.1016/j.biomaterials.2005.05.022

Wirth CJ, Rudert M (1996) Techniques of cartilage growth enhancement: a review of the literature. Arthrosc J Arthrosc Relat Surg 12:300–308. doi: 10.1016/S0749-8063(96)90062-6

Woodside SM, Bowen BD, Piret JM (1998) Mammalian cell retention devices for stirred perfusion bioreactors. Cytotechnology 28:163–175

Xu F, Xu L, Wang Q, et al (2014) 3D dynamic culture of rabbit articular chondrocytes encapsulated in alginate gel beads using spinner flasks for cartilage tissue regeneration. Biomed Res Int 2014:1–10. doi: 10.1155/2014/539789

Xu P, Lu Y (2016) Comparison of Bone Marrow-derived Mononuclear Cells vs. Mesenchymal Stem Cells in Protecting Random-pattern Skin Flap Survival in Rats. J Stem Cell Res Ther 6:6–11. doi: 10.4172/2157-7633.1000355

Yamane S, Iwasaki N, Majima T, et al (2005) Feasibility of chitosan-based hyaluronic acid hybrid biomaterial for a novel scaffold in cartilage tissue engineering. Biomaterials 26:611–619. doi: 10.1016/j.biomaterials.2004.03.013

Yan LP, Wang YJ, Ren L, et al (2010) Genipin-cross-linked collagen/chitosan biomimetic scaffolds for articular cartilage tissue engineering applications. J Biomed Mater Res - Part A 95 A:465–475. doi: 10.1002/jbm.a.32869

Yan S, Zhang Q, Wang J, et al (2013) Silk fibroin/chondroitin sulfate/hyaluronic acid ternary scaffolds for dermal tissue reconstruction. Acta Biomater 9:6771–6782. doi: 10.1016/j.actbio.2013.02.016

Yokoyama A, Sekiya I, Miyazaki K, et al (2005) In vitro cartilage formation of composites of synovium-derived mesenchymal stem cells with collagen gel. Cell Tissue Res 322:289–298. doi: 10.1007/s00441-005-0010-6

Yoon HH, Bhang SH, Shin J-Y, et al (2012) Enhanced Cartilage Formation via Three-Dimensional Cell Engineering of Human Adipose-Derived Stem Cells. Tissue Eng Part A 18:1949–1956. doi: 10.1089/ten.tea.2011.0647

Zang M, Zhang Q, Davis G, et al (2011) Perichondrium directed cartilage formation in silk fibroin and chitosan blend scaffolds for tracheal transplantation. Acta Biomater 7:3422–3431. doi: 10.1016/j.actbio.2011.05.012

Zaucke F, Dinser R, Maurer P, Paulsson M (2001) Cartilage oligomeric matrix protein (COMP) and collagen IX are sensitive markers for the differentiation state of articular primary chondrocytes. Biochem J 358:17–24. doi: 10.1042/0264-6021:3580017

Zhang K, Qian Y, Wang H, et al (2010a) Genipin-crosslinked silk fibroin/hydroxybutyl chitosan nanofibrous scaffolds for tissue-engineering application. J Biomed Mater Res - Part A 95:870–881. doi: 10.1002/jbm.a.32895

Zhang L, Li K, Xiao W, et al (2011) Preparation of collagen-chondroitin sulfate-hyaluronic acid hybrid hydrogel scaffolds and cell compatibility in vitro. Carbohydr Polym 84:118–125. doi: 10.1016/j.carbpol.2010.11.009

Zhang L, Su P, Xu C, et al (2010b) Chondrogenic differentiation of human mesenchymal stem cells: A comparison between micromass and pellet culture systems. Biotechnol Lett 32:1339–1346. doi: 10.1007/s10529-010-0293-x

Zhang Z, Cui H (2012) Biodegradability and biocompatibility study of poly(chitosan-g-lactic acid) scaffolds. Molecules 17:3243–3258. doi: 10.3390/molecules17033243

Zhao J, Griffin M, Cai J, et al (2016) Bioreactors for tissue engineering: An update. Biochem Eng J 109:268–281. doi: 10.1016/j.bej.2016.01.018

Zheng R, Duan H, Xue J, et al (2014) The influence of Gelatin/PCL ratio and 3-D construct shape of electrospun membranes on cartilage regeneration. Biomaterials 35:152–164. doi: 10.1016/j.biomaterials.2013.09.082

Publications

1. **P. Agrawal**, K. Pramanik, A. Biswas and R. K. Patra. "*In vitro* cartilage construct generation from silk fibroin- chitosan porous scaffold and umbilical cord blood derived human mesenchymal stem cells in dynamic culture condition" *Journal of Biomedical Materials Research Part A* 2018;106(2):397–407. John Wiley & Sons. DOI: 10.1002/jbm.a.36253
2. **P. Agrawal**, K. Pramanik and A. Biswas. "Chondrogenic differentiation of human mesenchymal stem cells on silk fibroin/chitosan- glucosamine scaffolds in dynamic culture", *Regenerative Medicine*. 2018;13(5):545-558. Future Medicine Group. DOI: 10.2217/rme-2017-0159
3. **P. Agrawal**, K. Pramanik, V. Vishwanath, A. Biswas, A. Bissoyi and P. K. Patra. "Enhanced chondrogenesis of mesenchymal stem cells over silk fibroin/chitosan-chondroitin sulfate three dimensional scaffold in dynamic culture condition" *Journal of Biomedical Materials Research Part B- Applied Biomaterials.* 2018;106(7):2576–2587. John Wiley & Sons. DOI: 10.1002/jbm.b.34074

Manuscript under revision

4. **P. Agrawal** and K. Pramanik. "Fabrication of cartilage construct by differentiation of human mesenchymal stem cells over glucosamine, chondroitin sulfate loaded silk fibroin/chitosan matrix under dynamic culture", *Differentiation*. Elsevier.

Related publications

5. **P. Agrawal** and K. Pramanik. "Chitosan-poly vinyl alcohol nanofibers by free surface electrospinning for tissue engineering applications" *Journal of Tissue engineering and regenerative medicine* 2016;13(5):485–497. Springer. DOI: 10.1007/s13770-016-9092-3
6. **P. Agrawal**, K. Pramanik and A. Bissoyi. "Novel blowspun nanobioactive glass doped polycaprolactone/ silk fibroin composite nanofibrous scaffold with enhanced osteogenic property for bone tissue engineering" *Fibers and Polymers* 2018. Springer.

Conference papers

1. **P. Agrawal** and K. Pramanik. Enhanced chondrogenesis of mensenchymal stem cells over glucosamine and chondroitin sulfate incorporated silk fibroin/ chitosan scaffold in dynamic culture condition. *National Conference on Tissue Engineering & Regenerative Medicine* 2017 at NIT Rourkela, India.
2. **P. Agrawal** and K. Pramanik. Nanofibers preparation by free-liquid surface electrospinning for cartilage tissue engineering. *International Conference on Nanomedicine and Nanobiotechnology* 2016 at University Pierre and Marie Curie, Paris, France.
3. **P. Agrawal** and K. Pramanik. Preparation of silk fibroin, chitosan and poly ethylene oxide scaffolds for cartilage tissue engineering. *2nd International Conference on Tissue Engineering & Regenerative Medicine* 2013 at NIT Rourkela, India.

Biography

PARINITA AGRAWAL

agrawalparinita@gmail.com

Educational Qualification

2018: Ph.D. (Biotechnology and Medical Engineering)
National Institute of Technology, Rourkela, Odisha, India

2013: M.Tech. (Biotechnology)
National Institute of Technology, Rourkela, Odisha, India

2010: B.Tech. (Biotechnology)
Dr. D.Y. Patil Biotechnology and Bioinformatics Institute, Pune, Maharashtra, India

Honours and Awards

- Institute Silver Medallist for being the topper of M.Tech. 2013 batch in the Department of Biotechnology and Medical Engineering, NIT Rourkela, Odisha, India
- Ministry of Human Resource and Development (MHRD) scholarship for qualifying Graduate Aptitude Test in Engineering (GATE) 2011 in Biotechnology, Score: 396

Research Interest

Tissue engineering, stem cell isolation and culture, scaffold fabrication

Personal Details

Permanent Address	C-225, Annapurna Vihar, C.S.E.B (West) Korba- 495451, Chhattisgarh, India
Date of Birth	13th April, 1988
Language Known	English, Hindi
Nationality	Indian